2020

Representations of Reward and Movement in Drosophila Dopaminergic Neurons

Aryeh Zolin

REPRESENTATIONS OF REWARD AND MOVEMENT IN *DROSOPHILA* DOPAMINERGIC NEURONS

A Thesis Presented to the Faculty of

The Rockefeller University

in Partial Fulfillment of the Requirements for

the degree of Doctor of Philosophy

by

Aryeh Zolin

June 2020

REPRESENTATIONS OF REWARD AND MOVEMENT IN *DROSOPHILA* DOPAMINERGIC NEURONS

Aryeh Zolin, Ph.D.

The Rockefeller University 2020

The neuromodulator dopamine is known to influence both immediate and future behavior, motivating and invigorating an animal's ongoing movement but also serving as a reinforcement signal to instruct learning. Yet it remains unclear whether this dual role of dopamine involves the same dopaminergic pathways. Although reward-responsive dopaminergic neurons display movement-related activity, debate continues as to what features of an individual's experience these motor-correlates correspond and how they influence concurrent behavior.

The mushroom body, a prominent neuropil in the brain of the fruit fly *Drosophila melanogaster*, is richly innervated by dopaminergic neurons that play an essential role in the formation of olfactory associations. While dopaminergic neurons respond to reward and punishment to drive associative learning, they have also been implicated in a number of adaptive behaviors and their activity correlates with the behavioral state of an animal and its coarse motor actions. Here, we take advantage of the concise circuit architecture of the *Drosophila* mushroom body to investigate the nature of motor-related signals in dopaminergic neurons that drive associative learning. *In vivo* functional imaging during naturalistic tethered locomotion reveals

that the activity of different subsets of mushroom body dopaminergic neurons reflects distinct aspects of movement. To gain insight into what facets of an animal's experience are represented by these movement-related signals, we employed a closed loop virtual reality paradigm to monitor neural activity as animals track an olfactory stimulus and are actively engaged in a goal-directed and sensory-motivated behavior. We discover that odor responses in dopaminergic neurons correlate with the extent to which an animal tracks upwind towards the fictive odor source. In different experimental contexts where distinct motor actions were required to track the odor, dopaminergic neurons become emergently linked to the behavioral metric most relevant for effective olfactory navigation. Subsets of dopaminergic neurons were correlated with the strength of upwind tracking regardless of the identity of the odor and remained so even after the satiety state of an animal was altered. We proceed to demonstrate that transient inhibition of dopaminergic neurons that are positively correlated with upwind tracking significantly diminishes the normal approach responses to an appetitive olfactory cue. Accordingly, activation of those same dopaminergic neurons enhances approach to an odor and even drives upwind tracking in clean air alone.

Together, these results reveal that the same dopaminergic pathways that convey reinforcements to instruct learning also carry representations of an animal's moment-by-moment movements and actively influence behavior. The complex activity patterns of mushroom body dopaminergic neurons therefore represent neither purely sensory nor motor variables but rather reflect the goal or motivation underlying an animal's movements. Our data suggest a fundamental coupling between reinforcement signals and motivation-related locomotor representations within dopaminergic circuitry, drawing a striking parallel between the mushroom body dopaminergic neurons described here and the emerging understanding of mammalian dopaminergic pathways.

The apparent conservation in dopaminergic neuromodulatory networks between mammals and insects suggests a shared logic for how neural circuits assign meaning to both sensory stimuli and motor actions to generate flexible and adaptive behavior.

To Aba and Ema

for unconditional love and support

To Ruth

the love of my life

for always being on my team

and reminding what's important

Acknowledgements

I would like to recognize and acknowledge the people who contributed directly to the work presented in my thesis. Raffi Cohn, a former graduate student in the lab, first appreciated the relationship between mushroom body dopaminergic activity and the movements of the fly, laying the foundation for this project. In addition, he designed the closed loop olfactory paradigm that was vital to our ability to understand the nature of motor-related signaling in mushroom body dopaminergic pathways and performed the experiments in which flies were presented with a pseudo-random white noise moving airstream. Raffi also contributed to the intellectual development of this project through frequent conversations and discussions of data. Raffi has been a mentor and a friend throughout my PhD and I am grateful to have had the opportunity to work with him so closely.

This project was a collaboration with Adrienne Fairhall and her student, Rich Pang. Rich performed the principle component analysis, generated the linear filters predicting dopaminergic neuron activity from behavior, the partial correlations between dopaminergic neurons, the cross-correlation matrices demonstrating the relationship between dopaminergic neuron activity and past, present, and future behavior, and the nested linear models predicting dopaminergic responses to odor from behavioral responses to odor. Their principled and quantitative approach to our datasets helped us better understand the nature of mushroom body dopaminergic signaling and greatly contributed to this project.

I was only able to design, develop, and build a tethered fly walking system in our lab with the help of Gaby Maimon and Jonathan Green, who provided early guidance and advice. Jim Petrillo and the entire Rockefeller Precision Fabrication Facility were instrumental in the design and assembly of the tethering and dissection chambers that allowed us perform all of our *in vivo* functional imaging experiments. The developer of FicTrac software, Richard Moore, was responsive and helpful in troubleshooting while setting up the system under our two-photon microscope.

Thomas Graham, a former postdoc in the lab, designed the behavioral chambers, optogenetic experimental system, and fly tracking software that allowed us to assay behavioral responses to odor in freely moving animals and assess how optogenetic inhibition and activation of select dopaminergic populations affected anemotaxic behaviors. Patrick Stock, an engineer in the lab, provided technical support and designed a novel positive pressure experimental system to assay olfactory responses in freely moving animals to CO_2.

Andy Siliciano, a talented MD-PhD student, is continuing our investigation into how ongoing mushroom body dopaminergic neuron activity affects downstream pathways and behavior. It has been a pleasure to work with him and I look forward to seeing his future progress.

The Ruta lab is a supportive and engaging environment and I am lucky to have had the opportunity to interact on a daily basis with such intelligent and passionate scientists. Eva Luderowski helped start the lab and Ianessa Morantte continues to keep it running smoothly and is a wonderful resource for general scientific advice and information. Conversations among Ruta

lab members, both formal ones in lab meetings and informal ones, has greatly contributed to my growth as a scientist. I'd especially like to thank Josie Clowney, Laura Seeholzer, Andy Siliciano, and my bay-mate Annie Handler for their comments, advice, thoughts, support, and friendship throughout this experience.

I would like to thank the members of my faculty advisory committee, Cori Bargmann, Jim Hudspeth, and Jeremy Dittman, for their advice throughout my PhD that helped shape and develop the work presented here today. I am also grateful to Sandeep Datta for serving as the external examiner of my thesis committee.

Most of all, I want to express tremendous gratitude to my first bay-mate, mentor, and advisor, Vanessa Ruta. Vanessa came into lab on the Sunday before my rotation was set to start to teach me fly dissections so that I could maximize my time in her lab in spite of my abridged MD-PhD rotation timeline. From that moment on she has been incredibly generous with her time and energy and has supported me throughout this process. When crises emerged and obstacles seemed insurmountable, her calm and confident support kept me going. Vanessa is overflowing with insights and ideas and the work I present in this document would not have been possible without her unwavering support and intellectual guidance. She pushes me to think deeply about scientific questions and to critically approach both my own data and that of others. Above all, Vanessa is a genuinely caring advisor and educator who tethers her own success as a mentor and lab head to the success of her students and trainees. She stands as an inspiration and is my model for what it means to be a scientist.

The Rockefeller University is a special place to do science and I am privileged to have had the opportunity to study here. I'd like to the thank the Dean's Office – Cris Rosario, Emily Harms, Stephanie Fernandez, Sid Strickland, Marta Delgado, and Kristen Cullen – for making life as a student as easy as possible and for always working to smooth over the bumps in the road. I am indebted to all of the invertebrate neuroscience BSVMRYKYZ labs at Rockefeller for creating a curious, engaged, and supportive community that provided helpful questions, feedback, and ideas throughout my PhD. I would like to especially to thank Wanhe Li, Zikun Wang, Meg Younger, and Cheng Lyu for interesting discussions, advice, and help over the past six years

Finally, I would like to thank all of my friends and extended family for making my life fuller and richer and for always asking how my flies are doing.

All of the good things in my life are because of the unconditional love, support, and dedication of my parents, Ronnie and Elliot Zolin. I will never be able to adequately express how grateful I am for all they have done for me. Thank you both for everything.

Lastly, Ruth Singer, my brilliant wife, fills my life with joy, love, and meaning. She has kept me sane and happy through this long and often turbulent process and has provided immeasurable support. I could not have done it without her.

Table of Contents

Chapter 2

Chapter 3

Chapter 6

List of Figures

List of Abbreviations

ACV	Apple cider vinegar
CO_2	Carbon dioxide
cAMP	Cyclic adenosine monophosphate
DAN	Dopaminergic neuron
DDC	Dopa-decarboxylase
GPi	Globus pallidus interna
Gr43a	Gustatory receptor 43a
KC	Kenyon cell
LH	Lateral horn
LTM	Long-term memory
MB	Mushroom body
MBON	Mushroom body output neuron
PAM	Protocerebral anterior medial
PPL	Protocerebral posterior lateral
PN	Projection neuron
RPE	Reward prediction error
SNc	Substantia nigra pars compacta
SNr	Substantia nigra pars reticulata
STM	Short-term memory
TH	Tyrosine hydroxylase
VTA	Ventral tegmental area

Chapter 1

Introduction

1.1 Neuromodulation Produces Flexible Neural Circuits

The Spanish neuroscientist and father of neuroanatomy Santiago Ramón y Cajal claimed that the structure of the brain was a reflection of the universe[1]. Indeed, the brain is charged with the monumental task of faithfully representing the diverse and intricate features of the physical world while simultaneously transmitting specific instructions to the body to exert precise control over the individual's actions. All of our perceptions of the universe and all of our interaction with it occur through neurons. As Cajal noted, the brain's structure, its connectivity and anatomy, was believed to dictate how information was relayed into, within, and from it and was therefore

considered its fundamental property and the key to understanding its operation[2,3]. There is no doubt that anatomy is an integral element of the central nervous system. Multiple aspects of the environment and complex motor commands are translated into the frequency of action potential firing and patterns of neural activity, the interpretation of which is dictated by the connective organization of sensory and motor circuits[4–7]. Likewise, higher order neural and cognitive processes, such as memory, language, and attention, have been localized to discrete neuropils and regions within the brain, underscoring the importance of having functionally specific circuits playing dedicated roles[4,5,8–15]. The physical organization of the brain and the specific connections between neurons – the connectome – provides the form within which neural circuits function and proscribes their activity. The connectome need not be static and certain neural processes can be attributed to changes in anatomic connectivity between neurons. Synaptogenesis is thought to underlie certain forms of learning[16–18] and synaptic pruning is vital for proper development[19,20]. In addition, cyclic behaviors, such as sleep, are accompanied by changes in the physical structure of the underlying neural pathways[21].

Even a dynamic connectome, however, cannot account for the brain's remarkable ability to flexibly adapt to meet the myriad and immediate needs of an animal[22–24]. Identical stimuli can generate profoundly different behavioral responses in a hungry individual compared to a sated one[25–32]. Within seconds of the sight of a predator or the whiff of a potential mate or reproductive rival there are alterations in how sensory stimuli are represented and how motor commands are relayed to peripheral pathways[33–41]. A saccade immediately shifts the flow of information through the retina[42,43]. Developing a separate and discrete circuit for every possible contingency or constructing new circuits as needed would be slow, require tremendous energy, and ultimately be

unwieldy and impractical (if not impossible). It has become increasingly clear, then, that the intricate wiring of neural circuits do not necessarily dictate their functional activity. Studies of the most basic nervous systems, like that of the nematode *Caenorhabditis elegans*, a model organism with a completely mapped connectome, or even simple circuits, like the stomatogastric ganglion of the crab *Cancer borealis*, reveal that only subsets of interconnected neurons become active in response to a sensory cue, during a movements, or while performing a task[22,23,44–46]. While anatomic connectivity may constrain the limits of neural systems, their *functional connectivity* is arguably more important and integral to understanding their physiological operation. Neural circuits must be able to adapt and the proper functioning of the nervous system depends on the ability of circuits to flexibly modulate their activity such that their properties can be emergently defined by the individual's experience, context, immediate requirements, and long-term needs.

The functional properties of neural circuits are defined, modified, and made flexible by the activity of a class of molecules known as neuromodulators. Unlike classical neurotransmitters, such as glutamate or GABA, that rapidly alter the voltage across a cell membrane, neuromodulators, such as serotonin, dopamine, and norepinephrine, cause diverse effects on the excitability and functionality of their post-synaptic targets[4,22,23,47]. Internal states, such as sleeping, fighting or flight, mating/reproduction, aggression, hunger, attention, stress, or strong emotions are made manifest by the activity of neuromodulators[48–62]. By reconfiguring the activity of neural pathways, these signaling molecules allow animals to adapt to a dynamic and rapidly shifting environment and modify behavior to meet an internal need or perform a desired task[22–24]. The changes wrought by neuromodulators can be rapid, but also have the potential to be long-lasting, creating alterations in circuit function that can last a lifetime. This ability to drive synaptic

plasticity has therefore made neuromodulators a key component of the neural pathways that underlie learning and memory, enabling experience to influence future behavior[63–67].

The importance of neuromodulators to normal neurophysiology is evident in the diseases that arise from perturbations to their activity. An inability to effectively control internal state due to impaired neuromodulation is the hallmark of a number of psychiatric disorders, including obsessive compulsive disorder, post-traumatic stress disorder, attention deficit hyperactivity disorder, bipolar disorder, depression, and schizophrenia[68–72]. Interestingly, even more mundane processes such as locomotion, require flexible circuit adaptation and defective neuromodulation can also lead to movement deficits such as those observed in Parkinson's disease[73]. Animal behavior that unfolds over multiple timescales, from milliseconds to years, depends on the flexibility of neural circuits that is made possible by neuromodulators.

1.2 The Complexity and Multifunctionality of Neuromodulatory Pathways

Given their vital role in controlling the activity of neural circuits, neuromodulators have been the subject of intense and focused study and great progress has been made in understanding how molecules like serotonin, dopamine, or norepinephrine reconfigure the functional properties of downstream pathways to ultimately produce adaptive behaviors[22–24,47,74–76]. Less well understood, however, are neuromodulatory circuits themselves. Within a specific experimental paradigm and from the perspective of an isolated circuit, it is often possible to infer what information is conveyed by a neuromodulatory pathway. During reinforcement learning in

primates and rodents, for instance, dopaminergic activity strongly correlates with reward and this signal is believed to change the functional connectivity of a circuit to produce novel behaviors[66,77]. Similarly, in the gill and siphon withdrawal reflex of *Aplysia*, serotonin release likely represents the punitive electric shock that indicates an aversive context and triggers defensive actions[78–81]. Norepinephrine is almost certainly signaling wakefulness and arousal as animals transition into and out of sleep[50,53,82]. These neuromodulatory networks, however, exhibit ongoing activity that contains multiple different sensory, motor, and task-related correlates[52,65,83–90]. The relationship between these signals and specific cognitive variables or features of an animal's experience is unknown and their contribution to an animal's behavior is poorly understood. Answering these questions is crucial to gaining a coherent understanding of how neuromodulatory networks operate coordinately to produce adaptive and flexible behavior.

The complexity and multifunctionality of neuromodulatory pathways is nowhere better illustrated than in the case of the ubiquitous neuromodulator dopamine.

1.3 Dopaminergic Signaling is Implicated in a Diverse Array of Different Neural Processes and Pathophysiologies

In 1817 James Parkinson first described the constellation of motor deficits that would eventually become the hallmark of the movement disorder that now bears his name[91]. It was not until the 1960s, however, that depletion of the neuromodulator dopamine was identified as the causative pathology in Parkinson's disease[73,92–99]. Since that discovery, perturbations in

dopaminergic signaling have been implicated in a wide array of seemingly distinct neural processes and pathophysiologies beyond movement, including learning and memory[100–104], sleep and circadian rhythms[105], habit formation and drug addiction[106–108], schizophrenia[109–111], attention deficit hyperactivity disorder[112], and depression[113]. The multiple distinct functions ascribed to dopamine contrast with the extremely small number of dopaminergic neurons in the mammalian central nervous system: dopamine is expressed in less than .0005% of neurons in the human brain, all of whose cell bodies are confined to a small number of discrete subcortical regions[5,114]. Despite extensive research, dopamine remains incompletely understood and it is unclear how the limited population of dopaminergic neurons can participate in such a diverse array of different neurological functions. As will be explored more fully in the coming sections, dopamine is a prime example of a neuromodulatory network whose function can be understood within the confines of given experimental paradigm, but whose ongoing activity and contribution to ongoing behavior remains ambiguous. It has therefore been a major goal of both neuroscience and clinical neurology to describe the anatomic and functional logic of dopaminergic circuitry, identify the variables encoded by dopaminergic neuron activity, and understand how dopamine affects downstream neural pathways to shape behavior.

1.4 Neuromodulation by Dopamine

As a neuromodulator, dopamine causes diverse effects on the excitability and functionality of its post-synaptic partners[4,22]. In mammals, five dopamine receptors, all G-protein coupled, have been identified that are each associated with distinct downstream signaling cascades[75]. Dopamine

acts via these receptors to reorganize and modify both pre- and post-synaptic function. By altering the probability, size, or timing of neurotransmitter release, dopamine can tune the pre-synaptic elements of circuits. Similarly, by modifying the sensitivity to calcium or other second messengers or by adjusting the concentration, distribution, or kinetics of neurotransmitter receptors, dopamine can control how post-synaptic neurons respond to equivalent upstream signals. Thus dopamine can act to both rapidly and persistently tune the activity of neural pathways by diverse means and at multiple levels[76,115–120]. Dopamine can also acts beyond the strict confines of synaptic structures, diffusing through the extracellular space to affect more distant neurons and larger neural circuits more broadly[121].

Although dopamine can variably and dynamically affect its targets, the different dopamine receptor signaling pathways generally seem to operate in parallel, in cooperation, or in opposition within the same larger circuits[4,75,121,122]. Distinct molecular pathways alone, therefore, cannot account for the wide array of functions ascribed to dopamine.

1.5 Control of Movement by Dopamine

Perturbations of dopaminergic neurotransmission result in severe motor dysfunction[73,96–99,123–127] that is thought to arise from altered signaling within and from the basal ganglia[128–131], a prominent subcortical structure in the vertebrate brain. The basal ganglia is composed of a number of discrete nuclei, including the striatum, globus pallidus, substantia nigra, and the subthalamic nucleus (Figure 1.1)[4]. Dopamine released by neurons residing in the substantia nigra pars compacta

Figure 1.1 | Midbrain Dopaminergic Neurons Coordinate the Output of the Basal Ganglia to Control Movement. Schematic of the direct (left) and indirect (right) pathways of the mammalian basal ganglia. Substantia nigra pars compacta (SNc), globus pallidus externa (GPe), globus pallidus interna (GPi), subthalamic nucleus (STN). Substantia nigra pars reticulata is not shown but, similar to GPi, receives inhibitory input from striatum, excitatory input from the STN, and has GABAergic projections to the thalamus.

Figure 1.1

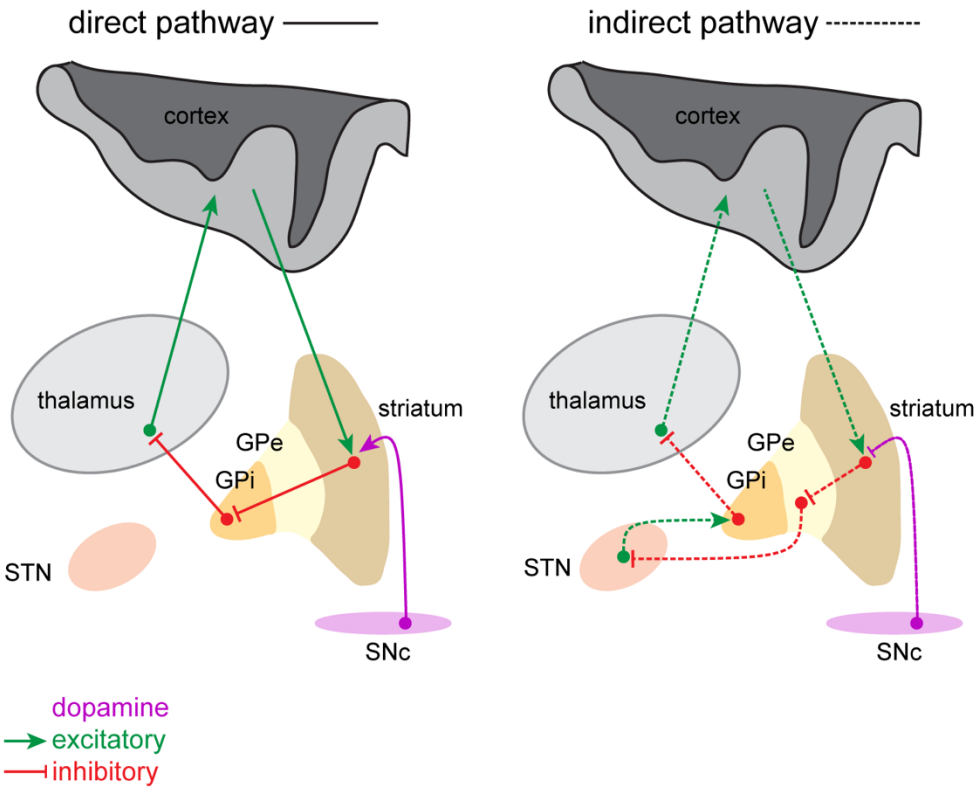
direct pathway
indirect pathway
cortex
cortex
thalamus
thalamus
striatum
striatum
GPe
GPe
GPi
GPi
STN
STN
SNc
SNc
dopamine
excitatory
inhibitory

(SNc) is believed to act by gating the output of the basal ganglia in the canonical cortico-basal ganglia-thalmo-cortical loop. Movement-related information from the cortex enters the basal ganglia by way of the striatum, where GABAergic medium spiny neurons (the primary intrinsic neurons of the striatum) receive excitatory cortical inputs and project to other interconnected basal ganglia nuclei. Ultimately, efferents from the globus pallidus interna (GPi) and substantia nigra pars reticulata (SNr) innervate the thalamus, which in turn projects axons back to the cortex, completing the circuit and closing the loop (Figure 1.1)[122].

The basal ganglia's functional interactions with thalamic and cortical motor circuits are composed of two distinct pathways defined by the dopaminergic receptors they express and how they are affected by dopamine: the direct and indirect pathways. In the direct pathway, dopamine activates and potentiates medium spiny neurons via the D1 receptor, allowing them to be stimulated by their cortical inputs and leading eventually to the activation of thalamic neurons that excite their cortical targets to promote and invigorate movement. In the indirect pathway, the GABAergic outputs of the GPi and SNr are tonically active and block cortical-projecting thalamic neurons to suppress movement. The activity of medium spiny neurons expressing the inhibitory D2 dopamine receptor is reduced by dopamine, relieving this blockade and allowing for the desired action to proceed. Dopamine is therefore thought to act as the critical regulator of action selection, permitting and driving the performance of a specific motor output while simultaneously preventing the expression of alternatives (Figure 1.1)[122,130–136].

The symptoms associated with dopaminergic pathologies are well-aligned with this model of dopaminergic control of basal ganglia output. Depletion of dopamine results in a suppression

of the direct pathway and continuous activation of the indirect pathway, producing the bradykinesia and akinesia that is pathognomonic of Parkinson's disease[73,99,122]. Excessive dopamine produces the inverse pattern of activity, leading to the dyskinesias and dystonias seen as a result of pharmacological or pathological increases in striatal dopamine levels[96,122,130].

Consistent with a motor control circuit, recordings from medium spiny neurons reveal that their activity is tightly linked to the kinematics of movement and the motor-action syllables that are concatenated to produce naturalistic behavior[137–142]. Additionally, activation of direct and indirect pathways has the predicted opposing effects on locomotion[132,133,143,144]. Although neurons in both the direct and indirect pathways have been reported to be similarly activated by movement[145], there appears to be subsecond decorrelations between the two pathways as animals initiate a new motor action that are consistent with a framework in which the two circuits work in opposition to shape moment-by-moment kinematics and the broader structure of naturalistic movement[146].

While the basal ganglia's role in modulating movement is well established[122], major questions persist regarding dopamine's functional role within this structure. Most strikingly, the vast majority of studies find no appreciable relationship between the activity of dopaminergic neurons and an animal's spontaneous movement[147–154]. The low levels of tonic dopaminergic neuron firing and the slowly (seconds to minutes) varying concentration of dopamine within the striatum that have been widely reported[155,156] are inconsistent with the rapid and dynamic control dopamine is believed to exert on the direct and indirect pathways of the basal ganglia to shape and

coordinate movement. Intriguingly, dopaminergic neurons appear to be strongly activated by rewarding sensory stimuli like an appetitive food or drink[152–154].

New neuronal recording technologies have provided novel insights into the activity of dopaminergic pathways and these data posit potential models of how dopamine may control movement. Before they can be fully appreciated, however, an understanding of the signals that dominate dopaminergic activity, namely those related to reward, is required.

1.6 Dopamine Signals Reward and Reinforcement to Instruct Learning

Although locomotor deficits are the most overt result of lesioning dopaminergic populations[125–128], the neuromodulator has been most extensively studied in the context of learning and the formation of associations. Early recordings from mammalian dopaminergic neurons demonstrated that they were responsive to unexpected rewards and stimuli predictive of reward, with little evidence of movement-related signaling[77,150–154,157–166]. The seminal observation that as animals learned to associate an initially neutral sensory stimulus with an appetitive reward, the dopaminergic response shifted from the reward itself to the now reward-predictive sensory cue led to a model in which dopaminergic neurons encode reward-prediction errors (RPEs) that indicate whether an animal's experience was better or worse than expected[77,153,154,166,167]. In this way, dopamine allows animals to continuously track the relationships among the myriad elements in their environment and develop causal links between different variables and their own experiences.

The ability of dopaminergic circuitry to communicate both expectations and outcomes and update its activity with experience has made it a powerful platform to understand how neural circuits achieve learning. Studies of dopaminergic signaling have provided insight into how an animal's experience is translated into altered patterns of neural activity and how this neural plasticity ultimately leads to the emergence of learned behaviors that can be either transient or long-lasting[22,168,169]. Furthermore, RPE fits well with the theoretical framework that has developed to explain how neural circuits flexibly and dynamically alter their activity during learning[170–175].

The discovery of diverse dopaminergic subpopulations, including those responsive to aversive stimuli[164,165,169,176–178], novelty[179–182], and those that are bidirectionally modulated by rewarding and punitive experiences[183], have expanded the understanding of dopamine beyond RPE to include a more general representation of value that is nonetheless believed to subserve learning. Studies in the zebra finch, for example, have identified dopamine as the "critic" in the actor-critic model of song learning, indicating to juvenile birds when they have succeeded and when they have erred in reproducing their mentor's song and allowing young males to develop their own unique song through trial and error[184–186]. The actor-critic model has been applied more broadly to describe how dopamine functions within circuits to instruct multiple types of learning, including sensory associations, procedural memory, and the development of refined motor skills[187–190]. In this way, dopamine acts as a general reinforcement signal that allows experience to bias an animal's future behavior towards desired outcomes.

In addition to producing motor deficits, perturbations of dopaminergic pathways also interfere with multiple types of learning. Dopaminergic signaling is necessary for the formation of

associations[101–104,191], the development of new motor programs[185,192], and sequence learning (connecting temporally linked patterns of cues and actions to achieve an outcome)[193–197]. Exogenous activation of dopaminergic pathways is capable of endowing neutral cues with a positive valence[100,107,147,198–202], cementing dopamine as a critical element of the circuitry underlying associative learning. Furthermore, signaling RPEs, or a more general representation of expectation or value that drives reinforcement, is consistent with dopamine's purported function in a number of the neural processes and pathophysiologies in which the neurotransmitter is implicated, including addiction, habit formation, and the psychiatric disorders of schizophrenia and depression[106–113,175].

Dopamine's vital role in associative learning is well established and conserved throughout the animal kingdom[150,154,157,203–205]. While patterns of dopaminergic neuron activity support its function in learning[77,154,166], they contrast with the neuromodulator's equally clear role in coordinating and regulating movement.

1.7 Reconciling Dopamine's Role in Reinforcement Learning and Movement

For decades researchers have strived to explain the dual role of dopamine in both learning and motor control. Conflicting findings have made it difficult for a consensus to emerge and there is still no clear and coherent understanding of how the relatively small number of dopaminergic neurons affects these apparently distinct neural processes. Extensive study, however, has provided

a number of models and frameworks that attempt to resolve dopamine's apparently multifaceted functionality.

Early electrophysiological recordings from individual dopaminergic neurons revealed that they had two distinct modes of activity. Dopaminergic neurons exhibited a baseline level of tonic activity, with relatively regular and periodic firing of action potentials. When presented with an unexpected reward or reward-predicting cue, however, these neurons exhibited sharp increases in activity, firing phasic bursts of action potentials at a high frequency[77,155,166,206]. This phasic spiking was believed to instruct learning and drive synaptic plasticity, while control of movement was ascribed to the ongoing and slowly varying tonic mode of activity[207–211]. In support of this model, the concentration of dopamine within the striatum correlates with certain features of movement, such as velocity, orientation, and posture, over a timescale of seconds to minutes[212]. Furthermore, broad and non-specific pharmacological increases in dopamine concentration improve the motor symptoms associated with the death of dopaminergic neurons and is still the mainstay of Parkinson's disease therapy[93,97]. Therefore, while the slowly varying, tonic levels of striatal dopamine set the overall tone of the basal ganglia to regulate the general level of arousal and movement, phasic bursts of dopamine at specific locations and times alter synapses to drive the plasticity that underlies learning.

Technological advancements have allowed for more extensive and precise recording from dopaminergic neurons that have challenged the tonic/phasic model. The discovery of rapid and phasic movement-related activity in dopaminergic neurons during spontaneous locomotion suggests that their influence on an animal's motor output is not solely limited to the slow and tonic

fluctuations. Instead of the same neurons controlling both learning and movement, recent evidence posits the existence of distinct dopaminergic subpopulations, some conveying information about reward or value and others relaying motor signals[213–217]. Dopamine neurons originating in the ventral tegmental area (VTA) and projecting to limbic structures in the ventral striatum (the mesolimbic pathway) appear to be primarily reward responsive, while the activity of dopamine neurons in the SNc that project to the dorsal striatum (the nigrostriatal pathway) is mainly reflective of an animal's movements. Accordingly, exogenous stimulation of movement-correlated dopaminergic neurons can trigger, promote, and invigorate locomotion[213,214]. This understanding of dopaminergic circuitry is further supported by the clinical observations: the death of SNc dopamine neurons is associated with motor deficits and altered activity in the mesolimbic pathway is thought to underlie dopamine-related psychiatric disorders[73,98,99,106,111,113]. Thus the diverse roles of dopamine may arise from anatomically segregated and functionally specialized circuits such that distinct subsets of dopaminergic neurons encode reinforcement and motor signals.

While dopamine's role in learning and movement have generally been considered and addressed separately, emerging evidence argues that they may not be completely independent variables. Reward prediction signals in dopaminergic neurons appear to be gated by locomotion initiation[218] and learning has been shown to strengthen and alter, not create, pre-existing representations of motor actions in dopaminergic neurons[199]. In addition, dopaminergic activity appears to ramp up as animals walk to approach distant rewards[148]. The functional parallels associated with the mesolimbic and nigrostriatal pathways are further undermined by reports of movement-related activity in supposedly learning and reward oriented VTA dopaminergic neurons

and RPEs in SNc dopaminergic neurons that are thought to control an animal's motor output[199,216,219,220].

Efforts to explain these observations have posited that dopamine neurons are relaying information regarding the motivation of an animal[156,179,221–223]. The concept of motivation links reward and movement together: a motivational cue could invigorate a motor action while also signaling a change in an animal's internal state following a sensory stimulus that is predictive of reward, thereby also instructing learning. The correlation of dopaminergic activity with an animal's engagement in a learned task[147,223,224] further supports this interpretation of the dopamine signal. It is unclear, however, if dopamine's representation of motivation is a true synthesis of reward- and motor-related signaling or an additional and separate function of an already complex dopaminergic network[147,156,179,198,204,225,226].

There are still major outstanding questions regarding the nature of dopaminergic circuitry. Recordings reveal that individual midbrain dopaminergic neurons exhibit multiplexed representations in which the kinematics of movement and task-related variables are encoded by the very same neurons that respond to rewards[220]. The meaning and function of these multiplexed signals are a subject of ongoing debate and speculation. Additional evidence suggests that these dopaminergic correlates of movement reflect an expectation of reward from a motor action utilized in a learned task, indicating that they may subserve learning rather than shape concurrent behavior[199]. In contrast, attempts to model movement-related signaling in midbrain dopaminergic neurons as motor-specific RPEs have been unsuccessful[227]. Therefore, the utility, the features of an animal's experience that are being represented and the functional effects of that neural activity

on downstream pathways and ultimately behavior, of motor-related activity in reward-signaling dopaminergic neurons remains poorly understood.

Answering these questions and reconciling the disparate roles of dopamine has proven challenging in part due to the complexity and technical inaccessibility of mammalian midbrain dopaminergic networks, which are anatomically and functionally heterogeneous and intricately innervate diverse target neuropils[228–230]. Moreover, dopaminergic activity has mainly been investigated in highly trained animals performing established tasks, where it is not necessarily possible to dissociate an animal's movements, motivations, expectations of reward, and sensory associations, as all these variables become inherently intertwined as a result of learning[147,148,160,198,218,227]. As a consequence it has been difficult to directly connect the heterogeneous and multiplexed activity of dopaminergic neurons with their role in both learning and motor control.

To circumvent these obstacles and address basic questions about what features of an animal's experience are encoded in the activity of a dopaminergic neuromodulatory network and how its ongoing activity impacts concurrent behavior, we turned to the simpler model animal, *Drosophila melanogaster*.

1.8 Using *Drosophila melanogaster* to Study Dopaminergic Neuromodulatory Pathways

The use of a reduced and experimentally tractable model system can provide critical insight into the fundamental underpinnings of complicated biological processes that generalize across the animal kingdom. For over a century, beginning with the seminal work of Thomas Hunt Morgan, the fruit fly *Drosophila melanogaster* has been critical to the study of many different fields of biology, including genetics, development, immunology, and neuroscience[231–233]. Despite the several hundred million years of evolutionary divergence separating insects and mammals, discoveries in the fly have provided a deep and invaluable understanding of our own physiology and have revealed that many essential mechanisms and pathways are conserved across the two species[231–234]. Although the *Drosophila* brain lacks the structures analogous to those found in vertebrates, it has been the source of key neurobiological insights into basic molecular and circuit mechanisms and has proven to be a powerful platform to study neurophysiology[234].

Decades of research on *Drosophila* provides us with a broad knowledge of its biology and a powerful set of tools that allow for a detailed study of neural circuits. The Gal4/UAS system developed for the fruit fly, coupled with a wide array of promoter lines, offer select genetic access to neural populations of interest[235–238]. In addition, optogenetic and thermogenetic tools enable the rapid and reversible modulation of neural activity to interrogate how individual neurons and larger populations affect behavior as well as adjacent circuits[238–240].

The fly is especially well suited to the study of neuromodulation as its large behavioral repertoire is a testament to the power of neural circuit flexibility. Despite possessing only ~100,000 neurons, the fly demonstrates a range of diverse and varied behaviors made possible by neuromodulators. The neurons in the fly's visual system are rapidly tuned to optimize their activity for either flight or walking[241]. They engage in persistent odor tracking[242–244] and perform elaborate courtship and mating rituals[38,245–247] that can be modified by their satiety state and need to seek out sources of food[26,28,30–32,57,58,248–250]. Flies can even form positive and negative associations that may be transient or long-lasting depending on the nature of the formative experience[251–253]. The neuromodulatory pathways of the fly's brain thus act from the periphery to higher order integrative centers to sculpt and shape the behavior of the animal across multiple timescales, from moment-by-moment processing of sensory information and control of locomotion, to prolonged behavioral and internal states, to permanent changes in circuit output.

To interrogate neuromodulatory pathways we specifically focused on the mushroom body, a prominent neuropil in the brain of the fruit fly richly innervated by dopaminergic neurons that plays an essential role in the formation and expression of olfactory associations[254,253,255,256]. Although primarily studied in the context of learning, the mushroom body and its associated dopaminergic populations affect multiple different flexible and adaptive behaviors[248–250,257–281]. The relationship between the ongoing activity in the mushroom body dopaminergic neurons and the neuropil's diverse functions remains poorly understood. The simple and organized architecture of the mushroom body, however, facilitates a detailed investigation of neural circuit function and allows us to address basic questions regarding what variables are reflected in the ongoing activity of a neuromodulatory circuit and its role in shaping an animal's behavior[238–240].

1.9 The Mushroom Body of *Drosophila melanogaster*

The mushroom body (MB), a conserved and well-defined insect brain structure (Figure 1.2A), was first described in the mid 19th century by French biologist Félix Dujardin[282]. Although it was initially loftily presented as the source of free will and intelligence[283], it was not until over a century later in the 1980s and early 1990s that it was demonstrated to be an associative learning center, endowing insects with the ability to form memories[284,285]. The capacity of insects to form associations, especially that of the fruit fly, *Drosophila melanogaster*, which will avoid or approach an initially neutral odor after it has been paired with an aversive or appetitive outcome[252], has provided a powerful model system to study the molecular pathways and the functional circuit architectures that underlie neural plasticity and learning[234]. The MB has been most comprehensively studied in *Drosophila*, where chemical ablation or exogenous perturbation of its activity severely impairs the ability of the fly to learn[254,284–287]. Furthermore, mutant studies have localized the activity of genes vital for proper memory formation to the MB[288–297]. Thirty years of extensive research has established the MB as the primary neural circuit for olfactory associative learning in *Drosophila*[298–301].

The MB is formed by approximately 2,000 third-order, odor-responsive intrinsic neurons termed Kenyon cells (KCs)[256,302]. In the calyx of the MB, the KCs receive olfactory input from Projection neurons (PNs) emanating from the antennal lobe[256,303,304]. The PNs are divided into approximately fifty subgroups, each with dendrites in a different antennal lobe glomerulus that receives input from all the olfactory sensory neurons expressing the same odorant receptor[305–309]. Each KC extends a small number of dendritic claws (~3 to ~10) into the calyx to stochastically

Figure 1.2 | Compartmentalized Anatomic Organization of the *Drosophila* Mushroom Body. (A) MB neuropil within the *Drosophila* brain with KCs labeled in blue (left). In the output lobes of the MB, KCs form *en passant* synapses with MBONs that innervate discrete regions or compartments within the lobes. Each of these compartments is co-innervated by the axons of DANs. Right: Composite image showing compartmentalized innervation of the γ5 compartment by DANs (magenta), MBONs (green), and a single KC axon highlighted with photoactivatable GFP (cyan). **(B-C)** Schematized structure of the MB highlighting the inputs and outputs of the γ lobe. **(B)** Compartmentalized organization of the γ2-γ5 MBONs. Activation of the γ2/γ3 MBONs induces approach behaviors while activation of γ4/γ5 biases animals towards avoidance. **(C)** Compartmentalized organization of γ2-γ5 DANs. Lateral γ2/γ3 DANs respond to painful electric shock and underlie the formation of negative olfactory associations. Medial γ4/γ5 DANs respond to appetitive sugar reward and underlie the formation of positive olfactory associations.

Figure 1.2

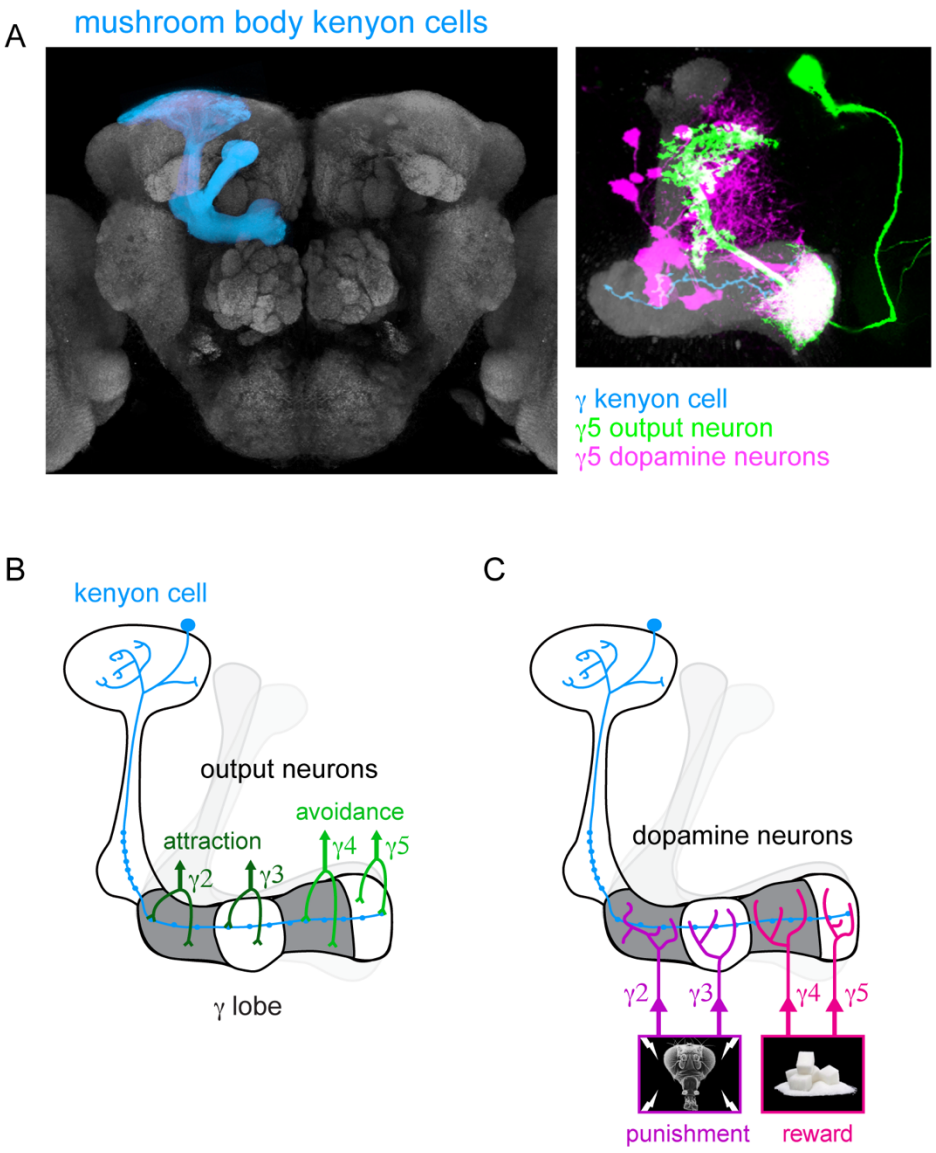
A
mushroom body kenyon cells
γ kenyon cell
γ5 output neuron
γ5 dopamine neurons
B
kenyon cell
output neurons
avoidance
attraction
γ4
γ5
γ2
γ3
γ lobe
C
dopamine neurons
γ2
γ3
γ4
γ5
punishment
reward

receive synaptic input from a fraction of the roughly fifty PN channels (Figures 1.2B,C)[310–317]. The random and combinatorial wiring between PNs and KCs allows odor information to be represented in a vast neural state space that is capable of capturing the complexity of the chemical world. The sparse activity of unique KC ensembles encodes odor identity[315–317] and is especially well-suited to a circuit whose function is to assign value to diverse and potentially arbitrary sensory stimuli based on experience[317–320].

From the calyx, each KC sends a single axon into the pedunculus of the MB. At the terminus of the pedunculus, the fasciculated KC axons project into the five output lobes of the MB: the dorsally (vertically) oriented α and α' lobes and the medially (horizontally) oriented β, β', and γ lobes. A portion of the KCs bifurcate at the end of the pedunculus to send branches into either the α and β lobes or the α' and β' lobes while the remaining KCs extend a single axon into the γ lobe (Figure 1.2)[256,302]. These anatomic distinctions have been elaborated upon to divide the KCs into three broad categories, αβ, α'β', and γ KCs, that each possess distinctive electrophysiological properties[321], developmental timelines[322–324], and are thought to play separate roles in the different forms of memory displayed by *Drosophila* (short-term vs. long-term vs. anesthesia-resistant vs. anesthesia-sensitive)[251,325–338].

Within the output lobes the KC axons form *en passant* synapses with the efferent neurons of the MB: the mushroom body output neurons (MBONs). The dendrites of each MBON innervates a spatially segregated and restricted area of the lobes such that they tile across the lobes creating 15 non-overlapping compartments innervated by one to three individual efferent neurons (Figure 1.2B)[256,302,339]. MBONs are necessary for the expression of olfactory memories[340–344] and

the activity of individual MBONs can bias an animal towards avoidance or approach behaviors[339]. There are only 34 MBONs resulting in a massive reduction in coding space as information is transferred from KCs to MBONs. This anatomy posits that within the lobes of the MB, a representation of odor identity in KCs is transformed into a representation of general value or valence by the MBONs[256,339,345] such that patterns of MBON activity can drive animals to avoid and approach an olfactory stimulus[339].

In addition to the dendrites of MBONs, each discrete compartment of the lobes is also innervated by the axons of a small population of dopaminergic neurons (DANs) that signal reward and punishment (Figures 1.2A,B)[205,256,302,346–349]. This compartmentalized anatomic organization immediately suggests a model for how dopaminergic reinforcement drives associative learning[256]. The MB DANs are activated by appetitive and punitive stimuli such as a sugar reward or an aversive electric shock and these reinforcement cues drive distinct patterns of activity across the MB DANs (Figure 1.2B)[205,348–351]. DAN activity is necessary during training for animals to form associations. Exogenous activation of subsets of DANs are sufficient to instruct learning and endow odors with valence and meaning to shape future olfactory behavior[352–357]. Dopamine release within a compartment tunes the strength of synaptic connections between the KCs and the MBONs, allowing the same odor cue to drive either approach or avoidance behavior depending on an animal's past experience[345,351]. Like their mammalian counterparts, MB DANs thus appear to signal reward and punishment to drive reinforcement and instruct learning.

Despite the MBs established and well-characterized role in olfactory associative learning, earlier and more recent studies alike suggest that the neuropil plays a more extensive role in

shaping the fly's behavior. Beyond olfactory memory, the MB is implicated in innate odor preference[248,249,358,359], visual learning[360], sleep and circadian rhythm[257–263], temperature preference[264,265], oviposition choice[266], courtship behavior[267,268], decision-making[250,269,270], attention[271], maintenance of flight bouts[272], discrimination and reaction to novelty[361], and signaling satiety and hunger to control food foraging behavior[273–276]. Many of the MB's purported functions are related to the movements of the animal and, intriguingly, the structure has also been suggested to control and modulate the fly's locomotion itself[277–281].

All of these non-learning functions of the MB involve the DANs, suggesting that their activity does more than simply drive plasticity in KC-MBON synapses to alter future olfactory behavior and may be rapidly modulating the output of the MB to influence an animal's immediate actions. Understanding the ongoing activity of the MB DANs, then, is key to unraveling the neuropil's diverse roles in shaping adaptive behavior. Interestingly, recent studies have uncovered correlations between the gross motor actions of an animal and the activity of DANs innervating the γ lobe of the MB, a population that responds to rewarding and punishing cues and plays an essential role in the formation of olfactory associations[351,362].

The ongoing, motor-correlated activity in these DANs is not well described and its function is unclear. Like many neuromodulatory systems, then, the MB DANs appear play important roles in diverse neural processes and the connection between their ongoing activity and an animal's behavior is poorly understood. The simple, organized, and stereotyped anatomy of the MB allows us to examine the same neurons across different contexts. The MB, therefore, offers an opportunity to explore what is encoded in the ongoing activity of a neuromodulatory circuit. Specifically, we

will examine movement-related signals in a dopaminergic population with a clearly defined role in reinforcement learning, investigate what is represented in these multiplexed patterns of activity, and determine how they affect concurrent behavior.

1.10 Investigating Ongoing Activity in Mushroom Body Dopaminergic Neurons

In my thesis work I took advantage of the concise circuit architecture of the MB to gain insight into the heterogeneous and varied activity of a neuromodulatory pathway, specifically the dual nature of reward and movement-related signals observed within a dopaminergic pathways.

In Chapter 2 I describe which features of an animal's experience are encoded in the ongoing activity of DANs innervating the γ lobe of the MB. I demonstrate that the different subpopulations of the MB DANs have distinct behavioral and sensory correlates, some oriented to reflecting reward and others that contain multiplexed representations of both reinforcing sensory cues and specific aspects of the fly's movements. These representations of movement are not stereotyped, suggesting they do not encode the specific kinematics of movement but rather some other higher order cognitive variable nonetheless intimately related to the fly's motor actions.

In Chapter 3 I explore the nature of the movement-related signals in the DANs. I describe the development of a closed loop olfactory paradigm that allows us to record from DANs while flies perform goal-directed and sensory-triggered behaviors. I observe that in the context of an

olfactory stimulus, the DANs correlate with neither the odor stimulus alone, nor the physical kinematics of movement, but rather the strength and robustness of the behavioral response to the odor.

In Chapter 4 I further probe our conclusions from Chapter 3, examining how changing an animal's internal drive to track an appetitive food odor alters both behavior and neuronal responses to olfactory stimuli.

In Chapter 5 I investigate how the ongoing DAN activity alters the fly's concurrent behavior. With the use of optogenetic reagents I demonstrate that the representations of behavioral responses to odor within MB DANs play an active role in shaping real-time behavior.

In Chapter 6 I provide a discussion of my results. I explore the implications of my findings on our understanding of the MB and dopaminergic networks more broadly. I also suggest future studies and describe ongoing experiments in the lab that attempt to understand how movement-related activity in MB DANs affects KCs and MBONs to control and coordinate the net output of the MB.

Chapter 2

Representations of Reward and Movement by Mushroom Body Dopaminergic Neurons

2.1 Introduction

The neuromodulator dopamine determines future behavior by directing learning but is also critical for the proper coordination of locomotion[73,99–101]. Dopaminergic representations of rewarding or punishing stimuli are believed to signal reinforcement to drive the synaptic plasticity that underlies learning[100,166,200], but the function of movement-related activity is less well understood[209,223,224]. The basic logic of dopaminergic pathways, therefore, remains unclear. The same midbrain dopaminergic neurons that underlie learning have also been argued to control movement by setting the overall tone of motor circuits. Their activity is therefore thought to reflect

an animal's general level of arousal[212] or other internal state variables such as motivation or expectation[156,179,209,225]. Accordingly, dopaminergic activity correlates with an animal's engagement in a learned task and ramps as animals approach distant rewards[147,148]. Alternatively, distinct dopaminergic neurons may encode the fine-scale kinematics of physical locomotion[213–217], consistent with a role for dopaminergic pathways in action selection. Under this model, anatomically separate dopaminergic populations are thought to rapidly initiate changes in movement, reconfiguring the activity of circuits to promote and invigorate a given motor program[130–136].

Recent recordings reveal that individual midbrain dopaminergic neurons exhibit multiplexed representations, with rapid and phasic fluctuations in their activity that correlate with the kinematics of motion while also responding to rewards[220]. These observations fit neither a tonic/phasic model, which confines phasic bursts of dopaminergic activity to the signaling of reward, nor a model of dopaminergic circuitry consisting of separate learning and motor channels. The size, diversity, and complexity of mammalian dopaminergic systems make it challenging to gain an understanding for the relationship between the various sensory and motor correlates that have been observed in these pathways.

To explore the logic of dopaminergic pathways we focused on the MB of the fruit fly, *Drosophila melanogaster*. With only ~120 dopamine neurons (DANs) and a mere 34 output neurons (MBONs), this neuropil represents a significantly simplified system in which to explore the functional operation of a dopaminergic circuit[256]. MB DANs are responsive to reward and punishment and are essential for the formation of olfactory associations[205,348,351–357]. The ongoing

activity of certain subsets of these DANs has also been correlated with the coarse motor actions of the fly[351,362]. The simple and organized architecture of the MB therefore offers the opportunity for a detailed investigation of how movement is reflected in the activity of a dopaminergic circuit with an established role in learning[238–240].

Although the MB is innervated by ~15 subsets of DANs, we focus here on the DANs that extend axons into the medial portion of the γ lobe of the MB: the γ2, γ3, γ4, and γ5 DAN subpopulations (Figure 2.1). These neurons bidirectionally respond to rewarding and punishing sensory stimuli such as sweet and nutritive sugars and punitive electric shock. These responses to reinforcing sensory stimuli regulate the formation of short-term associations [332,352,354–356,363,364]. Yet, these same DANs also exhibit correlations with an animal's coarse motor activity[351,362]. This movement-related signaling was initially described in the context of tethered flies suspended in mid-air that alternate between periods of quiescence and periods of chaotic movement where they flail their limbs in an uncoordinated manner. In this preparation, γ2 and γ3 DAN activity increases during bouts of flailing, while the activity in γ4 and γ5 DANs is diminished. The reciprocal pattern appears during periods of quiescence (Figure 2.1)[351]. γ2 DAN activity likewise was specifically elevated during periods of tethered locomotion on a spherical treadmill[362]. It is of note that according to these observations, each DAN subpopulation relates the same information concerning the behavior of the fly: any single γ lobe compartment equally (but potentially inversely) represents whether an animal is still or in motion.

These bidirectional patterns of DAN activity mirror those observed in response to reward and punishment: γ4 and γ5 DANs are activated by appetitive stimuli like sugar in accord with

Figure 2.1 | Mushroom Body Dopaminergic Neuron Activity Reflects Both Salient External Sensory Stimuli and Internal Behavioral State. Schematic of MB DAN activity during punitive electric shock and flailing (left), which are both accompanied by increased activity in γ2/γ3 DANs (thick lines) and decreased activity in γ4/γ5 DANs (thin lines) and during appetitive sugar reward and quiescence (right), which are accompanied by the reciprocal pattern of DAN activity.

Figure 2.1

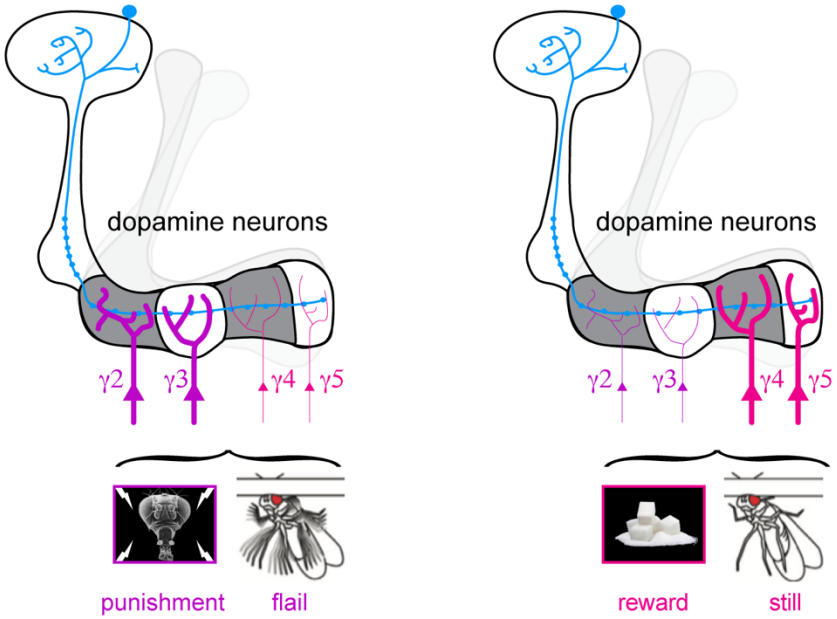
dopamine neurons
γ2
γ3
γ4
γ5
punishment
flail
dopamine neurons
γ2
γ3
γ4
γ5
reward
still

evidence that these pathways can drive the formation of positive associations. Conversely, γ2 and γ3 DANs are activated by punitive experiences, such as a painful electric shock, and their exogenous activation during the presentation of a neutral odor induces subsequent avoidance (i.e. a negative association) (Figure 2.1)[205,348,352–357]. Dopaminergic signaling of reward and punishment appears to be coordinated, with increases in γ4 and γ5 activity being accompanied by decreases in γ2 and γ3 activity and vice versa. Therefore, just as any single γ lobe compartment can represent motion or stillness, each can also equally (but potentially inversely) reflect the presence of a positive or negative reinforcing stimulus.

The striking correspondence between the bidirectional patterns of DAN activity associated with flailing and punitive electric shock suggest that behavioral context may itself serve as a reinforcement to subserve learning. The DANs therefore may be broadly categorizing any particular moment as either appetitive or aversive and rather than influencing the concurrent actions of an animal, this activity allows an animal's behavioral and internal state to influence future odor processing[351,362].

The ongoing DAN activity, however, could also contribute to the MB's role in flexibly shaping the fly's real-time behavior[248,249,257–265,268,270,272–275]. Motor-related activity in a population of dopaminergic neurons that signal reinforcement and facilitate learning offers an intriguing parallel to mammalian dopaminergic pathways that also instruct learning and regulate movement. The ongoing DAN activity may therefore be facilitating movement and playing an active role in shaping concurrent behavior. Understanding how movement is encoded in the activity of the simplified dopaminergic pathways of the MB will provide insight into what features of an animal's

experience they represent and how their ongoing activity influences the fly's real-time locomotion. However, it remains unclear how tonic DAN activity corresponds to an animal's actions in a more ethologically relevant and naturalistic behavioral context as an animal navigates through its environment.

To gain a detailed description of how the activity of the γ DANs relates to the moment-by-moment changes in behavior associated with the fly's natural motor output, we therefore adapted an experimental paradigm to record from DANs during naturalistic and spontaneous locomotion.

2.2 Monitoring Mushroom Body Dopaminergic Neuron Activity During Reward and Spontaneous Locomotion

To explore how dopaminergic pathways in the *Drosophila* MB coordinately represent reward- and movement-related variables, we monitored their activity in head-fixed animals walking on a spherical treadmill. We adapted an experimental paradigm in which tethered flies were able to walk naturalistically on an air supported foam ball[365–369]. By recording the rotation of the ball, we quantified multiple aspects of the fly's locomotion, including an animal's fictive position on a 2D plane, forward velocity, and change in heading over time (Δheading/Δt or turning velocity)[370]. To simultaneously record the activity of the DANs, we expressed a synaptically localized variant of the genetically encoded calcium indicator GCaMP (sytGCaMP6s) using the tyrosine hydroxylase (TH) and dopa-decarboxylase (DDC) promoters[351,371], allowing us to visualize calcium influx in DAN axon terminals innervating the different compartments that tile

across the MB output lobes. In addition, flies were presented with microliter volumes of a 1M sucrose solution[351,372], allowing us to compare the DAN activity evoked by reward and locomotion within the same trials (Figure 2.2A).

As described above, we focused on the subset of DANs innervating the γ lobe (γ2-γ5). In addition to their role in olfactory learning and the correlation of their activity with the gross motor output of an animal[332,351,352,354–356,362–364], the γ lobe can also be synchronously imaged within a single optical plane, allowing for high temporal resolution of DAN activity compatible with the rapid speed of a fly's movement during naturalistic locomotion (Figure 2.2A).

As previously documented, ingestion of a sucrose reward evoked bidirectional changes across the γ lobe DANs[351], robustly activating DANs innervating the γ4 and γ5 compartments while suppressing activity in the γ2 and γ3 DANs. Interestingly, complex patterns of dopaminergic neural activity emerged during spontaneous movement that deviated from the simple pattern of bidirectional signaling across compartments observed as animals alternate between flailing and quiescence. Prominent fluctuations in DAN activity were observed prior to and after sugar consumption that appeared to be temporally aligned to an animal's locomotion (Figure 2.2B).

Representations of reward and locomotion may be conveyed by the same DAN neurons or distinct subsets of reward- and movement-responsive neurons innervating each compartment. To address this question, we simultaneously imaged the soma of γ4 DANs expressing soluble GCaMP6s and confirmed that their activity was highly correlated due to shared fluctuations in all neurons as an animal spontaneously walked (Figure 2.3A). We further probed the possibility

Figure 2.2 | Mushroom Body Dopaminergic Neurons Coordinately Represent Reward and Movement-Related Variables. (A) Schematic of the experimental system for simultaneous recording of locomotion and MB DAN>sytGCAMP6s activity (left). The parameters of locomotion monitored during experiments are displayed as they are quantified by FicTrac software or subsequently calculated. Illustration of the anatomy of the mushroom body within the *Drosophila* brain (bottom right). Expression of sytGCaMP6s in DANs innervating the MB γ lobe (top right). **(B)** Overlay of four individual flies' net motion and compartmentalized DAN>sytGCaMP6s activity during spontaneous locomotion and during ingestion of 1 M sucrose solution (as indicated by maroon line beneath each trace). **(C)** Ratio of the magnitude of sugar-related activity to movement-related activity in the γ DANs. One-way ANOVA, $p=1.7311\times10^{-15}$. **(D)** Change in magnitude of movement-associated MB DAN activity after ingestion of 1M sucrose solution. One-way ANOVA, p=0.0052.

Figure 2.2

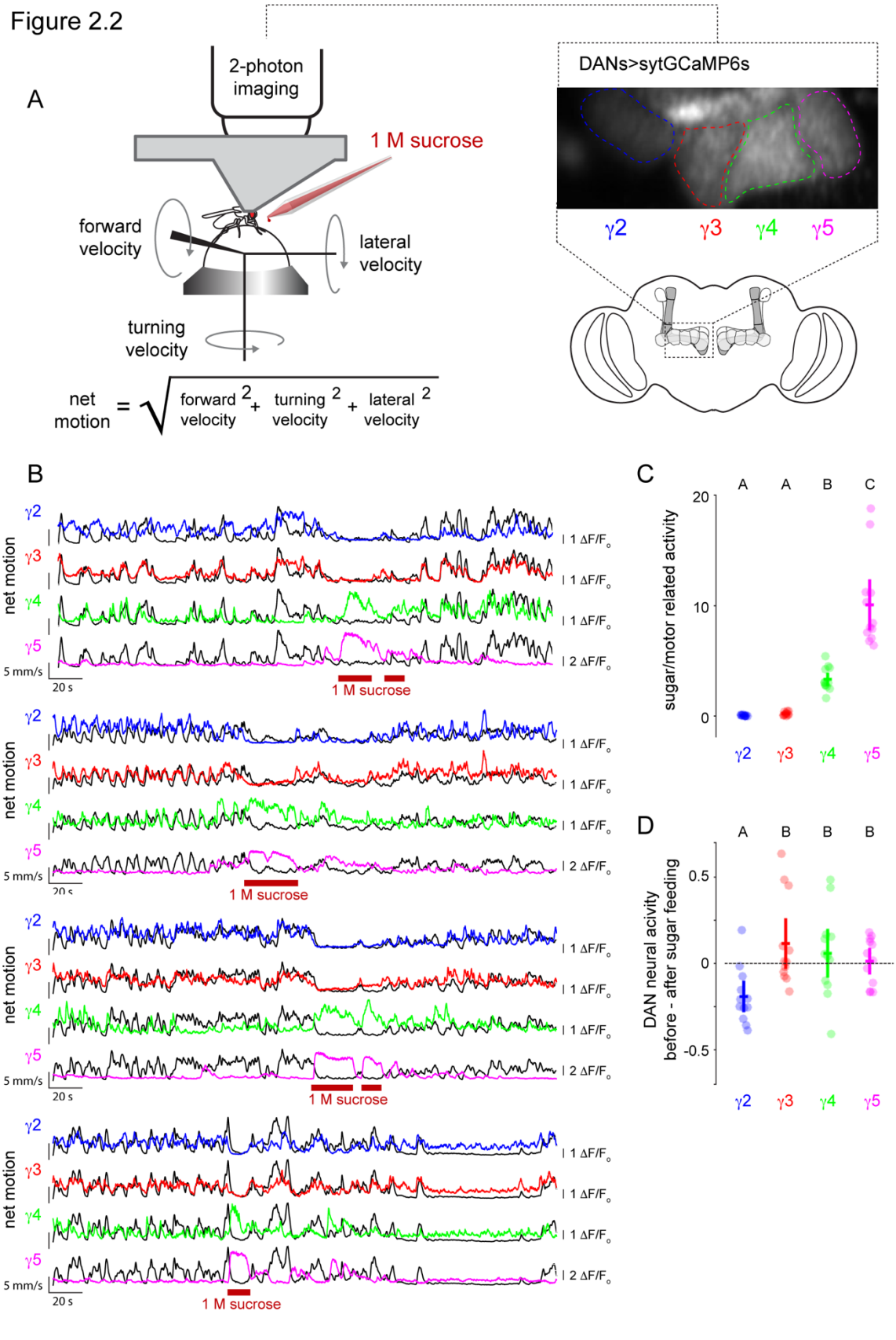
A
2-photon imaging
1 M sucrose
forward velocity
lateral velocity
turning velocity
net motion = √(forward velocity² + turning velocity² + lateral velocity²)
DANs>sytGCaMP6s
γ2 γ3 γ4 γ5
B
net motion
γ2
γ3
γ4
γ5
1 ΔF/F
2 ΔF/F
5 mm/s
20 s
1 M sucrose
C
sugar/motor related activity
A A B C
20
10
0
D
DAN neural acivity before - after sugar feeding
A B B B
0.5
0
-0.5

that distinct subsets of DANs innervating the same compartment had heterogeneous activity patterns during spontaneous locomotion using K-means clustering of DAN activity in the lobes. This analysis, however, revealed that the pixels comprising a compartment were highly correlated, independent of whether a compartment was innervated by a single (γ2) neuron or multiple (γ3, γ4, and γ5) DANs (Figure 2.3B). DANs targeting a single compartment thus appear to function as a unit implying that the same dopaminergic pathways that convey reinforcements to instruct associative learning also carry robust behavioral signals.

The relative magnitude of reward and motor-associated signals differed across the DANs innervating different compartments. While γ4 DANs were similarly activated by both sugar ingestion and locomotion, γ2 and γ3 DANs were activated only during walking bouts. Sugar-evoked responses in the γ5 DANs were significantly larger than baseline motor-associated fluctuations, indicating that any movement-related activity in this population occupied the lower end of these DANs' dynamic range (Figures 2.2B,C). We did not observe any overt qualitative changes in how DAN activity related to movement after flies were fed the sugar compared with before (Figure 2.2B), and while the magnitude of the movement-related signals increased slightly in γ2, there were no large quantitative changes in the period immediately after feeding (Figure 2.2D).

Figure 2.3 | Dopaminergic Neurons Targeting a Single Compartment Function as a Unit. **(A)** Activity of individual DANs innervating the γ4 compartment are positively correlated. γ4 DAN (MB312B) > soluble GCaMP6s activity during spontaneous tethered locomotion in four representative individuals. Forward velocity (top row), somatic GCaMP6s activity (middle row), and cross-correlation (Pearson correlation coefficient) between GCaMP6s signal in γ4 soma. **(B)** Expression of sytGCaMP6s in DANs innervating the MB γ lobe in five representative flies. Pixels in the γ lobe are color coded by K-means clustering analysis that distributed them into correlated subgroups that align with the compartmentalized architecture of the MB. Only periods of spontaneous locomotion when animals received no overt sensory stimulation were used to calculate K-means clusters.

Figure 2.3

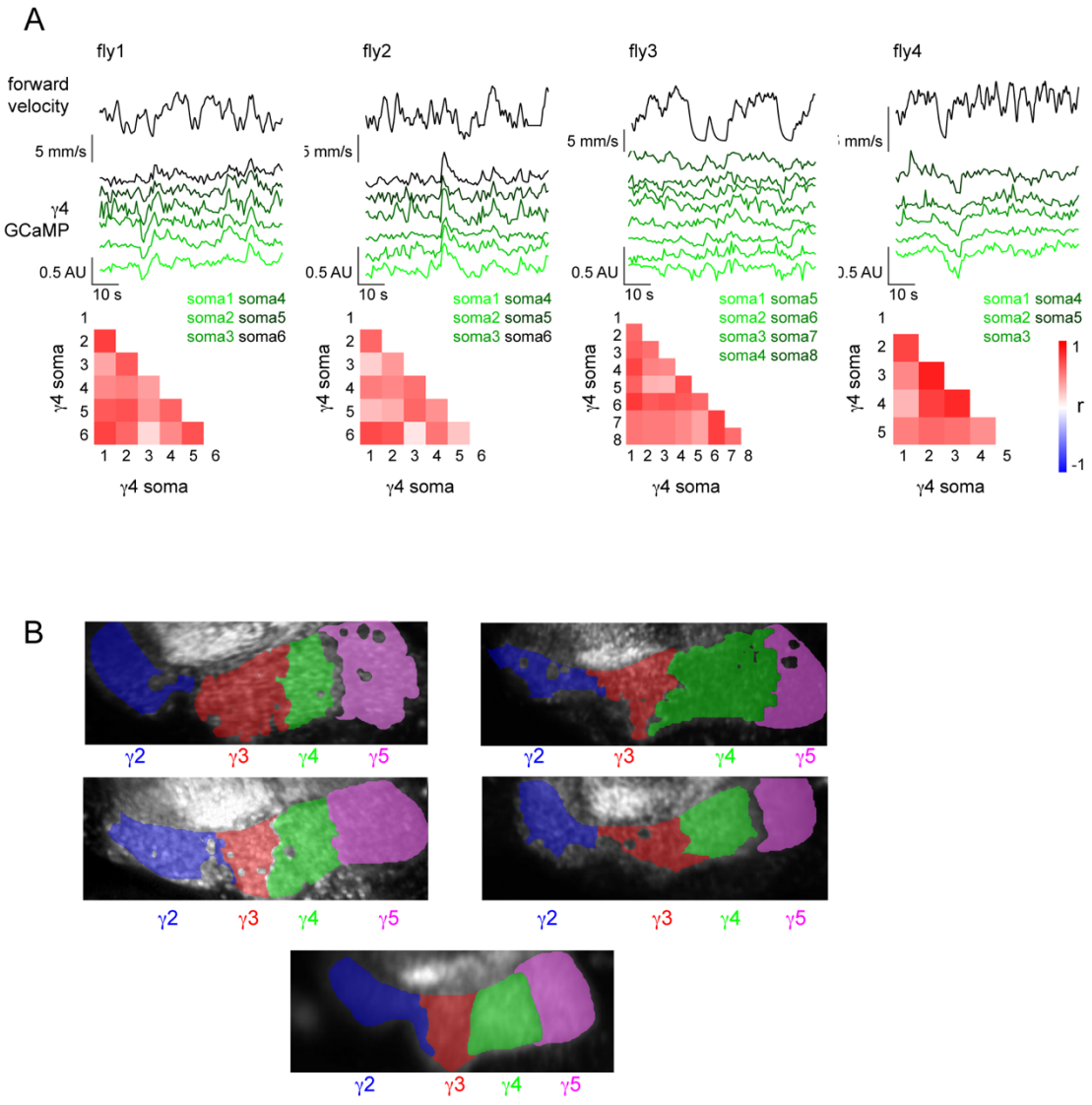
A
fly1
fly2
fly3
fly4
forward velocity
5 mm/s
γ4 GCaMP
0.5 AU
10 s
soma1 soma4
soma2 soma5
soma3 soma6
soma1 soma5
soma2 soma6
soma3 soma7
soma4 soma8
γ4 soma
r
1
-1
B
γ2
γ3
γ4
γ5

2.3 Mushroom Body Dopaminergic Neurons Innervating Different Compartments Reflect Distinct Facets of Motor Activity

While information about ongoing locomotor behavior could be uniformly broadcast across the brain[373], we observed that the DANs innervating different compartments correlated with distinct parameters of locomotion that unfolded over different timescales.

Tethered animals walking in the dark, in the absence of any overt sensory stimuli, alternated between spontaneous bouts of locomotion and quiescence (Figure 2.4A). γ3 DAN activity faithfully tracked the onset and offset of each bout of locomotion, such that whether an animal was walking or not (locomotor state) could be predicted from a logistic regression model with 87% confidence using the activity of this compartment alone (Figure 2.4B). γ3 activity remained low even during periods even when animal's stopped walking to groom, indicating that these DANs were specifically linked to locomotion and not limb movement generally (data not shown). In contrast to the consistency observed in γ3 DANs, the relationship between an animal's locomotor state and γ2, γ4, and γ5 DANs was far more variable. These other DANs did contain some predictive power regarding walking state, but given the strength and accuracy of γ3-generated model, including them as additional predictors along with γ3 only marginally improved the model's accuracy (Figure 2.4B).

The suggestion that dopamine may play a role in action selection and movement initiation[213,216,374–377] prompted us to focus on changes in DAN activity as animals initiated a bout of continuous movement after a pause in walking. We found that γ3 was consistently positively

Figure 2.4 | Dopaminergic Neuron Activity Reflects Locomotor State and is Modulated by the Onset of Movement. (A) Overlay of three representative animals' net motion and compartmentalized DAN>sytGCaMP6s activity during spontaneous locomotion. **(B)** Probability of accuracy of a logistic regression model predicting locomotor state (walking or not walking) based on DAN activity. N=27 animals. One-way ANOVA, $p=1.082\times10^{-12}$. **(C)** γ DAN activity during the initiation of movement. Top: average net motion ± 95% confidence interval as animals initiate sustained locomotion (≥3sec) following a pause (≥2sec). Bottom: heat map of $\Delta F/F_o$ in γ DAN subpopulations aligned to initiation of movement. Rows represent individual movement initiations ordered by average $\Delta F/F_o$ during the onset of locomotion (1sec to 2.5 sec after the start of movement) in the γ2 compartment (left) or γ4 compartment (right). F_o= average sytGCAMP6s activity from t=-2 to t=-0.5 seconds before the start of movement. White dashed lines indicates highest (above top line) and lowest (below bottom line) 20% average $\Delta F/F_o$ during the onset of locomotion. N=53 animals, 1060 movement initiations. **(D)** Pearson correlation coefficient between the increase in net motion and change in DAN>sytGCaMP6s activity during initiations of sustained movement (≥3s ec) following a pause (≥2 sec). Each row represents all the movement initiations performed by as single individual. Ordered by average motion-γ4 correlation for all starts within an individual animal. N=39 animals, 1043 movement initiations.

Figure 2.4

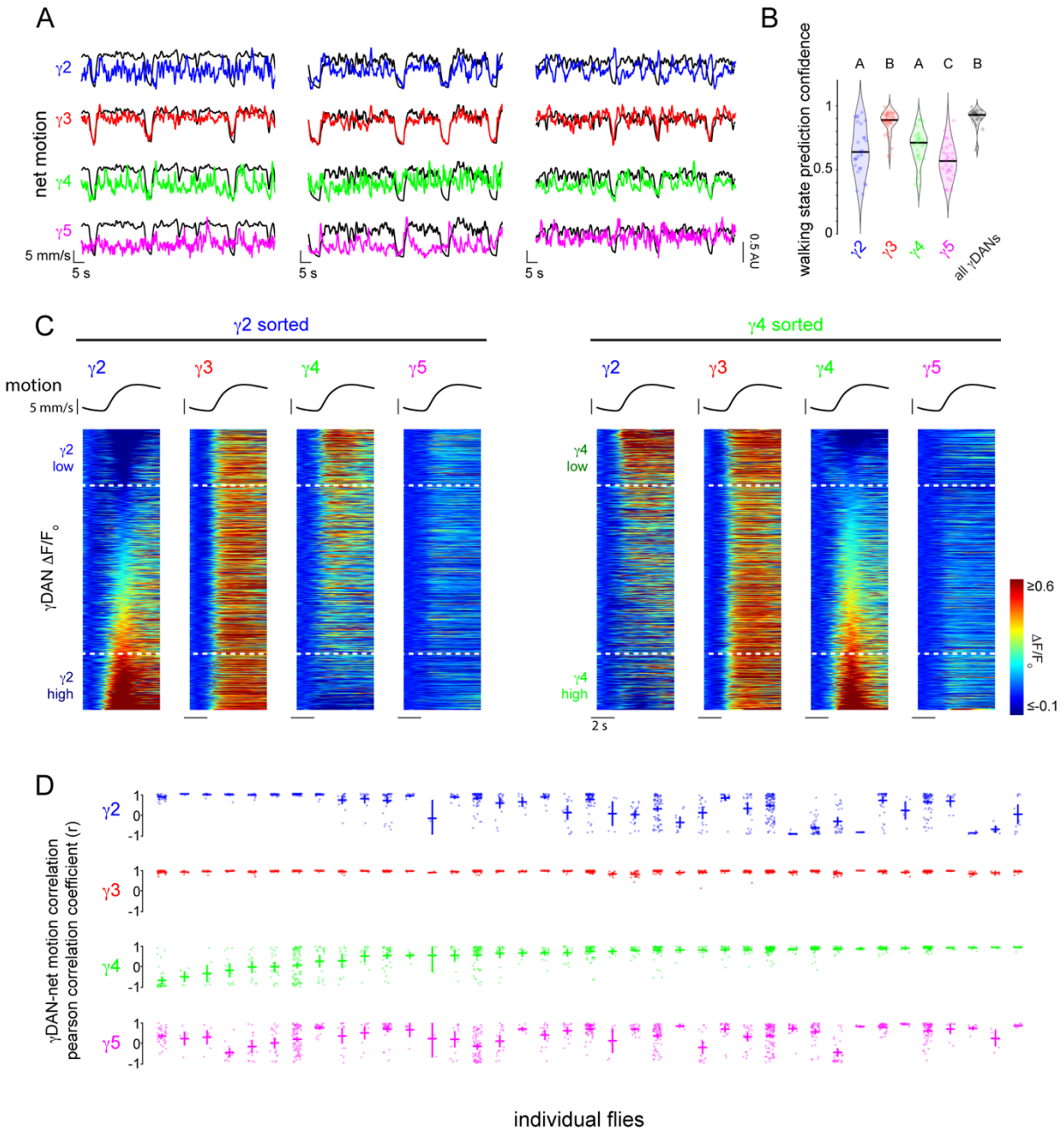
A
γ2
γ3
γ4
γ5
net motion
5 mm/s
5 s
5 s
5 s
0.5 AU
B
walking state prediction confidence
A
B
A
C
B
1
0.5
0
γ2
γ3
γ4
γ5
all γDANs
C
γ2 sorted
γ4 sorted
motion
5 mm/s
γ2
γ3
γ4
γ5
γ2 low
γ2 high
γ4 low
γ4 high
γDAN ΔF/F0
≥0.6
ΔF/F0
≤-0.1
2 s
D
γDAN-net motion correlation
pearson correlation coefficient (r)
1
0
-1
γ2
γ3
γ4
γ5
individual flies

correlated with movement and its activity reliably increased as flies initiated a bout of locomotion (Figures 2.4C,D). Although γ2 and γ4 DAN activity was unable to accurately predict an animal's locomotor state (Figure 2.4B), these populations were nonetheless strongly modulated as an animal initiated movement (Figure 2.4C). The relationship between γ2 and γ4 DANs with movement initiation, however, was highly variable both within and across individuals (Figures 2.4C,D). Whereas the start of a movement bout was reliably accompanied by an increase in γ3 DAN activity, we observed both decreases and increases in γ2 and γ4 activity even over the course of single recording session (Figures 2.4A,C,D).

The variability in γ2 and γ4 activity did not map onto any detectable differences in the kinematics of fly movement as they initiated locomotion nor did it relate to any other aspect of the bout, including its duration, the length of the preceding pause, or amount of time the fly had spent on the ball (Figure 2.5A). Furthermore, comparing locomotion bouts that were accompanied by the most divergent γ2 and γ4 activity revealed no overt differences in the fly's kinematics (Figure 2.5B). Bouts of locomotion onset that were indistinguishable by multiple behavioral metrics, including acceleration, speed, and turning velocity could be accompanied by opposing patterns of γ2 and γ4 DAN activity. Finally, in collaboration with Rich Pang, a graduate student in Adrienne Fairhall's lab at the University of Washington, we performed a principle component analysis of movement parameters as animals initiated locomotion and could identify no clear relationship between any of the dominant components and patterns of γ2 and γ4 DAN activity (Figure 2.6). Therefore, while γ3 activity invariantly tracked locomotor bouts independent of the heterogeneous kinematics of spontaneous movement, γ2 and γ4 activity was variable even for apparently identical bouts of movement initiation. γ5 DANs were relatively unaffected by the onset of movement

Figure 2.5 | Variability in Dopaminergic Neuron Activity at the Onset of Locomotion Is Not Related to Differences in The Physical Kinematics of Movement. (A) Relationships between the activity of γ2 (1st and 3rd rows, blue) and γ4 (2nd and 4th rows, green) DANs and behavioral variables during the initiation of movement. Average DAN $\Delta F/F_o$ defined as in Figure 2.4C. All behavioral variables are normalized by average values during bouts of continuous movement during the 5-minute recording trial. Behaviors are averaged over relevant time period relative to the onset of locomotion (t=0). Net motion, forward velocity, and |angular velocity|: t=1 to t=3. |Lateral velocity|: t=0 to t=1. Proportion of time moving after start is calculated over a 10 second period after initiation of locomotion. N=1060 movement initiations. All Pearson correlation coefficients are either weak ($|r|<0.18$) or not significant (see table below).

Pearson correlation coefficients (not corrected)

	net motion	forward velocity	turning velocity	|lateral velocity|	time on treadmill	proportion of time moving after start	bout length	stop length
γ2	-0.1306	-0.1791	n.s.	0.1586	n.s.	n.s.	n.s.	n.s.
γ4	n.s.	0.1266	-0.0723	-0.1524	-0.1549	0.0828	n.s.	n.s.

(B) DAN activity and parameters of locomotion during movement initiations when γ2 and γ4 DANs were most differentially active. Left: average γ2 $\Delta F/F_o$ (top row), net motion (2nd row), forward velocity (3rd row), turning velocity (4th row), |lateral velocity| (5th row), net acceleration (6th row), forward acceleration (7th row), turning acceleration (8th row), and lateral acceleration (9th row) ± 95% confidence interval as animals initiated sustained locomotion (as in Figure 2.4C) in 20% of starts with highest (dark blue, trials below lower white dashed line in Figure 2.4C) and lowest (light blue, trials above upper white dashed line in Figure 2.4C) average γ2 $\Delta F/F_o$. Right: Same as left but for γ4. All behavioral variables are normalized by average values during bouts of continuous movement during the 5-minute recording trial. N=212 movement initiations per grouping.

Figure 2.5

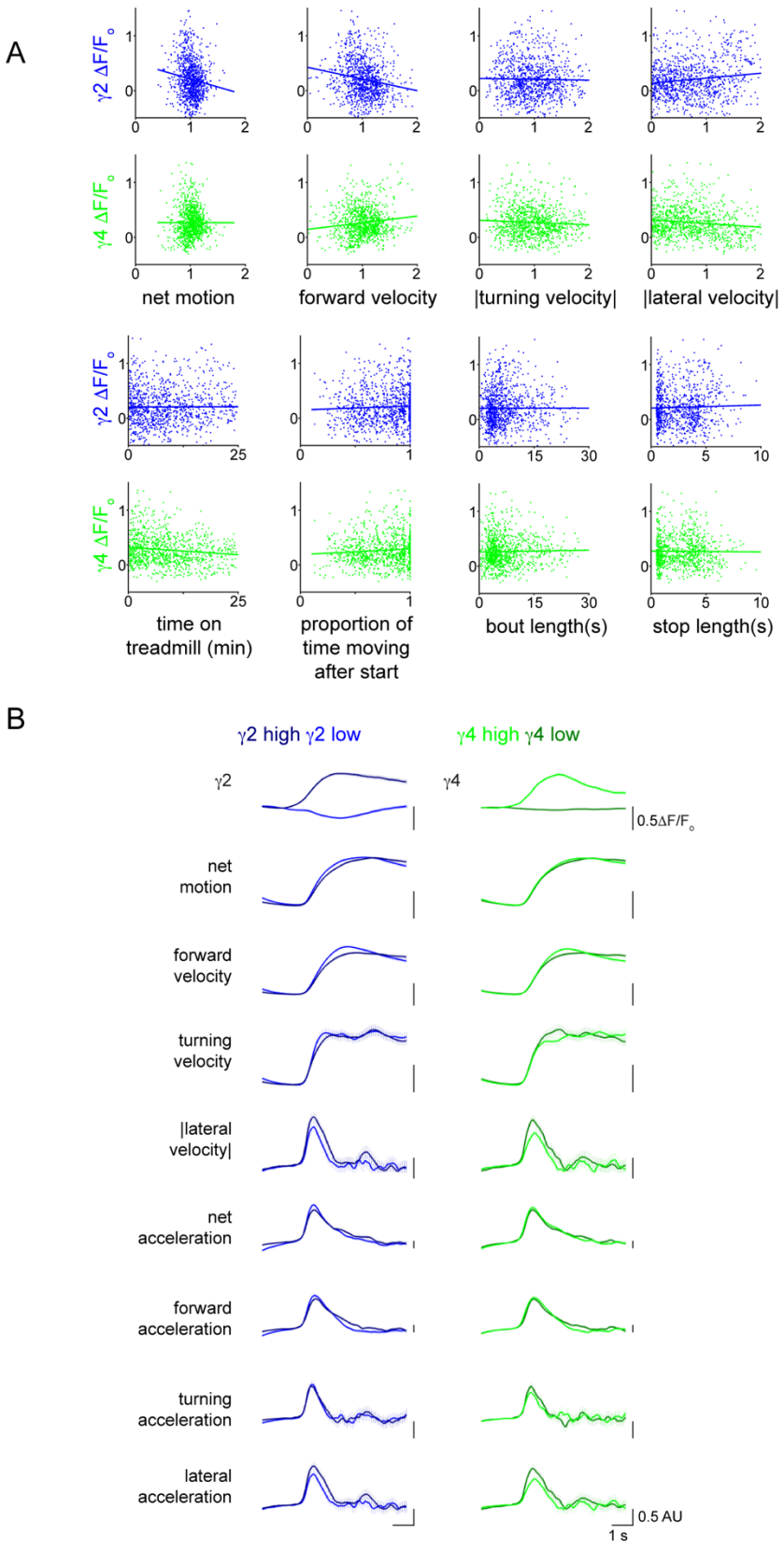
A
γ2 ΔF/F$_o$
γ4 ΔF/F$_o$
net motion
forward velocity
|turning velocity|
|lateral velocity|
time on treadmill (min)
proportion of time moving after start
bout length(s)
stop length(s)
B
γ2 high γ2 low
γ4 high γ4 low
γ2
γ4
0.5ΔF/F$_o$
net motion
forward velocity
turning velocity
|lateral velocity|
net acceleration
forward acceleration
turning acceleration
lateral acceleration
0.5 AU
1 s

Figure 2.6 | Principle Component Analysis Cannot Identify Behavioral Differences That Correspond to the Variability in Dopaminergic Neuron Activity at the Onset of Locomotion. Principal component analysis (PCA) of behavioral variables during the onset of movement. PCA was performed on net motion, forward velocity, turning velocity, and |lateral velocity| across a 4 second time window centered on instants of movement initiation (4 variables × 4 sec time window × 10Hz sampling = 160 initial variables per start). All behaviors were z-score normalized over the 4 sec window. **(A)** Additional proportion of variance explained by each additional principal component (PC) in PCA. **(B)** Most significant PCs. Left panel: mean z-score normalized behavioral variables during movement onset. Right panels: top 4 PCs along which the behavioral data maximally vary. **(C-D)** Relationship between most significant PCs and γ2 (C) and γ4 (D) $\Delta F/F_o$ (averaged during 2sec interval after movement onset). **(C)** Average γ2 $\Delta F/F_o$ vs projection of corresponding movement onset onto top four PCs (top row). All Pearson correlation coefficients are either weak (|r|<.2) or not significant (see table below). Pairwise comparison of top three PCs vs γ2 $\Delta F/F_o$ for all movement initiations (middle row) and highest and lowest 25% of γ2 $\Delta F/F_o$ (bottom row). **(D)** Same as in (C) but for γ4.

Significant Pearson correlation coefficients (not corrected)

	PC1	PC2	PC3	PC4
γ2	-0.1421	n.s.	0.1013	0.1939
γ4	n.s.	n.s.	-0.1250	-0.1980

Figure 2.6

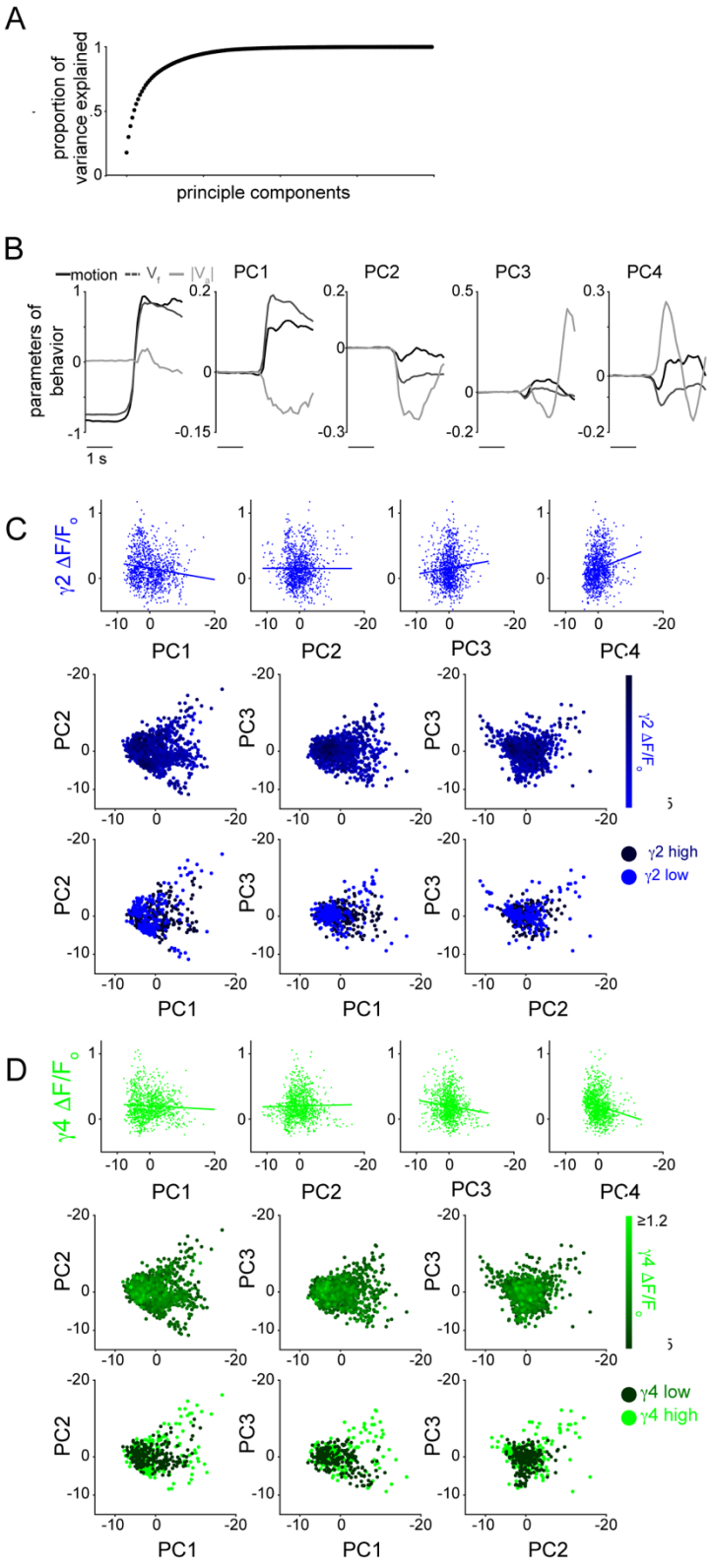
A
proportion of variance explained
principle components
B
motion
PC1
PC2
PC3
PC4
parameters of behavior
1 s
C
γ2 ΔF/F0
PC1
PC2
PC3
PC4
γ2 high
γ2 low
D
γ4 ΔF/F0
≥1.2
γ4 low
γ4 high

(Figure 2.4C), consistent with activity in this compartment being dominated by reward-related signaling. We therefore narrowed our focus to the γ2, γ3, and γ4 subpopulations to characterize the locomotor-related activity of DANs.

Although γ DAN activity was robustly modulated at the initiation and cessation of movement, we also observed rapid and large fluctuations in the DANs during periods of continuous locomotion. While γ3 DAN activity faithfully reflected whether an animal was walking or not, it failed to track the rapid fluctuations in an animal's velocity evident during periods of continuous walking with the same high fidelity. Rather, increases in forward velocity were associated with increased γ4 activity and decreased γ2 activity (Figures 2.7A,B), while increases in turning velocity were associated with increased γ2 and γ3 activity and decreased γ4 activity (Figures 2.7A,C). We thus see that DANs are reflecting changes in behavior on sub-second timescales. However, as seen for movement initiation, these relationships were not consistently observed across trials, even within the same individuals (Figure 2.7A).

To further explore how rapid changes in ongoing locomotion were reflected in the γ DANs, we again collaborated with Rich Pang to construct linear filters to quantitatively describe the relationship between DAN activity and either forward or turning velocity and then used these filters to predict DAN activity based on either behavioral parameter (Figures 2.8A-C). On average, the forward or turning velocity filters could account for 30-35% of the variance in DAN activity during locomotion, but this varied widely between flies, ranging from over 90% to less than 10%, further underscoring the dynamic relationship between DAN and motor activity (Figure 2.8D).

Figure 2.7 | Dopaminergic Neuron Activity Correlates with Changes in Forward and Turning Velocities. (A) Two representative overlays of γ DAN>sytGCaMP6s activity and forward velocity (top) and turning velocity (bottom) during periods of continuous locomotion (epoch designated by grey dashed box in top trace of net motion). DAN activity is normalized to minimum and maximum values during the selected bout of walking. **(B)** Average activity of γ DANs aligned to changes in forward velocity during bouts of continuous movement. N=9772 movements in 74 flies. **(C)** Average activity of γ DANs aligned to changes in turning velocity during bouts of continuous movement. N=11667 movements in 74 flies.

Figure 2.7

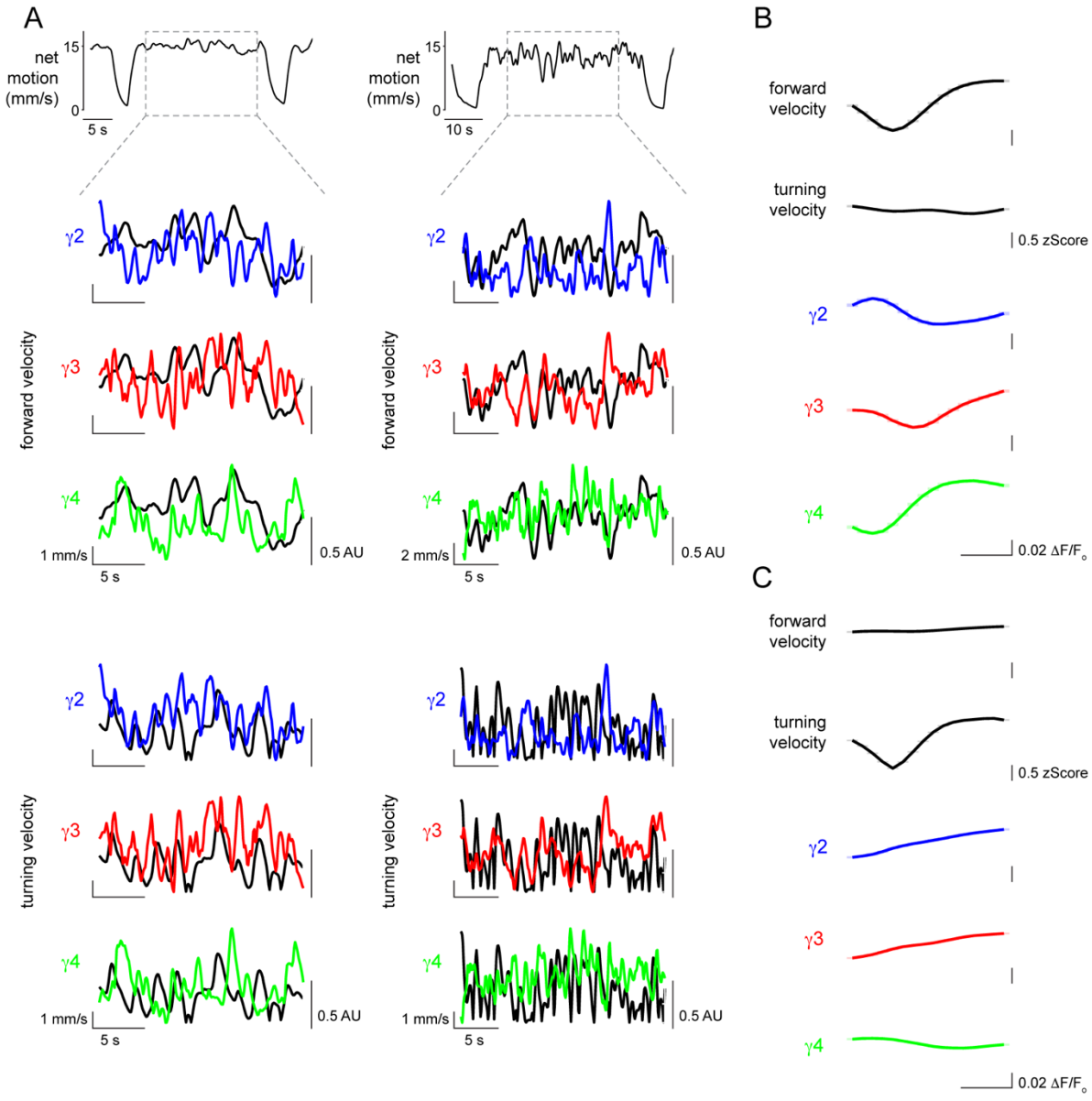
A
net motion (mm/s)
15
0
5 s
10 s
γ2
γ3
γ4
forward velocity
turning velocity
1 mm/s
2 mm/s
0.5 AU
B
forward velocity
turning velocity
0.5 zScore
0.02 ΔF/F0
C

Figure 2.8 | Dopaminergic Neuron Activity Can Be Predicted from Forward or Turning Velocity. (A) Linear filters predicting DAN activity during bouts of continuous movement using forward velocity (V_f, top) or turning velocity ($|V_a|$, bottom) centered on an eight second window as predictors ± 95% confidence interval. N=66 animals, 119 five minute trials. **(B)** Predicted DAN activity from linear filters in (A) based on forward velocity. Overlay of true γ2 (solid blue, 1st row), γ3 (solid red, 2nd row), and γ4 (solid green, 3rd row) DAN>sytGCaMP6s activity and predicted γ DAN activity generated by linear filters in (A) using forward velocity (dark gray). **(C)** Predicted DAN activity from linear filters in (A) based on turning velocity. Overlay of true γ2 (solid blue, 1st row), γ3 (solid red, 2nd row), and γ4 (solid green, 3rd row) DAN>sytGCaMP6s activity and predicted γ DAN activity generated by linear filters in (A) using turning velocity (light gray). **(D)** Proportion of variance in γ DAN activity explained by forward velocity and turning velocity. N=66 animals, 119 five minute trials. Paired t-test with Bonferroni correction, $p=1.02\times10^{-6}$ (*) and $p=3.07\times10^{-10}$ (**).

Figure 2.8

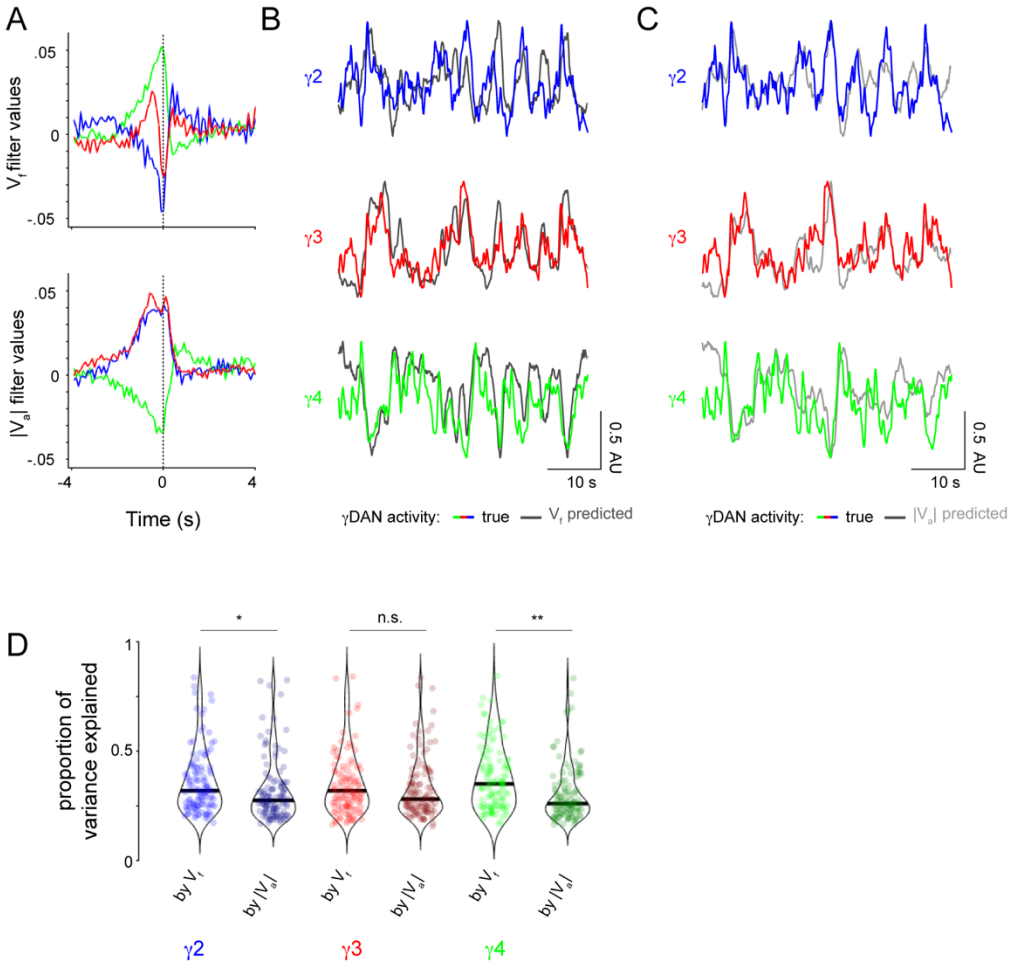
A
B
C
.05
0
-.05
V_t filter values
$|V_a|$ filter values
-4
0
4
Time (s)
γ2
γ3
γ4
0.5 AU
10 s
γDAN activity: true V_t predicted
γDAN activity: true $|V_a|$ predicted
D
*
n.s.
**
proportion of variance explained
1
0.5
0
by V_t
by $|V_a|$
γ2
γ3
γ4

Together, these analyses indicate that DAN activity patterns reflect diverse aspects of animal behavior that unfold at different timescales, encoding both rapid moment-to-moment fluctuations in an animal's velocity as well as slower changes in an animal's behavioral state (walking versus quiescence) that can persist for tens of seconds to minutes.

2.4 Dopaminergic Activity Appears to Precede Movement

The potential functions of a motor correlate can be constrained by determining if neuronal activity precedes or follows the physical action. Neuronal signals that occur prior to movement are expected to function in the motivation, planning, selection, or execution of an action[378–383], whereas neural activity following movement is more likely to convey behavioral feedback or other signals that could be used to evaluate an action's outcome[384–396]. In vertebrate systems, dopaminergic activity both anticipates action, where it acts to motivate, promote, and invigorate movement[213,214,216,223,374], but can also follows behavior, functioning as the "critic" in actor-critic models of dopaminergic based motor learning circuits[184–187,397]. Although our linear filters indicated that DAN activity trailed movement by a few hundred milliseconds, the ~500ms lag introduced by the slow calcium indicator GCaMP6s precluded our ability to draw conclusions about the temporal relationships between neural activity and movement. High speed imaging of either γ3 or γ4 DANs expressing the fast calcium indicator GCaMP6f[371], however, revealed that neural activity precedes the onset of locomotion and changes in forward velocity, respectively (Figures 2.9A,B). Furthermore, for both γ3 or γ4 DANs, a cross-correlation analysis revealed a

Figure 2.9 | Dopaminergic Activity Appears to Precede Movement. (A) Average γ3 DAN (MB441B) > soluble GCaMP6f activity and net motion aligned to the onset of locomotion. N=939 movement initiations in 27 flies. Cross-correlation peak at -151 ms, $p=1.86\times10^{-107}$, Wilcox sign-rank test across peak correlation times. **(B)** Average γ4 DAN (MB312B) > soluble GCaMP6f activity and forward velocity aligned to the increase in forward velocity during bouts of continuous movement. N=948 individual movements in 17 flies. Cross-correlation peak at -12 ms, $p=2.99\times10^{-208}$, Wilcox sign-rank test across peak correlation times. **(C)** Electrophysiological recording from individual γ3 DAN soma during spontaneous locomotion. Somatic spiking activity aligned to onset of locomotion. Thirteen movement initiations performed by two individual animals.

Figure 2.9

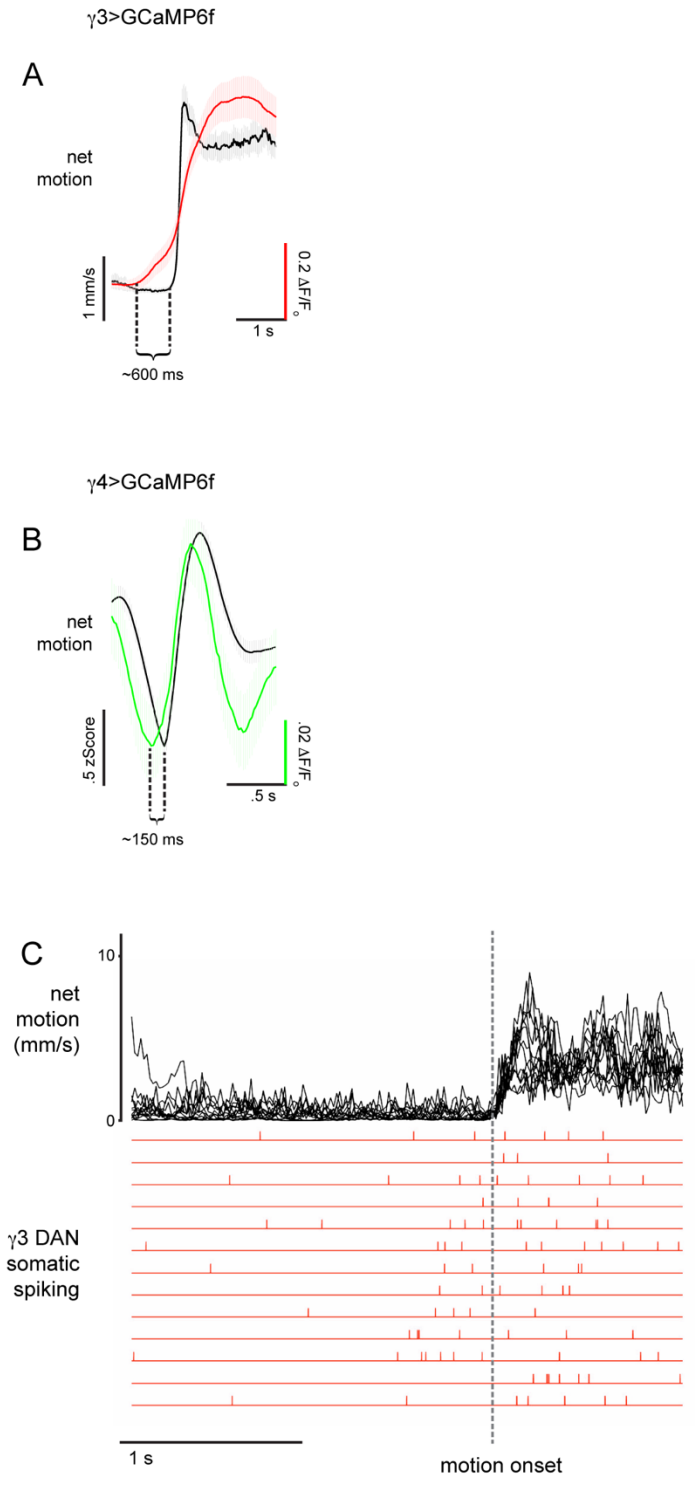
γ3>GCaMP6f
A
net
motion
1 mm/s
0.2 ΔF/F
1 s
~600 ms
γ4>GCaMP6f
B
net
motion
.5 zScore
.02 ΔF/F
.5 s
~150 ms
C
10
net
motion
(mm/s)
0
γ3 DAN
somatic
spiking
1 s
motion onset

significant peak when DAN activity was pushed forward in time. These data suggest that the activity of these MB DANs may anticipate, rather than reflect, behavior.

Despite our functional imaging experiments, we do not have sufficient evidence to conclusively prove that DAN activity precedes movement. Even our fast calcium indicator GCaMP6f introduces a temporal lag that results in some uncertainty in the alignment of DAN activity with movement. To address this concern, we performed preliminary electrophysiological recordings from individual γ3 soma, which demonstrated that they increase their frequency of action potential firing prior to movement initiation (Figure 2.9C). Even with this corroborating evidence, however, uncertainty persists as to the precise temporal relationship between neural activity and the rapid changes in the fly's motor output. Our quantification of behavior is limited to the movement of the spherical treadmill. Although we never observed limb movement not accompanied by rotation of the ball, we lack insight into the temporal delay between muscle contraction, leg motion, and movement of the treadmill. Although all available data suggests that DAN activity precedes movement, the limitations of our experimental system and the variability of DANs impedes our ability to draw strong conclusions regarding this point.

2.5 Intrinsic Network Dynamics of Mushroom Body Dopaminergic Circuitry

Despite their variable relationship to behavior, during periods of ongoing locomotion the DANs innervating different compartments were consistently correlated on a sub-second time scale

(Figure 2.10A). We calculated the partial correlations between DANs, controlling for potential relationships that arise from common behavioral signals. This revealed positive correlations between γ2 and γ3 DANs, γ3 and γ4 DANs, and γ4 and γ5 DANs while γ2 and γ4 DANs were strongly negatively correlated (Figure 2.10B). There appeared to be no strong relationship between γ5 and either γ2 or γ3 DANs. Some of these intrinsic dynamics between DANs corresponded to representations of movement, with an anticorrelation between the magnitudes of the γ2 and γ4 DAN responses to locomotion onset (Figure 2.10C) and changes in forward and turning velocity (Figure 2.7).

These network interactions partially mirror, but also deviate from, the coordinated and partially antagonistic responses of DANs evoked by flailing movement and external reinforcements like ingestion of a sugar reward or exposure to an aversive electric shock. The antagonism between γ2 and γ4 DANs can be at least partially explained by the anatomic evidence that the γ2 compartment is directly innervated by the inhibitory (glutamatergic) γ4 MBON. However, the remaining correlations between DAN populations appear to be an emergent and dynamic property, rapidly shifting within and between individuals. Thus the rich interconnections between DANs of different compartments[351,398–400] shape how behavioral features are represented by the DAN population such that opposing patterns of activity in the γ2 and γ4 compartments are evident during both movement initiation (Figure 2.4C and Figure 2.10C) and changes in forward and turning velocity during continuous locomotion (Figure 2.7 and Figure 2.8). Other aspects of the DAN network appear more flexible, such that γ3, for example, can rapidly shift and become correlated with either γ2 or γ4 during ongoing bouts of movement (Figures 2.10A,B).

Figure 2.10 | Intrinsic Network Dynamics of Mushroom Body Dopaminergic Circuitry. **(A)** Two representative overlays of DAN>sytGCaMP6s activity from pairs of γ DANs during bouts of continuous locomotion (epoch designated by grey dashed box in top trace of net motion, same as in Figure 2.7A). **(B)** Partial correlations between γ DAN subpopulations. N=74 animals, 178 five minute trials. One-way ANOVA, $p=1.73\times10^{-306}$. **(C)** Relationships between the activity of the different γ DANs during each individual initiation of movement. Pairwise comparisons of average $\Delta F/F_o$ during the onset of locomotion (1 sec to 2.5 sec after the start of movement) in the different γ DANs. Pearson correlation coefficient (r) indicated where relationship is statistically significant ($p<0.00001$). N=1060 movement initiations.

Figure 2.10

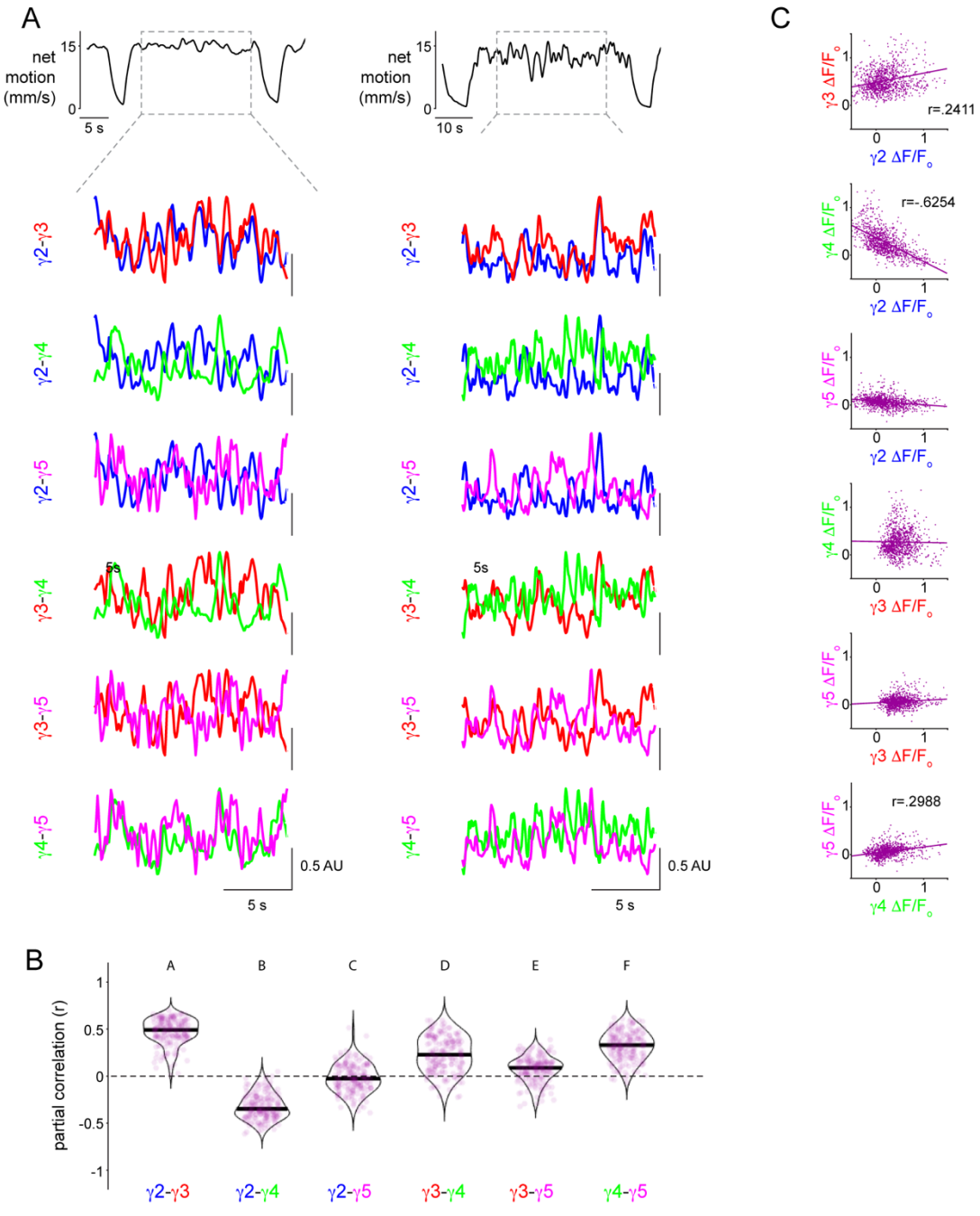
A
net motion (mm/s)
15
0
5 s
10 s
γ2-γ3
γ2-γ4
γ2-γ5
γ3-γ4
γ3-γ5
γ4-γ5
5s
0.5 AU
5 s
C
γ3 ΔF/F0
r=.2411
γ2 ΔF/F0
γ4 ΔF/F0
r=-.6254
γ5 ΔF/F0
r=.2988
B
partial correlation (r)
1
0.5
0
-0.5
-1
A
B
C
D
E
F

2.6 Discussion

Dopaminergic neurons have been reported to signal reinforcement to instruct learning[77,101,166,193] , reflect and set an overall level of activity indicative of an internal state[155,156,179,209,225,401], and encode an animal's rapid accelerations and shifts in movement to promote specific motor actions to shape the structure of real-time locomotion[132,133,213–217]. These often conflicting reports have stimulated an ongoing debate as to how dopamine plays such diverse and varied roles. There may be distinct dopaminergic subpopulations dedicated to specific functions or the same pathways could perform multiple tasks in parallel.

Our study of the MB indicates that both of these modes of dopaminergic circuitry can coexist simultaneously. Within the MB, the very same neurons that respond to reinforcing sensory cues to instruct learning also contain a rich and detailed representation of the moment-to-moment motor actions of an animal. Motor-correlates, however, are not equivalent across the dopaminergic subpopulations. While certain subsets of DANs, such as γ5, appear to be dedicated to signaling the rewarding nature of sensory stimuli, others contain multiplexed representations of both external reinforcements and movement (γ2, γ3, and γ4). Both the rapid changes in movement, such as accelerating or turning, that occur over the course of hundreds of milliseconds, as well as slower shifts in behavioral state that occurred over tens of seconds to minutes were differentially encoded by these DAN subpopulations. Similarly, MB DANs have been proposed to control behavior that unfolds over even longer periods, such as sleep cycles[259,260,262,263], suggesting that these populations are reflecting locomotor behavior over multiple timescales, from hours and days to fractions of seconds.

Just as distinct motor-correlates were observed across the γ lobe, representations of the reward varied between compartments as well. Individual DAN subpopulations have been reported to respond to different stimuli or have been implicated in the ability of a sensory modality to act as a reinforcer[348,350,354,363]. We find that even responses to a single stimulus vary across the different DAN subsets. Although both γ4 and γ5 DANs were activated by sugar, we noted that activity in γ5 usually increased prior to that of γ4. Simultaneous monitoring of the fly's behavior demonstrated that this earlier activity was concurrent with the forelimbs of an animal touching the approaching sugar droplet (data not shown). The DANs innervating the γ lobe have been subdivided into populations that underlie the formation of long-term memory (LTM), in which a nutritive sugar is required as a reinforcer, and short-term memory, (STM) where a non-nutritive but sweet tasting compound is sufficient to instill a transient association[334,336,352–355,363]. Different DAN subsets have been proposed to receive input from different sensory pathways, explaining their distinct and parallel roles in memory formation[332,354,363]. Our functional imaging data supports this model and provides evidence of differential representations of rewarding sugar within the MB DANs. In our preparation, γ4, which is implicated in STM formation, appears to respond to only to the ingestion of the sugar, while γ5, which is associated with LTM, appears to respond to both the ingestion and peripheral tasting of it. Consistent with our findings, the gustatory receptor 43a (Gr43a) is required for LTM formation and Gr43a-expressing neurons are believed to feed only into LTM-associated DANs like γ5. Gr43a-expressing neurons are found throughout the fly's body, but are enriched in the forelimbs[402], which are in contact with the approaching sugar droplet when we observe increased γ5 activity. These observations suggest that the γ4 and γ5

compartments represent distinct features of a stimulus that may emerge from different connectivity with afferent sensory pathways.

Differential input onto the separate dopaminergic subpopulations may likewise explain their non-equivalent representations of movement. Motor planning circuits controlling rapid accelerations during continuous locomotion may specifically link to γ2 and γ4 DANs, while pathways associated with more stable behavioral states connect to γ3 DANs. Similarly, motor circuits would not be predicted to be in contact with the dendrites of γ5 DANs. Despite a great deal of overlap in their dendritic arbors, specific DANs extend projections into distinct neuropils that would allow for differential input[256].

Segregated inputs onto DANs may be matched by distinct outputs. Preliminary evidence from our lab (data not shown) and others suggest connections between specific MBONs and neurons that innervate the fan-shaped body[256,339], a structure within the central complex with a well-defined role in navigational control of movement[367–369,403,404]. The connections between MBONs and downstream pathways may be specific and segregated such that the activity of any one can only affect a limited range of behaviors. This theoretical connectivity would match behavioral data indicating that only a fraction of the MBONs can alone bias an animal towards avoidance or approach[339]. If MBONs are dedicated to modulating a discrete set of behaviors, then it would be logical for their corresponding DANs to reflect only the relevant sensorimotor variables. Alternatively, DAN activity in different compartments may be relayed by MBONs to downstream integrators, allowing multiple different features of the animal's context and experience to influence a wide range of behaviors. In support of this model, combinatorial

activation of MBONs that alone do not alter behavior can have profound effects on avoidance and approach[339].

In support of an integration of the MB's efferent signal, anatomic and functional studies suggest rich interconnections between the inputs and outputs of the MB[351,398,400,405]. Activation of individual MBONs produces distinct patterns of DAN activity across the lobes[351], demonstrating that the DANs receive recurrent input from efferent pathways. A potential explanation of the heterogeneous and variable relationship between DANs and movement that we observe is that the activity of each DAN subpopulation may be the product of both distinct and unique sensorimotor inputs and recurrent feedback from MBONs innervating separate compartments. If the strength of these inputs is dynamic, then the dominance of a given modality on an individual DAN subset and on the MB as a whole could be flexibly controlled such that the relative strength of a correlation between DANs and a behavior or sensory stimulus would wax and wane. Such a system would permit cross-talk between sensory and motor aspects of the fly's experience as they exert shifting and varying levels of influence on the net output of the MB and the fly's behavior. The different patterns of DAN activity observed in flailing flies compared with flies walking on a treadmill similarly imply that ongoing DAN activity is flexibly dependent on the fly's immediate behavioral context. Although our partial correlation analysis suggests that network patterns of activity exist independent of sensorimotor variables, it is clear that the functional relationships between DANs are not absolute, but rather an emergent property that can change as animals move through their environment. Therefore representations of sensory and motor variables can map onto intrinsic circuit dynamics, while at the same time specific motor actions or external cues can reconfigure DAN activity patterns to promote a given network state. The activity in any one DAN compartment

may therefore be biased towards correlating with certain sensorimotor variables because of specific synaptic inputs, but at the same time be functionally flexible, tunable to the activity of other compartments to align with a relevant context, internal state, or external environment. Just as neuromodulation by dopamine imparts flexibility to its downstream targets, dopaminergic networks themselves may be functionally flexible.

Ongoing efforts to use electron microscopy to reconstruct the *Drosophila* brain's entire connectome and the use of genetically encoded markers of functional connections[25,406,407] will soon provide insight into the connectivity of both DANs and MBONs. In combination with functional analyses, these anatomic studies will greatly enhance our understanding of how the MB DANs dynamically interact with afferent, efferent, and recurrent pathways to influence behavior.

Our description of differential representations of reward- and movement-related activity across the MB DANs presents a striking parallel between insect and mammalian dopaminergic networks. The multiplexed encoding of reward- and movement-related variables within individual dopaminergic neuron and the heterogeneity between dopaminergic neurons that have been observed in the mammalian midbrain[199,213,214,216,220] are recapitulated in the *Drosophila* MB. We see a high degree of complexity, heterogeneity, and variability in just a fraction of the ~120 MB DANs, suggesting that the signaling of reward, representation of behavioral and internal states, and encoding of immediate movements are inherently interconnected processes linked within dopaminergic circuitry with a conserved functional logic. While the intricacy and size of vertebrate dopaminergic circuits presents a challenge to their study, the organized structure and simplicity of

the MB allows for an exploration of the nature and utility of these multifaceted signals with potential relevance to the physiology of mammalian dopaminergic pathways.

Individual dopaminergic neurons may be carrying representations of multiple variables simultaneously or they may be relaying a more complex and abstract feature of the fly's experience connected to both sugar ingestion and certain motor actions. The fact that the mapping between DAN activity and apparently indistinguishable behaviors is variable, coupled with our observation that DAN activity precedes the onset of movement, suggests that these neuromodulatory pathways are not simply encoding the detailed kinematics of locomotion, but are instead reflecting other, potentially higher order, cognitive variables that are nonetheless intimately related to the moment-by-moment movements of the fly. While our focus on spontaneous locomotion allowed us to isolate relationships between DANs and movement, it precluded any insight into the nature and meaning of these motor correlates. In the next chapter, I will relate how we developed tools to record from these DANs during goal-directed olfactory navigation and how these experiments provided insights into the nature and meaning of these representations of movement.

Chapter 3

Activity of Dopaminergic Neurons Correlates with the Strength of the Behavioral Response to Odor

3.1 Introduction

The complex and heterogeneous patterns of dopaminergic neuron activity, with their multiple sensory and behavioral correlates, have prompted an ongoing debate as to the nature and meaning of the dopamine signal[147,179,198,208,218,220,222,225,227]. Although specialized subpopulations of dopaminergic neurons exhibiting apparently dedicated responses to appetitive reward, punitive reinforcement, choice, movement initiation, velocity, orientation, or posture, have been reported[160,164,165,169,176–178,181,183,214–217,226,377], other studies have shown that individual dopaminergic neurons display multiplexed representations of both sensory cues and specific

parameters of movement[199,216,220]. One explanation for these findings is that dopaminergic neurons carry multiple distinct forms of information simultaneously, expressed through dissimilar and distinguishable patterns of activity[207,209,210,212]. Alternatively, representations of locomotion and reward conveyed by a single neuron have been proposed to reflect different aspects of the same unitary variable. For example, the correlation of mesolimbic dopaminergic neurons with both the latency to initiate a learned task and the delivery of reward after its successful completion suggests that this population encodes a single variable: an effort-to-value ratio representing the available reward relative to the amount of energy or level of exertion needed to achieve it[147]. In separate studies, the correlation of dopaminergic neurons with both sensory cues that predict reward in a learned task and specific motor actions used during the task argue that these sensory and motor correlates are analogous representations of the animal's expectations of a positive future outcome within a given context[199].

The question of what is encoded in the multiplexed activity of dopaminergic neurons remains unresolved. Attempts to establish a consensus have been hampered by the deep anatomic location, intricate pattern of innervation, and functional heterogeneity of mammalian dopaminergic systems[228–230], leading to conflicting reports and interpretations. The apparently flexible nature of dopaminergic pathways makes them inherently difficult to study in that their activity differs depending on the task parameters and requirements of a given experimental context. Different studies may therefore be examining distinct populations or the same functionally dynamic population in a distinct setting. Moreover, most studies of dopaminergic pathways have focused on animals engaged in learned tasks where it is difficult to distinguish movement-related

signals from representations of other variables related to the task, such as learned action, sensory association, reward expectation, or motivation[147,148,160,198,218].

Our study of the *Drosophila* MB as a representative dopaminergic system, as presented in Chapter 2, revealed that like their mammalian counterparts, DANs innervating the γ lobe exhibit multiplexed representations of both reinforcement stimuli and the moment-by-moment movements of the fly during naturalistic and spontaneous locomotion. The relationship between these two correlates is unknown: they may be distinct streams of information or they may be interconnected, representing two different aspects of a single variable. A thorough examination of the motor-related signals in DANs to determine what features of an animal's experience they correspond to will provide insight into the meaning of these signals. Such a study will likewise provide insight into the nature of complex patterns of dopaminergic activity observed throughout the animal kingdom.

The mapping between γ DAN activity and apparently indistinguishable behaviors was not stereotyped even within the same individual (see Chapter 2). In our experimental system, the animals were provided no overt sensory stimulation and other than their contact with the treadmill, they received no sensory feedback as a consequence of their actions. As DAN activity appears to precede movement initiation, one possible explanation for the variability we observe may be a disconnect between the intended and actual actions of an animal due to its inability to evaluate its movements in this artificial tethered paradigm. Indeed, in comparative studies where flies were transitioned from a sensory-unresponsive (open loop) setting to a context in which their behavior is capable of altering elements of their sensory environment (closed loop), important differences

emerged in how neural networks, especially those in higher brain centers, represent sensory and motor information[408]. In addition, in studies examining behavior when animals are deprived of sensory feedback, perception of velocity, orientation, and location are severely impaired and become disconnected from reality[409].

Alternatively, rather than encoding the detailed aspects of physical movement, the DANs may be reflecting a more abstract feature of the fly's experience. The correspondence between how certain movement parameters and reinforcing stimuli are represented by DANs (i.e. reciprocal patterns of γ2/γ4 activity during motion onset, forward acceleration, turning, sugar ingestion, and electric shock) suggests that variability may arise because the DANs are encoding a more general behavioral context that is independent of the animal's specific actions. Such a model of DAN activity would parallel findings in mammalian dopaminergic pathways that have been proposed to reflect motivation such that they correlate with the animal's engagement with a task and the vigor with which they perform it[147,148,156,225,410].

To probe these possibilities, we sought to monitor DAN activity as an animal locomoted in a sensory responsive environment and performed a purposive behavior with a clear and appreciable end-goal. We focused on odor tracking behavior because the MB serves as a major target of olfactory information[256,307,313] and has a well-established role in both the formation of olfactory associations[253,254,285,301,411] and in naïve responses to odor[248–250,358,359]. Animals use odor to detect the presence and proximity of food sources, conspecific mates or competitors, and predators or other threats. Animals rely on a combination of olfactory cues along with the ability to sense the strength and direction of airflow to bring them to the source of an odor. A well-

described strategy utilized by animals to locate the source of appetitive odors is anemotaxis, whereby an animal reorients in an airstream to turn upwind upon encountering an appealing olfactory stimulus, making anemotaxis a quantifiable behavior with an explicit purpose[412–421]. We therefore took advantage of a paradigm developed by a former student in the lab, Raffi Cohn, that allowed us to examine DAN activity as animals navigated in an airstream and responded to an olfactory stimulus. These experiments, combined with our knowledge of how the γ DANs encode spontaneous movements, present an opportunity to connect motor-related signals in DANs to an animal's goal-directed behavior.

In this chapter, I present our investigation into the nature of movement-related signaling in the γ DANs to determine the features of the animal's experience to which they correspond. I describe our use of a closed loop olfactory system to record MB DAN activity as animals actively tracked an olfactory stimulus, allowing us to gain insight into how goal-directed and sensory-triggered movements are represented by the MB DANs.

3.2 Goal-Directed Olfactory Behaviors

To explore the nature of movement-related signaling in the MB γ DANs we sought to record from these populations as animals performed goal-directed behaviors with appreciable ends, specifically anemotaxis, a common navigational strategy displayed by many insect species, including *Drosophila*[244,418–420,422–426].

To assess this behavior, we took advantage of an assay developed by Thomas Graham, a former postdoc in the laboratory, in which a cohort of 4-7 freely moving flies were recorded walking within in a small rectangular chamber (2 cm by 5 cm) in a constant laminar flow of clean air drawn from the surrounding environment. At designated times, air from the headspace of a bottle containing the appetitive food odor apple cider vinegar (ACV), was directed into the chambers without altering the net flow of air (Figures 3.1A,B). We found that flies displayed robust upwind tracking in response to a brief (1 second) pulse of ACV (Figure 3.1C). Animals tracked upwind primarily by reorienting, changing their heading, and walking in the upwind direction, although animals also increased their velocity as they moved towards the odor source (Figure 3.1D). A small fraction of animals were already walking in the upwind direction at the time of odor presentation and consequently responded to the odor solely by increasing their upwind speed (Figure 3.1E). These assays indicate that flies robustly respond to ACV by employing different navigational strategies depending on their immediate behavioral context when they encounter the odor.

To assess if these behavioral responses depended on an animal's internal satiety state, we compared tracking in fed and starved animals and found that, consistent with previous reports[275,276,427–431], fed flies displayed significantly diminished upwind tracking to ACV (Figures 3.2A,B). An animal's energy expenditure must be carefully regulated and it must balance the energetic costs of foraging with its metabolic requirements. Fed flies are less likely to engage in exploration and anemotaxis because their immediate need to locate a new food source is low. The upwind movement of their starved counterparts in response to ACV is therefore compelled by their ultimate end-goal of bringing themselves into contact with a presently needed food source. We

Figure 3.1 | Different Navigational Strategies for Appetitive Approach to Apple Cider Vinegar. (A) Illustration of the movements of freely moving flies before, during, and after presentation of ACV in behavioral chambers. **(B)** Illustration of chamber assay showing how airflow switches across manifolds between odor presentations to come from the top or bottom of the chamber on alternating odor presentations. Additional valves were used to switch airflow from glass bottle containing water to an odor-containing bottle. **(C)** Average upwind displacement (top) and proportion of animals walking upwind (bottom) ± 95% confidence interval before, during, and after a 1sec pulse of ACV in freely moving animals in our behavioral chambers. Presence of odor indicated by semi-transparent orange bar. N=15 cohorts, 300 odor presentations. **(D-E)** Behavioral responses of individual flies to ACV presentation when they were walking crosswind (D, N=637) or upwind (E, N=224) at the time of odor onset. Trajectories of individual flies (top). Average |heading| and upwind velocity ± 95% confidence interval (bottom). Presence of odor indicated by semi-transparent orange bar.

Figure 3.1

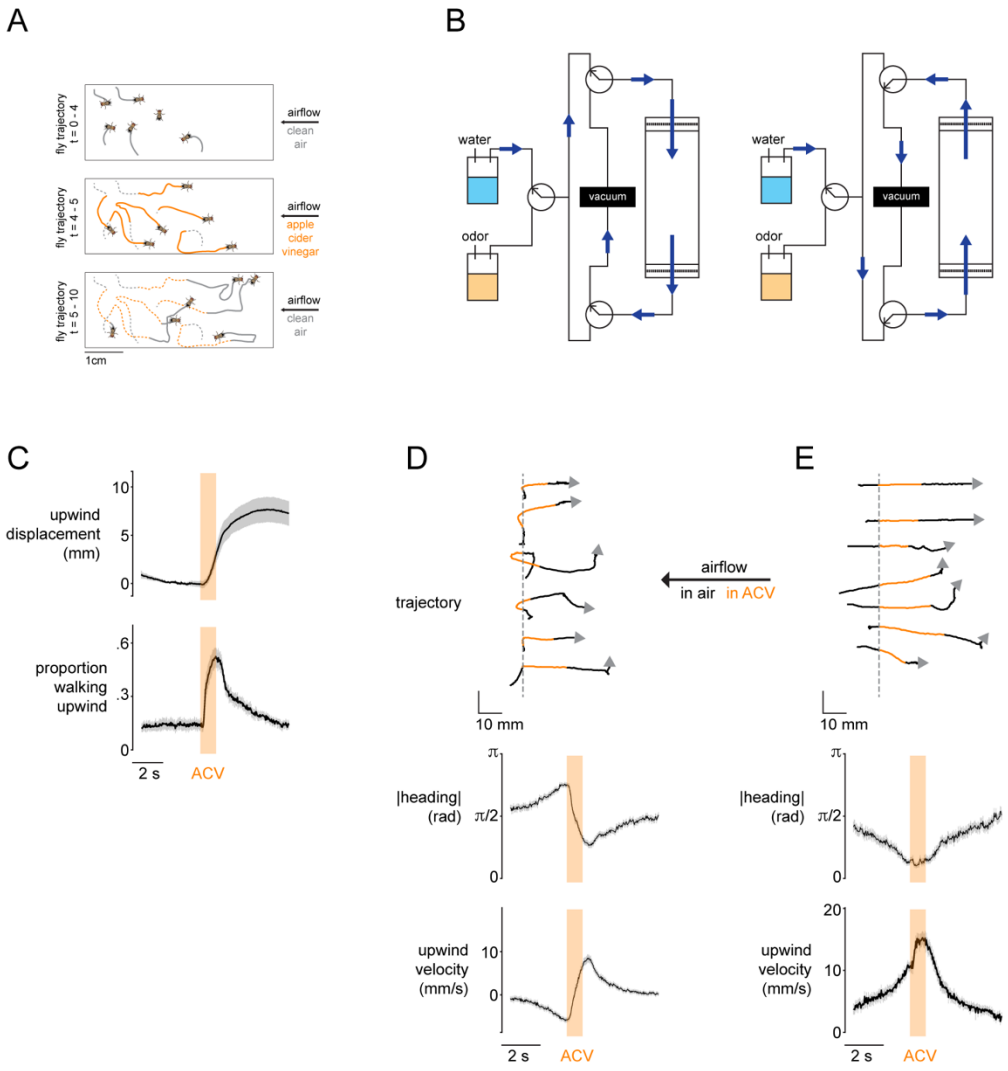
A
fly trajectory t = 0 - 4
airflow
clean air
fly trajectory t = 4 - 5
airflow
apple cider vinegar
fly trajectory t = 5 - 10
airflow
clean air
1cm
B
water
odor
vacuum
water
odor
vacuum
C
upwind displacement (mm)
10
5
0
proportion walking upwind
.6
.3
0
2 s
ACV
D
trajectory
10 mm
airflow
in air
in ACV
|heading| (rad)
π
π/2
0
upwind velocity (mm/s)
10
0
2 s
ACV
E
10 mm
|heading| (rad)
π
π/2
0
upwind velocity (mm/s)
20
10
0
2 s
ACV

Figure 3.2 | Upwind Tracking is Reduced in Fed Flies and Animals Display Diminished Approach to Carbon Dioxide. (A-B) Fed animals have diminished behavioral responses to ACV. **(A)** Average upwind displacement (top) and proportion of animals walking upwind (bottom) ± 95% confidence interval in 12-18 hour starved (black) and fed (maroon) flies before, during, and after a 1sec pulse of ACV in freely moving animals in our behavioral chambers. Presence of odor indicated by semi-transparent orange bar. N=15 cohorts, 300 odor presentations. **(B)** Fed animals have diminished behavioral responses to ACV. Upwind displacement (left), average upwind velocity (middle), and average |heading| of 12-18 hour starved (black) and fed (maroon) paired cohorts of animals during a 1sec presentation of ACV. Paired t-test with Bonferroni correction, $p=8.085\times10^{-7}$ (**), $p=2.166\times10^{-5}$ (*), and $p=2.053\times10^{-14}$ (***). N=15 cohorts, 300 odor presentations. **(C-D)** Flies have diminished behavioral responses to CO_2 compared to ACV. **(C)** Average upwind displacement (top) and proportion of animals walking upwind (bottom) ± 95% confidence interval in flies before, during, and after a 1sec pulse of either ACV (black) or CO_2 (grey) in freely moving animals in our behavioral chambers. Presence of odor indicated by area shaded in blue. N=55 cohorts, 550 presentations per odor. **(B)** Animals have diminished behavioral responses to CO_2 compared to ACV. Upwind displacement (left), average upwind velocity (middle), and average |heading| of paired cohorts of animals during a 1sec presentation of either ACV (black) or CO_2 (grey). Paired t-test with Bonferroni correction, $p=4.\ 5\times10^{-18}$ (*), $p=8.7\times10^{-26}$ (**), and $p=3.9\times10^{-45}$ (***). N=55 cohorts, 550 presentations per odor.

Figure 3.2

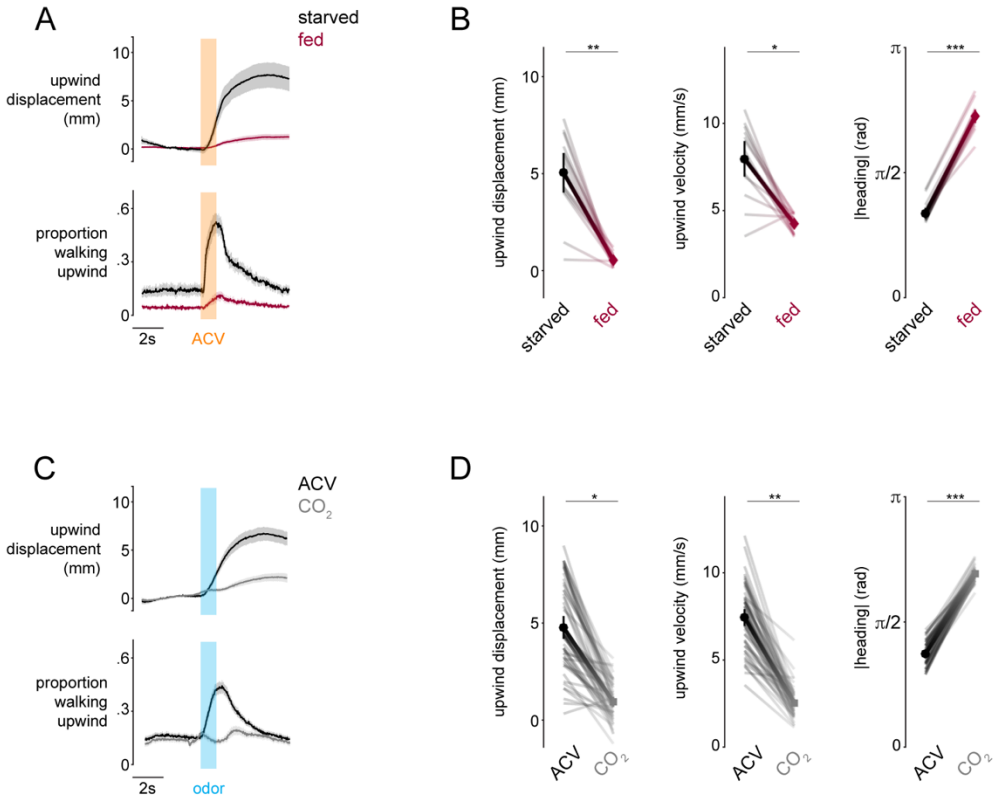
A
starved
fed
upwind displacement (mm)
10
5
0
proportion walking upwind
.6
.3
0
2s
ACV
B
upwind displacement (mm)
upwind velocity (mm/s)
|heading| (rad)
**
*
***
π
π/2
starved
fed
C
ACV
CO2
odor
D
ACV
CO2

also compared the behavioral responses evoked by ACV to those elicited by carbon dioxide (CO_2), an aversive chemical cue released by flies to signal stress[248,249,432–434]. Flies generally did not display upwind tracking to CO_2 and, on average, appeared to pause during CO_2 exposure and increase their upwind tracking after it was removed (Figures 3.2C,D). These experiments demonstrate that animals track towards appetitive food odors depending on their satiety state.

3.3 A Closed Loop Olfactory Paradigm

To replicate this odor-evoked anemotaxis under the microscope, we took advantage of a closed loop paradigm in which the heading of a tethered fly walking on the air-supported foam ball was yoked to the position of a tube carrying an airstream capable of rotating 360° around the animal (Figure 3.3A). Odor could also be injected into the airstream without changing the net flow, allowing us to observe how animals behaviorally responded to olfactory stimuli. This system therefore placed the animals in a virtual reality, allowing them to control their orientation relative to a clean airstream or odor plume by changing their turning velocity. As in freely moving animals, tethered flies in this paradigm frequently reoriented and maintained an upwind trajectory in response to the presentation of ACV, resulting in a net upwind displacement towards the fictive odor source (Figure 3.3B). This closed loop system thus allowed us to record from the DANs as an animal actively tracked towards a fictive odor source.

Figure 3.3 | The Closed Loop Experimental Paradigm Replicates Odor-Evoked Anemotaxis Under the Microscope. (A) Schematic of closed loop experimental paradigm (top) where the animal's instantaneous heading is relayed to a motor controlling the position of an air tube relative to the fly. Bottom: top-down view of a tethered fly showing the position of the air tube during upwind and crosswind movement. **(B)** Comparison of trajectories of freely moving and tethered flies during anemotaxis. Top: trajectories of individual freely moving flies in our behavioral chambers aligned to their positions at the beginning of a 1sec presentation of ACV. Trajectories include animal location 1sec before and 2 sec after odor. Bottom: Fictive 2D trajectory of tethered fly walking in closed loop and responding to four 10sec presentations of ACV over a 5 minute trial.

Figure 3.3

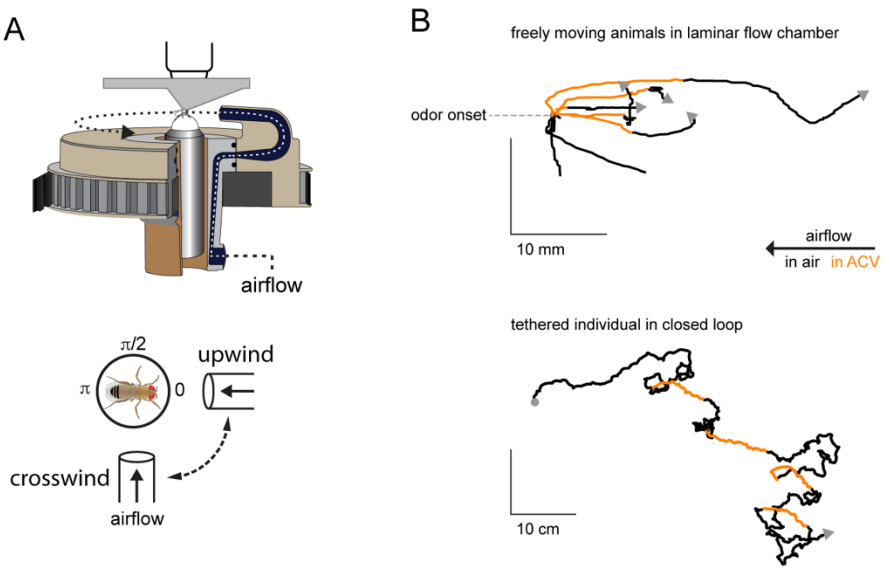
A
airflow
π/2
π
0
upwind
crosswind
airflow
B
freely moving animals in laminar flow chamber
odor onset
10 mm
airflow
in air
in ACV
tethered individual in closed loop
10 cm

3.4 Dopaminergic Neurons and Movement in Closed Loop

When animals walked in clean air in this closed loop system, the relationship between DAN activity and different behavioral variables appeared generally similar to those measured in flies walking in the absence of any overt external sensory feedback. γ3, for example, remained highly positively correlated with movement onset. Variability was still observed in how γ2 and γ4 DANs represented the onset of locomotion (Figure 3.4A), but these different neural signals were now, on average, associated with differences in an animal's movement as it initiated a walking bout. For example, depressed γ2 activity during movement initiation was generally associated with faster accelerations and a reorientation in the upwind direction. Similarly, elevated γ4 activity, on average, accompanied faster movement initiations with larger accelerations in the forward direction (Figure 3.4B). Variability persisted in the relationship between patterns of γ2 and γ4 DAN activity and how the animals were physically initiating locomotion and these correlations only emerged on average when comparing the most extreme neural differences. As these closed loop movements are still spontaneous, we are hesitant to draw strong conclusions. One possibility, however, is that these apparent differences in neural representations may be due to overall changes in brain activity when flies are in a sensory responsive environment[408]. Alternatively, as will be expanded upon in forthcoming sections, these differential representations may emerge due to differences in the goal of specific movements or the behavioral context of the animal when it is in a closed loop environment.

We observed comparable fluctuations in DAN activity associated with the rapid changes in forward and turning velocity that were noted during spontaneous bouts of locomotion in a

Figure 3.4 | Mushroom Body Dopaminergic Neuron Representations of Movement Initiation in Closed Loop. (A) Pearson correlation coefficient between the increase in net motion and change in DAN>sytGCaMP6s activity during initiations of sustained movement (≥3 sec) following a pause (≥2 sec) in animals spontaneously walking in closed loop. Ordered by average motion-γ4 correlation for all starts within an individual animal. N=32 animals, 452 movement initiations. **(B)** DAN activity and parameters of locomotion during movement initiations when γ2 and γ4 DANs were most differentially active in animals walking in closed loop. Left: average γ2 $\Delta F/F_o$ (top row), net motion (2^{nd} row), forward velocity (3^{rd} row), turning velocity (4^{th} row), |lateral velocity| (5^{th} row), net acceleration (6^{th} row), forward acceleration (7^{th} row), turning acceleration (8^{th} row), lateral acceleration (9^{th} row), and Δheading (10^{th} row) ± 95% confidence interval as animals initiated sustained locomotion (as in Figure 2.4C) in 20% of starts with highest (dark blue, trials below lower white dashed line in Figure 2.4C) and lowest (light blue, trials above upper white dashed line in Figure 2.4C) average γ2 $\Delta F/F_o$. Right: Same as left but for γ4. All behavioral variables are normalized by average values during bouts of continuous movement during the 5-minute recording trial. N=91 movement initiations per grouping.

Figure 3.4

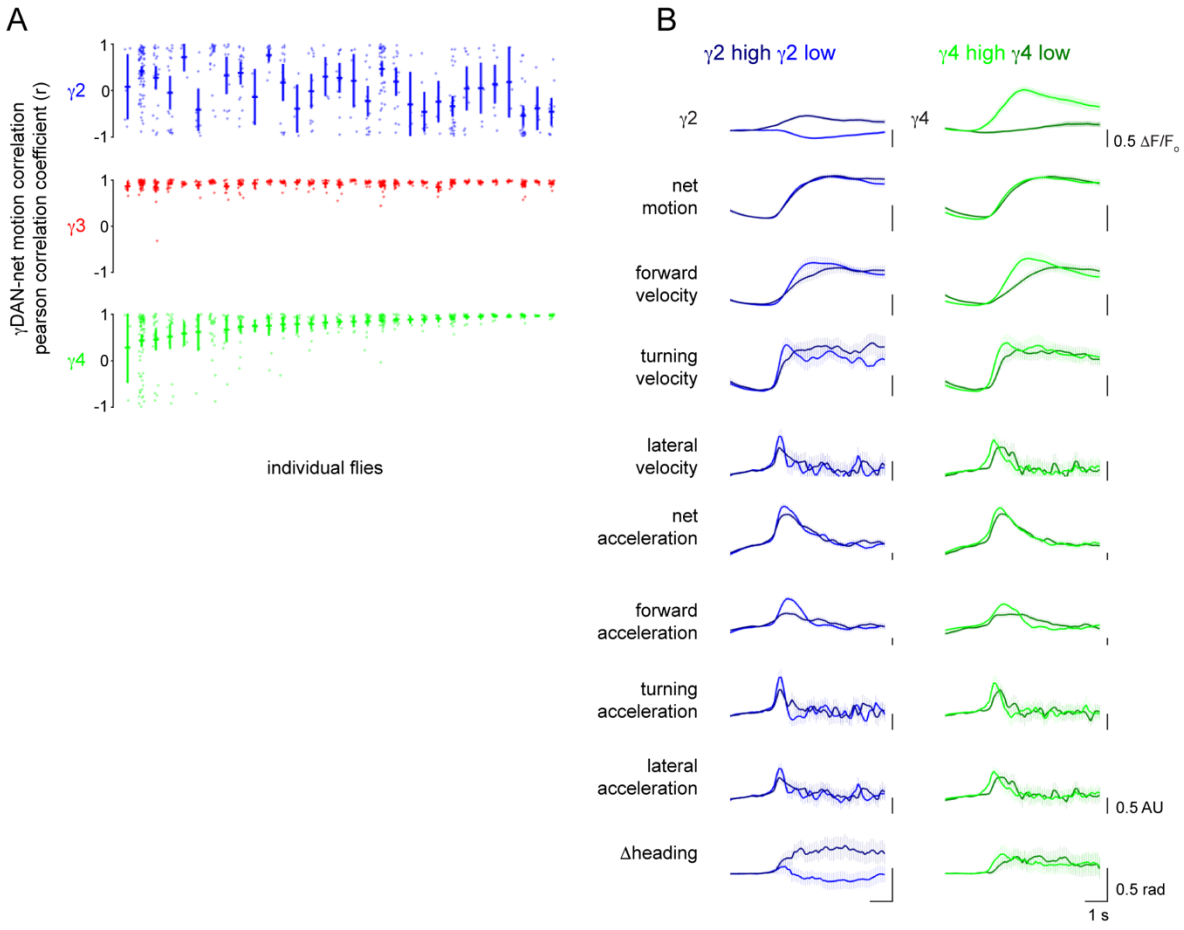
A
γDAN-net motion correlation
pearson correlation coefficient (r)
γ2
γ3
γ4
1
0
-1
individual flies
B
γ2 high γ2 low
γ4 high γ4 low
γ2
γ4
0.5 ΔF/F0
net motion
forward velocity
turning velocity
lateral velocity
net acceleration
forward acceleration
turning acceleration
lateral acceleration
0.5 AU
Δheading
0.5 rad
1 s

sensory-restricted environment (Figure 3.5A). Moreover, linear filters predicting DAN activity based on forward or turning velocity were similar when generated from either closed loop or spontaneous movement (Figure 3.5B). To further probe how representations of movement were altered in closed loop, we recorded from flies first without any overt sensory stimulation and then in closed loop where they could control their orientation relative to an airstream, allowing for comparisons within the same individual. These experiments revealed subtle but consistent differences between the two conditions (Figure 3.5A). To quantitatively assess how the relationships between DAN activity and movement were altered across conditions in the same fly, we constructed simple linear models from the activity of all the γ DANs and compared their ability to predict a specific behavioral parameter. We found that models predicting forward velocity were consistently improved when using DAN activity from animals in the closed loop context, explaining more of the variance with less residual error (Figure 3.5C). This appeared to be driven primarily by a higher correlation between γ4 DANs and forward velocity, as the coefficients associated with that compartment alone were significantly higher in closed loop (Figure 3.5D). Like differences in the neural representations of movement onset, this improved correlation between γ4 DANs and forward velocity may be due to a general increase in the coherence of neural activity when animals are in closed loop or may be specifically related to a different behavioral context that emerges when animals are in a sensory-responsive environment.

In all of our previous recordings of the γ DANs, we observed equivalent activity across the two hemispheres of the fly's brain. In closed loop, however, we noted a significant difference between the activity in the left and right γ4 compartments that appeared to relate to the turning velocity of a fly (Figures 3.6A,B). One possibility is that γ4 DANs carry information about the

Figure 3.5 | Mushroom Body Dopaminergic Neurons Encode Rapid Changes in Forward and Turning Velocity in Closed Loop. (A) Representative overlays of γ DAN>sytGCaMP6s activity and forward velocity during periods of continuous locomotion of two individuals walking spontaneously without any overt sensory input (SR, left) and in closed loop (CL, right). DAN activity is normalized to minimum and maximum values during the selected bout of walking. **(B)** Linear filters predicting DAN activity (as in Figure 2.8A) during bouts of continuous movement using forward velocity (top) or turning velocity (bottom) centered on an eight second window as predictors ± 95% confidence interval for animals walking in closed loop (CL, dark lines) and animals walking spontaneously without any overt sensory input (SR, light lines, same as in Figure 2.8A). CL: N=20 animals, 32 five minute trials. SR: N=66 animals, 119 five minute trials. **(C-D)** Representations of forward velocity in MB DAN network improves when animals are transitioned from SR to CL. Linear models predicting forward velocity from γ DAN activity during continuous locomotion under SR or CL conditions were compared within the same individuals. **(C)** Sum of the square of the residuals (left) and proportion of variance explained (right) from SR model compared to CL model. **(C)** Coefficients associated with the activity of the γ DANs in linear models generated from flies walking in SR and CL. Paired t-test with Bonferroni correction, $p<10^{-6}$ (***), $p<10^{-4}$ (**), $p<0.01$ (*). N=22 flies.

Figure 3.5

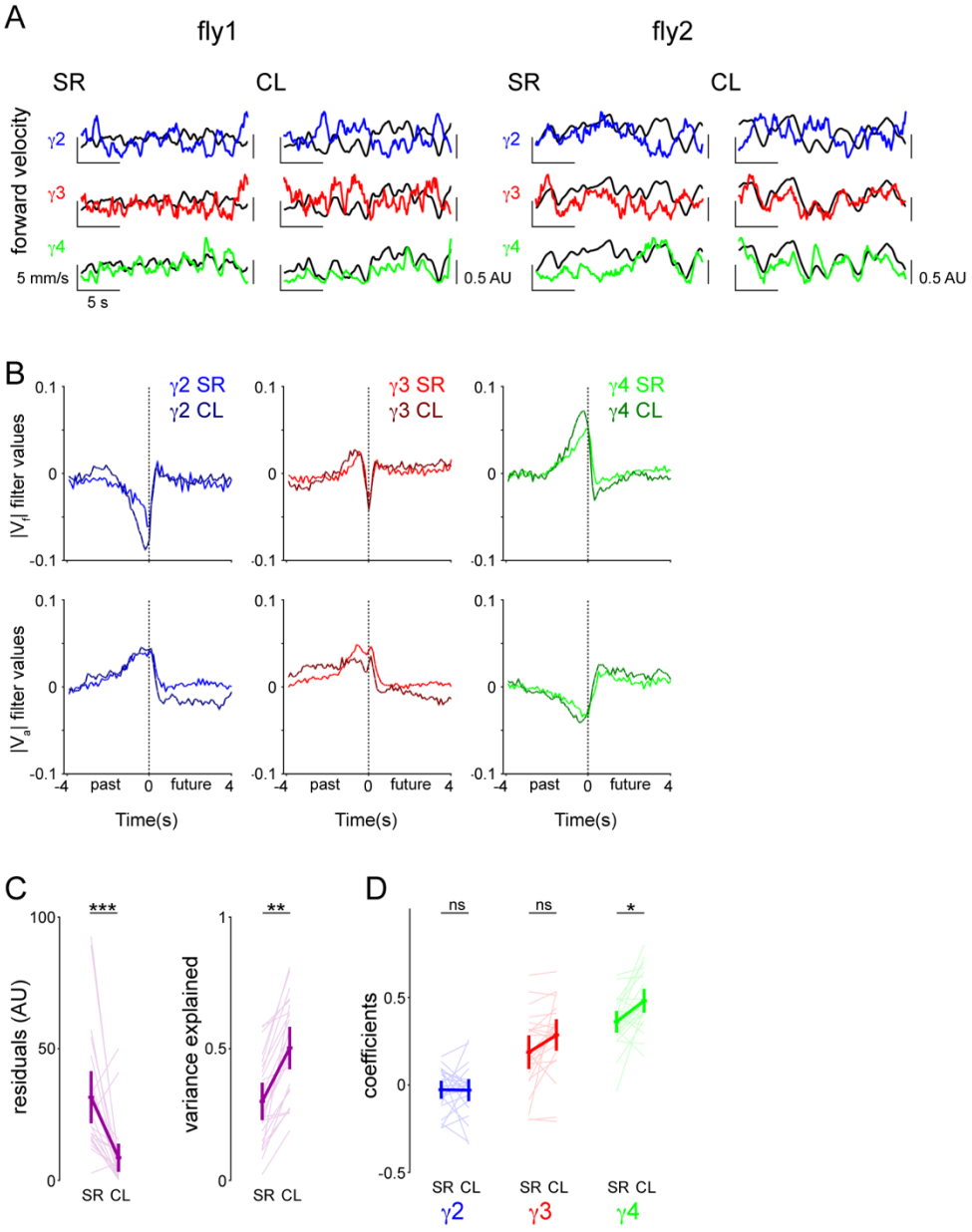
A
fly1
fly2
SR
CL
SR
CL
forward velocity
γ2
γ3
γ4
5 mm/s
5 s
0.5 AU
0.5 AU
B
γ2 SR
γ2 CL
γ3 SR
γ3 CL
γ4 SR
γ4 CL
|Vf| filter values
|Va| filter values
0.1
0
-0.1
-4
past
0
future
4
Time(s)
C
***
**
residuals (AU)
variance explained
100
50
0
1
0.5
0
SR CL
SR CL
D
ns
ns
*
coefficients
0.5
0
-0.5
SR CL
SR CL
SR CL
γ2
γ3
γ4

Figure 3.6 | Interhemispheric Difference in γ4 Dopaminergic Neuron Activity Reflects Change in Wind Direction Relative to the Fly. (A) Average interhemispheric difference in the activity of γ DANs aligned to turning movements performed during spontaneous locomotion in closed loop. γ DAN activity z-score normalized by average GCaMP signal during epochs of continuous movement. N=22 animals, 1113 individual turns. **(B)** Interhemispheric difference of γ4 DAN activity overlaid with turning velocity (top) or air tube velocity (bottom) in a representative example of a fly in closed loop (left, unshaded) and when being presented with a pseudorandom white noise pattern of air tube movement (right, grey shading). **(C)** Variance in γ4 DAN activity explained using only the fly's turning velocity, only the airstream's movement velocity, or both during presentation of the white noise pattern of air tube movements. N=3 flies, 5 total 5-minute trials each composed of alternating 1 minute periods of closed loop or white noise. Paired t-test with Bonferroni correction, $p<0.05$ (*).

Figure 3.6

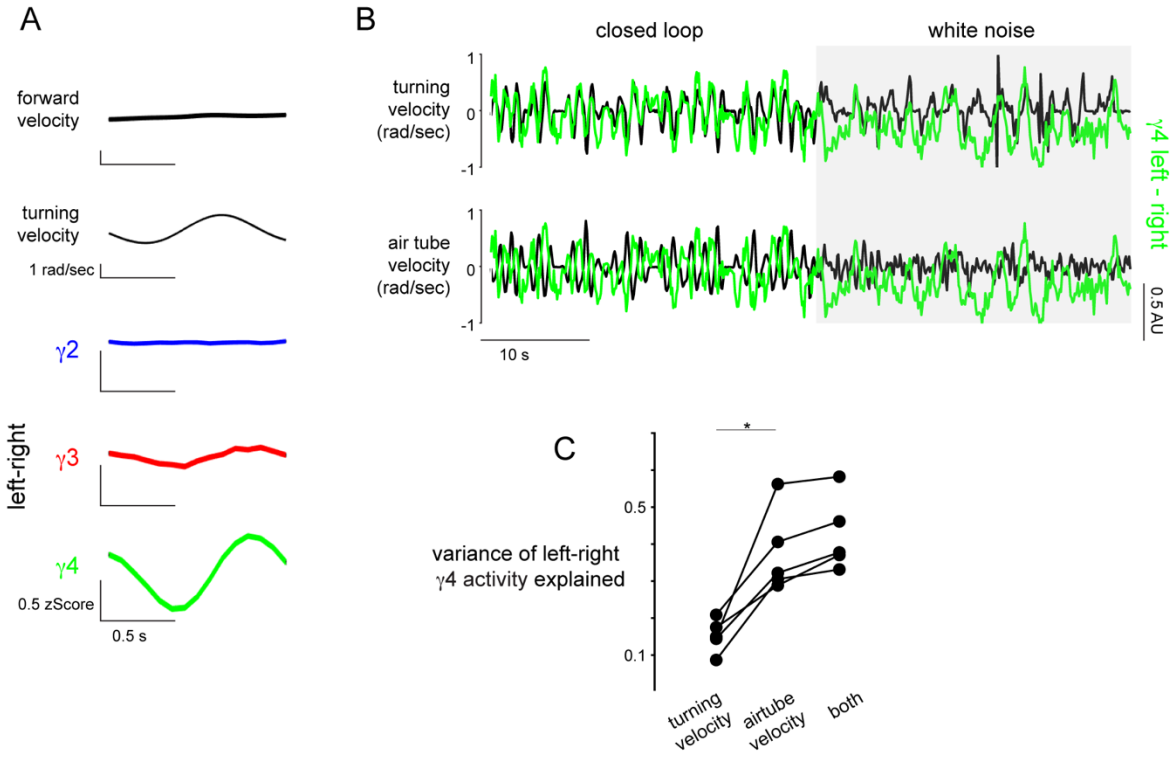
A
forward velocity
turning velocity
1 rad/sec
γ2
left-right
γ3
γ4
0.5 zScore
0.5 s
B
closed loop
white noise
turning velocity (rad/sec)
1
0
-1
air tube velocity (rad/sec)
10 s
γ4 left - right
0.5 AU
C
variance of left-right γ4 activity explained
0.5
0.1
*
turning velocity
airtube velocity
both

heading of an animal through the differential activity across the two hemispheres. Such a representation would only emerge in closed loop when the fly had a sensory cue with which to orient its heading. In closed loop, however, the position of the airflow around the animal is intrinsically yoked to the turning of a fly, raising the possibility that the inter-hemispheric difference could arise from changes in wind direction. To determine if this differential γ4 activity was related to the movement of the animal or contingent on its sensory experience, we recorded from the same animals in both closed loop and while providing them with a pseudorandom rotating airstream (a temporally filtered white noise pattern) unlinked from the fly's behavior. In closed loop, the difference in γ4 activity across the left and right hemispheres mirrored both the animal's turning and the change in air tube position (which are inherently tethered together); however, when behavior was uncoupled from the movement of the airstream, this was no longer the case. Although over a timescale of multiple seconds the inter-hemisphere difference superficially appeared to align with the animal's turning, over the finer time frame of hundreds of milliseconds the transient differences between the left and right γ4 DANs were more strongly associated with the rapid changes in the position of the air tube (Figure 3.6B). To quantitatively assess these relationships, we constructed a linear model to predict the left-right difference in γ4 activity during presentation of the white noise pattern from either behavior, air tube velocity, or both, and found that significantly more of the variance in γ4 activity was explained by the movement of the airstream, with little additional contribution from the turning behavior of the fly (Figure 3.6C). Therefore, riding on top of the movement-related γ4 DAN activity is a sensory representation of the changing direction of airflow around an animal.

3.5 Activity of Dopaminergic Neurons During Odor Tracking

In addition to the subtle differences in the neural representation of sensory and motor variables that emerged when animals were transitioned into closed loop, we examined the correlations between DAN activity and behavior during olfactory navigation and anemotaxis. We therefore presented flies walking in our closed loop system with 10 seconds of ACV interleaved with 30 seconds of clean air. We were able to capture a variety of behavioral responses to odor because although animals often reoriented to walk upwind, they also modulated their velocity and occasionally walked downwind or crosswind within the odor plume (Figure 3.7).

On average, γ4 DANs were activated by ACV. This odor is released by fruit and other organic matter that are a source of food for *Drosophila* and an advantageous location for egg-laying and larval development. ACV is therefore innately predictive of essential nutrients and rewarding food. The observed responses in γ4 are thus consistent with the sensitivity of this dopaminergic pathway to appetitive sensory cues. In contrast, γ2 DANs and γ3 DANs were inhibited or unresponsive to ACV stimulation (Figure 3.7A). A notable feature of odor-evoked DAN activity, however, was its variability, even between sequential trials within an individual animal (Figure 3.7B). This variation appeared related to the nature of the behavioral response to the odor. In particular, γ4 responses were strongest during trials when animals vigorously reoriented in the odor plume to track upwind and weaker when animals failed to alter their heading and continued to walk crosswind instead (Figure 3.7B). Plotting the magnitude of γ4 DAN responses as a function of the net upwind displacement in the odor plume revealed that γ4 DAN activity was correlated with the strength of the evoked tracking response (Figure 3.7C). γ2 DAN

Figure 3.7 | Mushroom Body Dopaminergic Neurons Encode the Strength of Behavioral Responses to Apple Cider Vinegar. (A) Triggered average of γ DAN $\Delta F/F_o$ before, during, and after odor presentation. Thick dark lines indicate average γ DAN activity. Translucent thin lines represent DAN activity from individual odor presentations. F_o= average sytGCAMP6s activity from t=-10 to t=0 seconds before the onset of odor. Orange bar indicates odor pulse. N=26 flies, 143 odor presentations. **(B)** Fictive 2D position and DAN>sytGCAMP6s activity as animals respond to odor stimuli. Top row: fictive 2D trajectory of a tethered animal as it walks in closed loop during two consecutive five minute trials. During each trial animals were presented with a continuous flow of clean air and received five 10sec presentations of the odor apple cider vinegar (ACV). Clean air presentation indicated in black and ACV presentation indicated in orange. Middle row: zoomed in depiction of indicated trajectories over 20 sec period centered on ACV presentation (10sec prior to odor and 10sec during odor). Bottom row: γ DAN $\Delta F/F_o$ before and during odor presentation (10 sec prior to odor and 10sec during odor). F_o defined as in (A). **(C)** γ2 and γ4 DAN activity during odor presentation is correlated with upwind displacement and change in absolute heading. Average γ DAN $\Delta F/F_o$ vs upwind displacement (left), Δ|heading| (middle), and Δforward velocity (right) during odor presentation. Upwind displacement normalized by average net motion during movement bouts. γ DAN $\Delta F/F_o$ is averaged over t=2 to t=10 sec after odor onset. F_o defined as in (A). Pearson correlation coefficient (r) indicated where relationship is statistically significant ($p<0.00001$ with Bonferroni correction). Fisher r-to-z transformation indicates significant differences in correlation coefficients for γ4-Δ|heading| and γ4-Δforward velocity relationship with $z=6.65$. N=26 flies, 143 odor presentations. **(D)** Upwind displacement in odor is determined by an animal's orientation rather than speed. Upwind displacement vs average Δ|heading| (left) and average Δforward velocity (right) during odor presentation. Points are color-coded by magnitude of average γ DAN $\Delta F/F_o$ in odor. Average γ DAN $\Delta F/F_o$ in odor is calculated as in (C) and average Δ|heading| and average Δforward velocity are calculated identically to average γ DAN $\Delta F/F_o$. Upwind displacement is normalized as in (C) Pearson correlation coefficient (r) for the relationship between upwind displacement and Δ|heading| is $r = -0.6000$ with $p=0.00001$. Pearson correlation coefficient (r) for the relationship between upwind displacement and Δforward velocity is $r=0.2878$ with $p=0.0005$. Fisher r-to-z transformation indicates significant differences in correlation coefficients with $z=8.28$. N=26 flies, 143 odor presentations. **(E)** Inverse correlation between odor responses in γ2 and γ4 DANs. $\Delta F/F_o$ of DAN>sytGCaMP6s in the γ2 vs γ4 compartments during odor presentation. $\Delta F/F_o$ average calculated as in (C). Pearson correlation coefficient (r) indicated where relationship is statistically significant ($p<0.00001$). N=26 flies, 143 odor presentations.

Figure 3.7

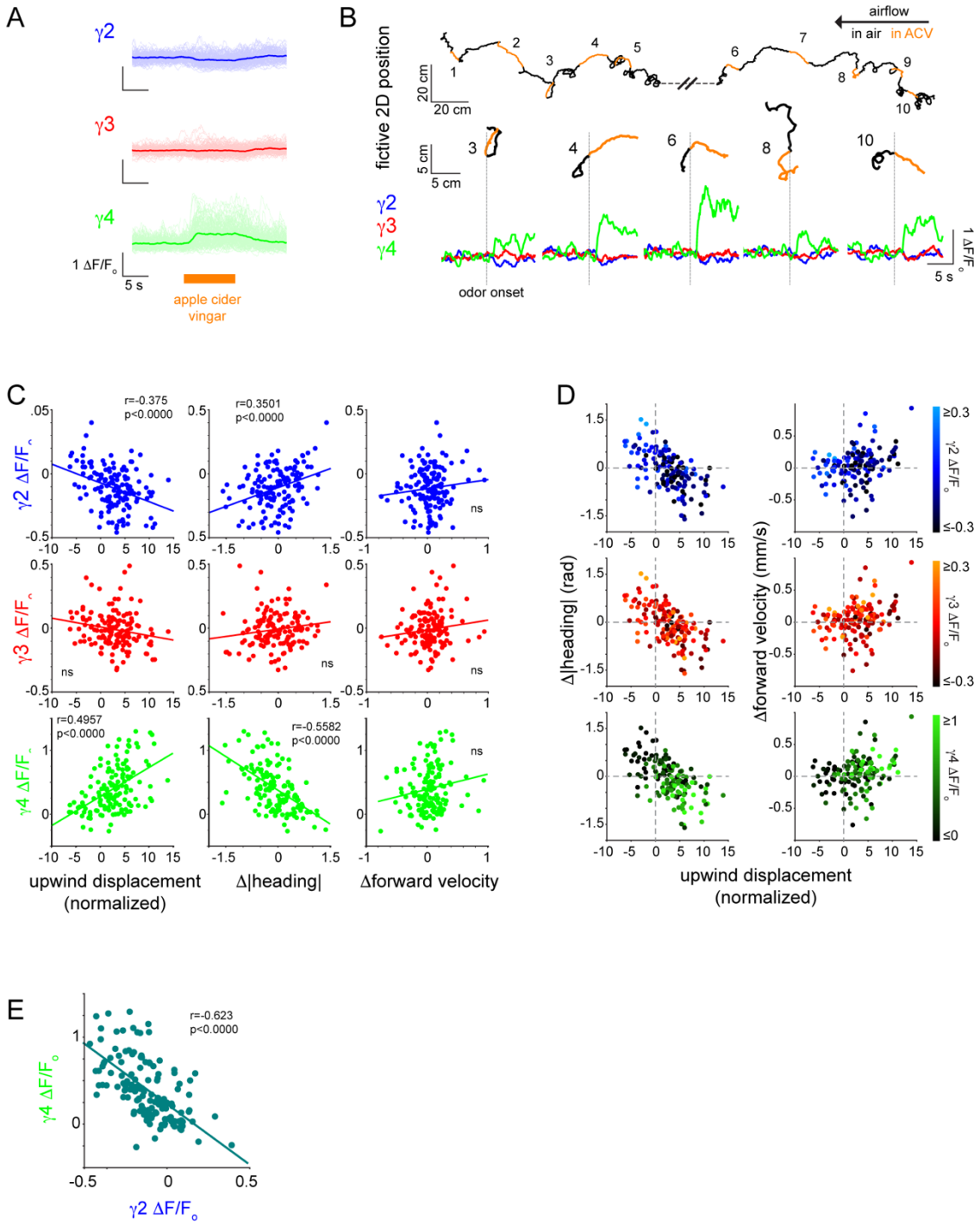
A
γ2
γ3
γ4
1 ΔF/F$_o$
5 s
apple cider vingar
B
fictive 2D position
airflow
in air
in ACV
20 cm
5 cm
odor onset
C
r=-0.375
p<0.0000
r=0.3501
p<0.0000
ns
r=0.4957
p<0.0000
r=-0.5582
p<0.0000
upwind displacement (normalized)
Δ|heading|
Δforward velocity
D
Δ|heading| (rad)
Δforward velocity (mm/s)
upwind displacement (normalized)
E
r=-0.623
p<0.0000

activity was also modulated by the strength of the behavioral response, with the largest inhibition apparent in trials where the net upwind displacement was greatest. Indeed the odor responses in γ2 and γ4 DANs were strongly anti-correlated (Figure 3.7E), indicating that the antagonistic interaction between these DANs was maintained during odor tracking. The dependence of DAN activity on tracking could not be explained by differences in the efficacy of odor stimulation when animals walked upwind or crosswind since KC responses to ACV were equivalent independent of the position of the odor tube (Figure 3.8A). Furthermore, these correlations were not apparent when animals walked in clean air (Figure 3.8B), suggesting they reflect an emergent property of the DAN network that arises when animals are engaged in odor tracking.

In the closed loop paradigm, flies tracked towards the fictive odor source predominantly by decreasing their absolute heading to reorient in the upwind direction, rather than increasing their forward velocity to walk faster (Figure 3.7D). While changes in the heading were well correlated with the magnitude of DAN responses, forward velocity was not, suggesting that DAN activity may be tuned to behavioral variables relevant to odor navigation (Figures 3.7C,D). To further explore the relationship between DAN activity and these behavioral variables during odor tracking, we calculated a cross-correlation matrix at various temporal offsets relative to the odor stimulus (Figure 3.9A). This analysis reveals how DAN activity at one time point correlates with past, present, and future behavior, with points along the diagonal reflecting real-time correlations while points below and above the diagonal are indicative of correlations with preceding or subsequent behavior, respectively. As expected from the linear filters (Figure 2.8A and Figure 3.5A), γ2 and γ4 DAN activity tracked an animal's current forward velocity in clean air, evident by the significant

Figure 3.8 | Odor Responses of Intrinsic Mushroom Body Neurons Are Not Sensitive to Direction of Airflow and Animal Orientation is Not Reflected in Dopaminergic Neuron Activity in the Absence of Odor. (A) $\Delta F/F_o$ of GCaMP6s activity in γ Kenyon cells (KCs) during a 10 sec presentation of ACV from different angles relative to the fly (left). F_o= average GCAMP6s activity from t=-10 to t=0 seconds before the onset of odor. Average $\Delta F/F_o$ of GCaMP6s in γ KCs during odor presentation at different orientations (right). One-way ANOVA, no statistical significance. **(B)** Linear filters predicting DAN activity (as in Figure 2.8A) during bouts of continuous movement using |heading| centered on an eight second window as predictors ± 95% confidence interval for animals walking in closed loop during the presentation of clean air. N=20 animals, 32 five minute trials.

Figure 3.8

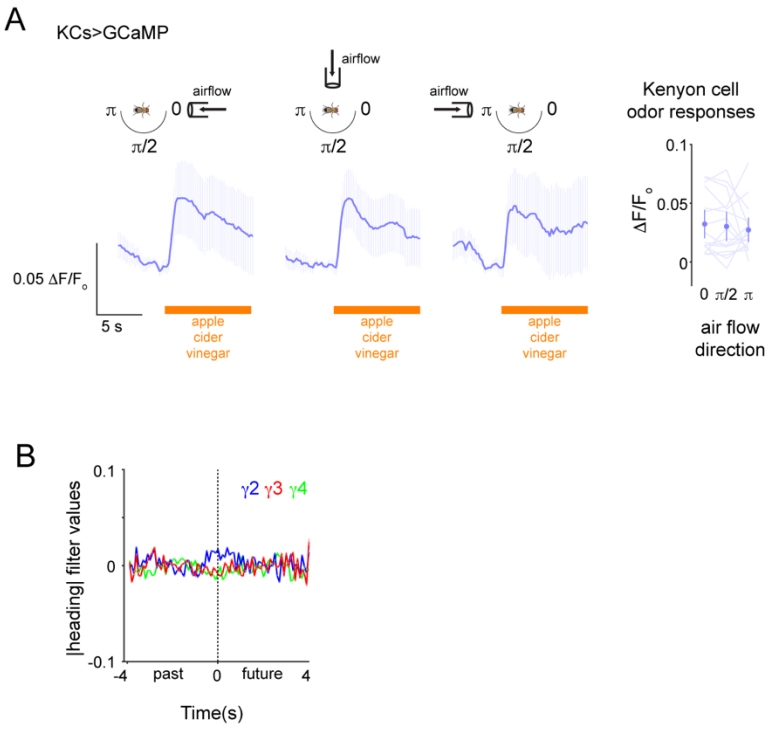
A
KCs>GCaMP
airflow
airflow
airflow
π
0
π/2
0.05 ΔF/F$_o$
5 s
apple cider vinegar
Kenyon cell odor responses
0.1
0.05
0
ΔF/F$_o$
0 π/2 π
air flow direction
B
γ2 γ3 γ4
|heading| filter values
0.1
0
-0.1
-4
past
0
future
4
Time(s)

Figure 3.9 | Mushroom Body Dopaminergic Neurons Correlate with Orientation in an Odor Plume and Anticipate Future Tracking. (A) Cross-correlation matrix between forward velocity (left) and |heading| (right) and γ DAN activity during the 10 sec prior to odor and the 10 sec during odor presentation. Diagonal represents real-time while points above and below represent the correlation of γ DAN activity with future and past behavior, respectively. **(B)** Same as (A) except centered on a 20 sec epoch during which only clean air is presented to the animal (10 sec offset from actual odor presentation). Colored points indicate statistically significant correlations ($p<0.05$). N=26 flies, 143 odor presentations.

Figure 3.9

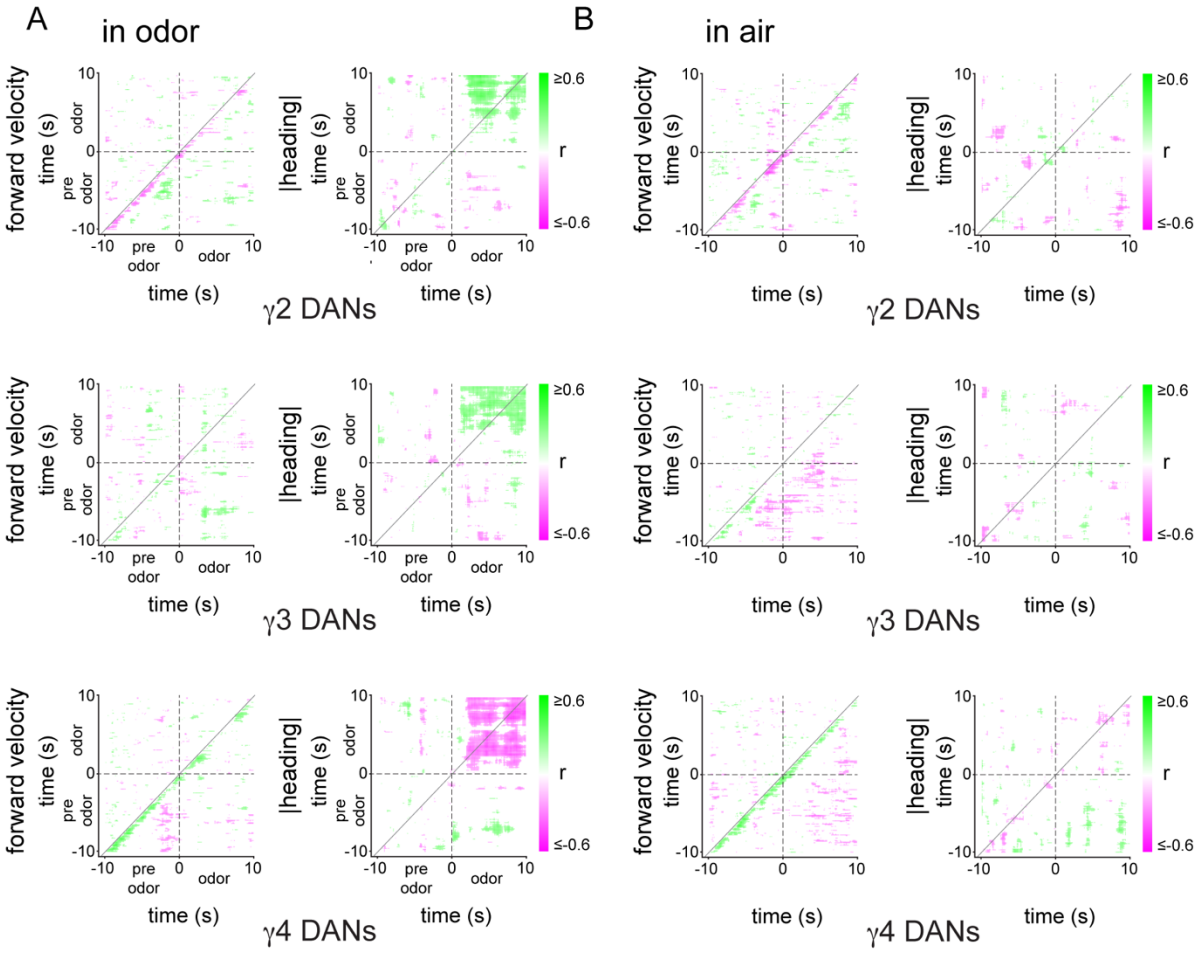
A
in odor
B
in air
forward velocity
time (s)
pre odor
odor
|heading|
r
≥0.6
≤-0.6
γ2 DANs
γ3 DANs
γ4 DANs

negative or positive correlations localized to the diagonal of the matrix. Within the odor plume, however, this relationship weakened and the DANs instead became correlated with the heading of an animal. Interestingly, the activity of all DAN subsets was significantly correlated with the future heading of an animal throughout the odor stimulation epoch, up to 8 seconds forward in time, suggesting that they carry predictive information about ensuing odor-tracking behavior. This anticipatory activity depended on the presence of the olfactory cue and was not apparent in the cross-correlations calculated for periods preceding or following odor stimulation when animals walked in clean air (Figure 3.9B).

One possible explanation for this anticipatory activity is that when animals initiate upwind tracking, they maintain an invariant trajectory throughout the end of the odor pulse. Indeed, calculating the autocorrelation of an animal's heading revealed that its current heading was correlated with its future heading for up to 3 seconds in advance (Figure 3.10A). However, this autocorrelation was similar in both clean air and odor, suggesting it reflects a general feature of how animals navigate when walking in this paradigm, and occurred over a narrower temporal window than the period over which DAN activity was predictive of odor tracking behavior (Figure 3.10B).

To further explore the possibility that DAN activity carries prospective information about odor-tracking behavior, we worked with Adrienne Fairhall and Rich Pang to build a nested model that quantified how much the past, present, or future heading of an animal contributed to predicting DAN activity in the initial epoch of an odor response (seconds 1-4 of the odor stimulus) (Figure 3.11A). While the heading of a fly prior to odor onset had a negligible contribution to DAN

Figure 3.10 | Anticipatory Dopaminergic Activity Is Only Present in the Odor Plume and Cannot be Accounted for by the Correlation Between Present and Future Heading. (A) Auto cross-correlation matrix of forward velocity (left) and |heading| (right) before and during odor presentation (same time period as in Figure 3.9A). **(B)** DAN activity is anticipatory of animal orientation during odor presentation. Cross correlation matrix of |heading| and γ DAN activity during odor presentation (same data as right upper quadrant of Figure 3.9A, right). Auto cross-correlation of heading (left, same data as right upper quadrant of (A)) does not contain same predictive capabilities. Colored points indicate statistically significant correlations ($p<0.05$). N=26 flies, 143 odor presentations.

Figure 3.10

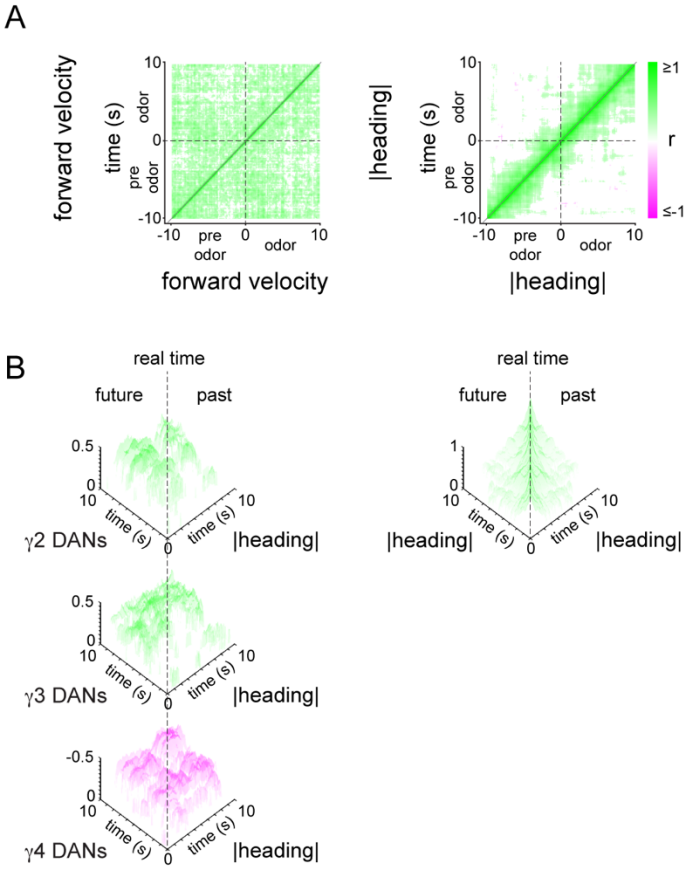
A
forward velocity
time (s)
pre odor
odor
forward velocity
|heading|
time (s)
pre odor
odor
|heading|
r
≥1
≤-1
B
real time
future
past
γ2 DANs
|heading|
γ3 DANs
|heading|
γ4 DANs
|heading|
real time
future
past
|heading|
|heading|

Figure 3.11 | A Nested Linear Model Demonstrates That Dopaminergic Neurons Encode Orientation in an Odor Plume and Anticipate Future Tracking. A nested linear model predicts γ DAN activity during the initial phase (t=1 to t=4) of odor presentation based on pre-odor heading (t=-10 to t=0), initial Δforward velocity (t=1 to t=4), initial Δ|heading| (t=1 to t=4), and future Δ|heading| (t=7 to t=10). **(A)** Schematic of the nested linear model to predict initial odor responses in γ DANs. Predictors are added to the model stepwise and difference in explained variance computed using F-test. **(B)** Additional variance in γ DAN activity explained by the nested linear model with the stepwise addition of each predictor. Colored lines represent model predictions when true odor presentations are the model's input. Black lines represent model predictions when a period of clean air presentation (10sec offset) are the model's inputs. F-test, $p<0.05$ (*), $p<0.01$ (**). N=26 flies, 143 odor presentations.

Figure 3.11

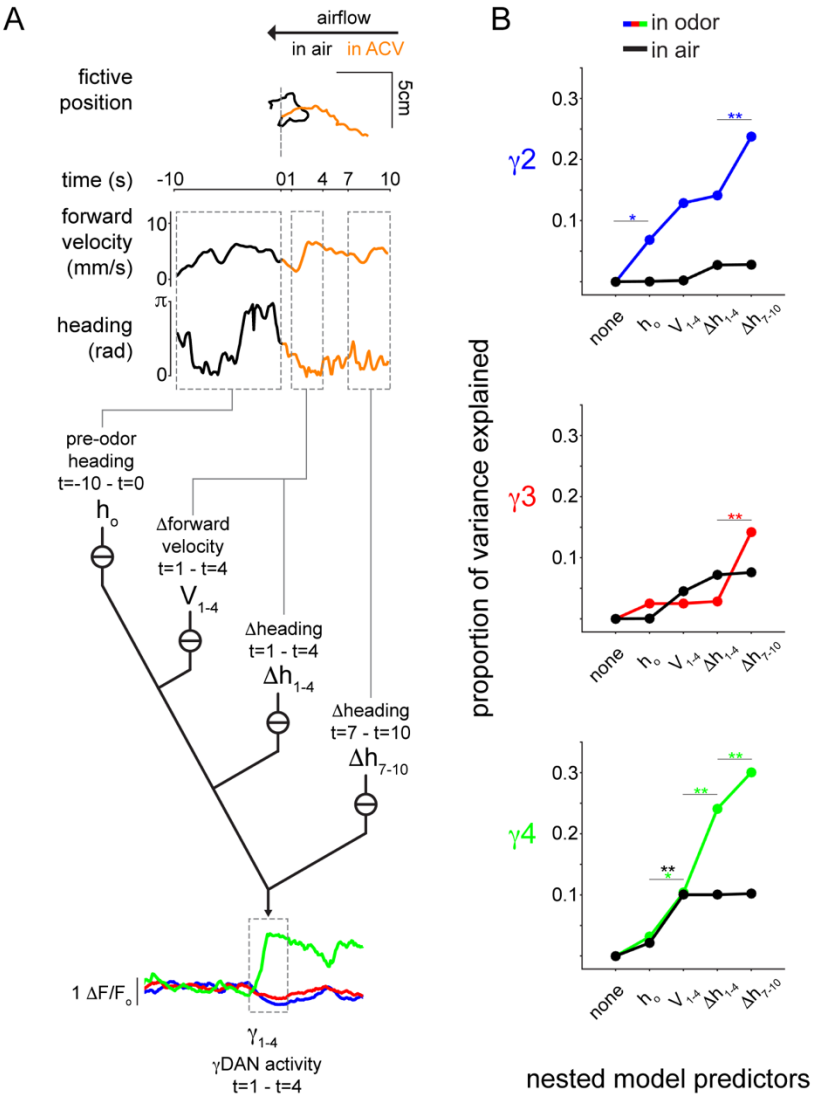
A
airflow
in air
in ACV
fictive position
5cm
time (s)
-10
01
4
7
10
forward velocity (mm/s)
10
0
heading (rad)
π
0
pre-odor heading t=-10 - t=0
h0
Δforward velocity t=1 - t=4
V1-4
Δheading t=1 - t=4
Δh1-4
Δheading t=7 - t=10
Δh7-10
1 ΔF/F0
γ1-4
γDAN activity t=1 - t=4
B
in odor
in air
γ2
γ3
γ4
0.3
0.2
0.1
proportion of variance explained
none
h0
V1-4
Δh1-4
Δh7-10
nested model predictors

activity, including the current heading of the animal significantly improved its ability to predict γ4 DAN activity. In contrast, the inclusion of future heading significantly improved the model's performance for all three γ DAN populations (Figure 3.11B).

Our data suggest that in the context of a sensory-driven behavior with an appreciable end-goal, like odor tracking, the MB DANs appear to neither strictly represent the odor cue, nor the kinematics of movement, but rather reflect an animal's behavioral response to the stimulus.

3.6 Dopaminergic Neurons Correlate with Different Movements Depending on an Animal's Behavioral Context

We sought to test our hypothesis that MB DAN activity was related to the behavioral response to the stimulus by requiring animals to alter the actions necessary to track towards the fictive odor source. We reasoned that the relationship between DAN activity and upwind tracking should be maintained even if implemented through distinct motor programs. As noted earlier, within a laminar flow chamber a small fraction of flies were already walking upwind prior to odor onset and these animals responded to ACV, not by reorienting, but by simply increasing their forward velocity to walk faster in the upwind direction towards the odor source (Figure 3.1D). We therefore modified the parameters of the closed loop system to bias tethered animals to walk upwind even in clean air and replicate this distinct odor tracking strategy. High wind speeds are known to trigger anemotaxis in *Drosophila*[435], so by increasing the airflow and restricting the air tube's movements to an 180° arc in front of the fly, we found that the animals walked upwind

almost continuously for several meters and responded to a pulse of ACV by maintaining their upwind trajectory and transiently increasing their forward velocity (Figure 3.12A).

Under these conditions, we observed a correlation between the magnitude of odor-evoked DAN activity and the net upwind displacement, similar to the relationship seen in the low airflow context (Figure 3.12B). An animal's heading, however, was no longer the primary behavioral determinant of how far an animal walked upwind and was only weakly correlated with DAN activity (Figures 3.12B,C). Rather, in the high airflow context, γ4 activity was strongly correlated with an animal's forward velocity, the behavioral feature most relevant to odor tracking (Figures 3.12B,C). In contrast, while animals tracking odors at lower wind speeds also occasionally modulated their forward velocity, it was neither correlated with an animal's upwind displacement nor DAN activity in that context (Figures 3.7C,D).

We next analyzed how different behavioral parameters contribute to DAN activity as animals tracked in high wind flow. Performing a cross-correlation analysis and building a nested model both reinforced that during odor presentation in the high airflow context DAN activity was predominantly correlated with forward velocity (Figure 3.13). While DAN activity was correlated with an animal's current forward velocity in clean air across all conditions, this relationship was selectively strengthened in the presence of the odor stimulus in high airflow. Furthermore, DAN activity now carried prospective information about an animal's future forward velocity (Figures 3.13A,B). Conversely, the current or future heading of an animal no longer meaningfully predicted DAN activity either within the odor plume or in clean air in this behavioral context (Figure 3.13C).

Figure 3.12 | Dopaminergic Neurons Correlate with Anemotaxically Relevant Movements. During continuous upwind walking, flies respond to ACV by increasing forward velocity and this behavior becomes emergently correlated with the γ DAN network. **(A)** Fictive 2D position (top two rows), |heading| (3rd row), forward velocity (4th row) and DAN>sytGCAMP6s activity (bottom row, $\Delta F/F_o$) as a representative animal responds to odor in closed loop while experiencing high airflow. Top-most panel: Fictive 2D trajectory of representative animal during a five minute trial when the animal received one 60sec ACV presentation. Clean air presentation indicated in black and ACV presentation indicated in orange. 2nd panel: zoomed-in depiction of above trajectory over 20sec period centered on ACV presentation (10sec prior to odor and 10sec during odor). 3rd panel: |heading| during above time window. 4th panel: forward velocity during above time window. Bottom panel: γ DAN $\Delta F/F_o$ before and during odor presentation (10sec prior to odor and 10sec during odor, same as above time window). F_o= average sytGCAMP6s activity from t=-10 to t=0 seconds before the onset of odor. **(B)** Under high flow conditions, upwind displacement in odor is determined by an animal's forward velocity rather than orientation. Upwind displacement vs average Δ|heading| (left) and average Δforward velocity (right) during odor presentation. Points are color-coded by magnitude of average γ DAN $\Delta F/F_o$ in odor. Average γ DAN $\Delta F/F_o$, average Δ|heading|, average Δforward velocity, and upwind displacement in odor are calculated as in Figure 3.7D. Pearson correlation coefficient (r) for the relationship between upwind displacement and Δ|heading| is r = -0.5744 with p=0.0001. Pearson correlation coefficient (r) for the relationship between upwind displacement and Δforward velocity is r=0.7023 with p<0.00001. N=22 flies, 41 odor presentations. **(C)** γ4 DAN activity during odor presentation is correlated with upwind displacement and change in Δforward velocity but not absolute heading. Average γ DAN $\Delta F/F_o$ vs upwind displacement (left), Δ|heading| (middle), and Δforward velocity (right) during odor presentation under high flow conditions. Upwind displacement and $\Delta F/F_o$ are calculated as in Figure 3.7C. Pearson correlation coefficient (r) indicated where relationship is statistically significant (p<0.01 with Bonferroni correction). Fisher r-to-z transformation indicates significant differences in correlation coefficients for γ4-Δ|heading| and γ4-Δforward velocity relationship with z=6.65.N=22 flies, 41 odor presentations.

Figure 3.12

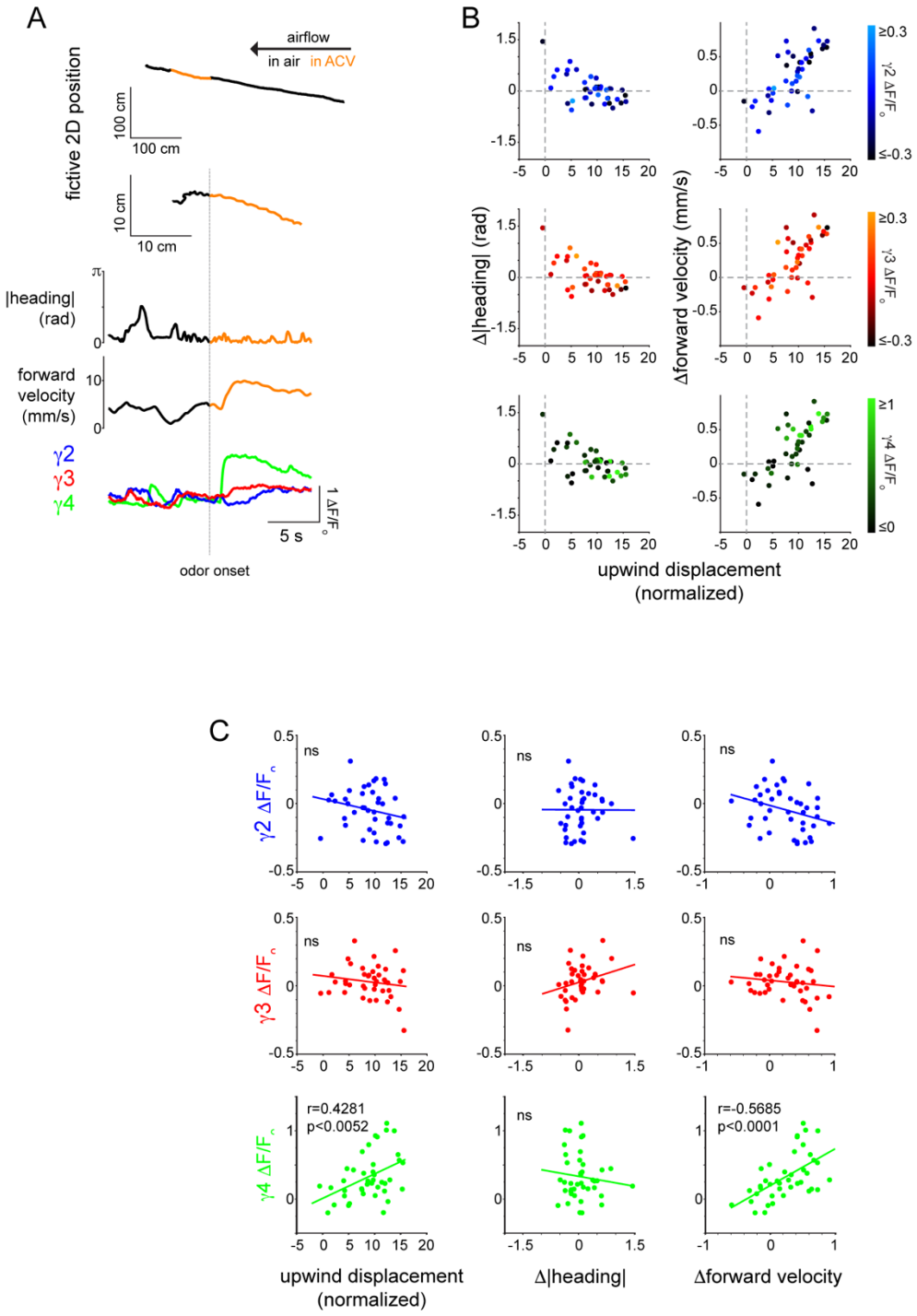
A
airflow
in air
in ACV
fictive 2D position
100 cm
100 cm
10 cm
10 cm
|heading| (rad)
forward velocity (mm/s)
γ2
γ3
γ4
1 ΔF/F0
5 s
odor onset
B
Δ|heading| (rad)
Δforward velocity (mm/s)
upwind displacement (normalized)
≥0.3
γ2 ΔF/F0
≤-0.3
≥0.3
γ3 ΔF/F0
≤-0.3
≥1
γ4 ΔF/F0
≤0
C
γ2 ΔF/F0
γ3 ΔF/F0
γ4 ΔF/F0
ns
r=0.4281
p<0.0052
r=-0.5685
p<0.0001
upwind displacement (normalized)
Δ|heading|
Δforward velocity

Figure 3.13 | Mushroom Body Dopaminergic Neurons Correlate with Forward Velocity in an Odor Plume in the High Airflow Context. (A) Cross correlation matrix between forward velocity (left) and |heading| (right) and γ DAN activity (as in Figure 3.9) as animals experience a high rate of airflow. Time window centered on odor presentation, depicting 10sec prior to odor and the 10sec during odor presentation. **(B)** Same as (A) except centered on a 20sec epoch during which only clean air is presented to the animal (10sec offset from actual odor presentation). Colored points indicate statistically significant correlations ($p<0.05$). N=22 flies, 41 odor presentations. **(C)** A nested linear model as in Figure 3.11A to predict γ DAN activity during the initial phase (t=1 to t=4) of odor presentation under high airflow conditions. Additional variance in γ DAN activity explained by the nested linear model with the addition of each predictor. Colored lines represent model predictions when true odor presentations are the model's input. Black lines represent model predictions when period of clean air presentation (10sec offset) are the model's inputs. F-test, $p<0.05$ (*), $p<0.01$ (**).

Figure 3.13

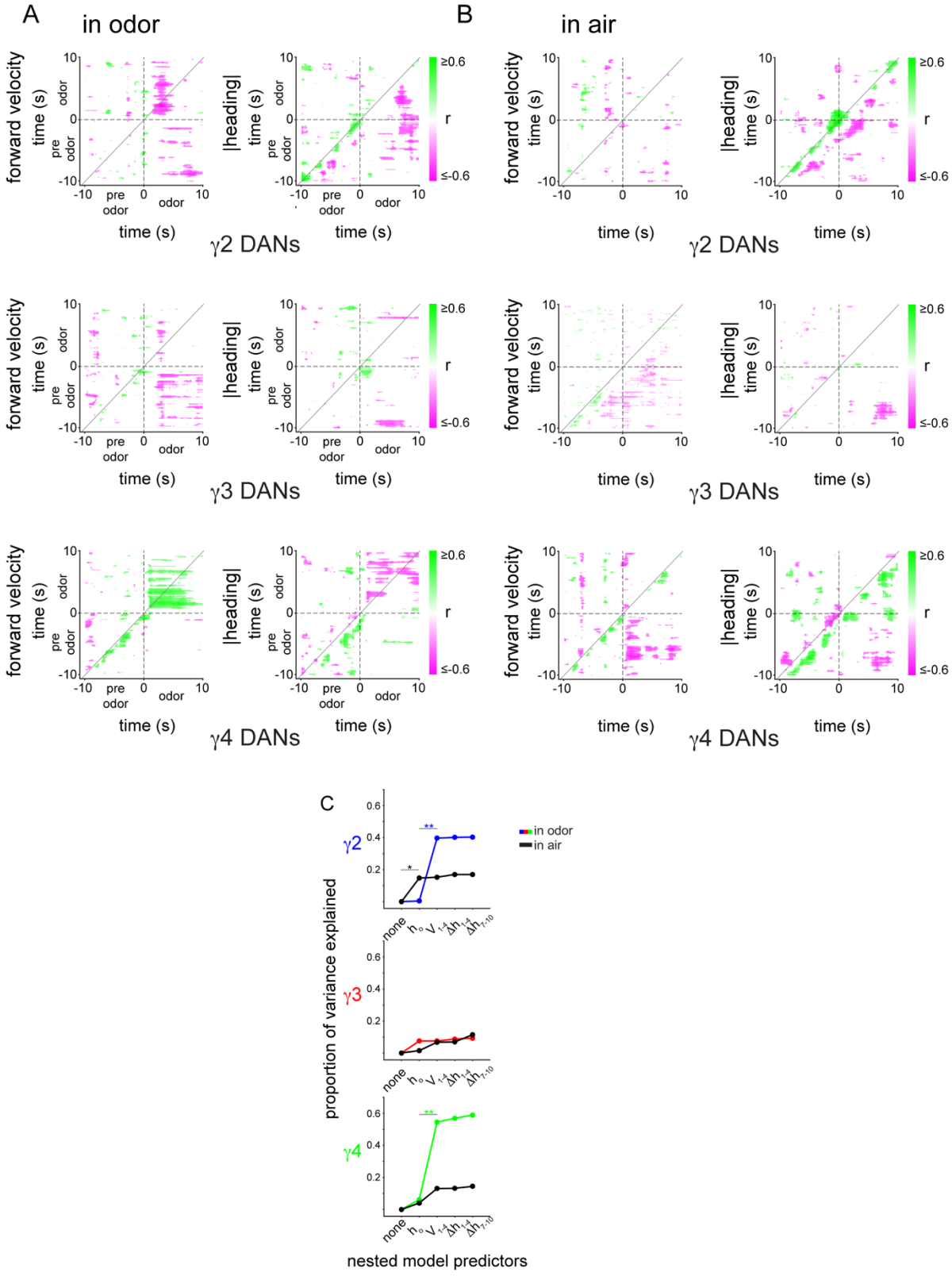
A
in odor
B
in air
forward velocity
time (s)
|heading|
r
≥0.6
≤-0.6
pre odor
odor
γ2 DANs
γ3 DANs
γ4 DANs
C
γ2
γ3
γ4
in odor
in air
proportion of variance explained
nested model predictors
none

Thus in the context of distinct olfactory navigation strategies, different behaviors that achieve the same goal appear to be similarly represented by DAN activity.

In the presence of a high airflow, flies spent the majority of time tracking upwind, even in the absence of an odor, while in low airflow, this approach behavior is only observed in the presence of an appetitive odor. We reasoned that if DAN activity was related to movements associated with approach or tracking behavior, there may be a representation of the animal's heading in clean air selectively in the high airflow context associated with animal's turns to maintain their upwind trajectory. Indeed, whereas the linear filters predicting DAN activity from heading in low airflow conditions showed no representation of the animal's orientation, when animals were engaged in extended bouts of anemotaxis in the presence of clean air alone, both γ2 and γ4 appeared to reflect the fly's immediate heading (Figure 3.14A). These data suggest that, across a range of different contexts, the DANs are consistently tuned to most relevant behavioral metric.

3.7 Dopaminergic Neurons Correlate with Strength of Approach Behaviors Independent of Odor Identity

Despite the fact that we recorded DAN activity in starved animals and ACV is an appetitive food odor, we nonetheless observed a number of trials when flies did not track upwind in the presence of this olfactory cue (Figures 3.7B-D). This is consistent with our observation that when freely moving animals in our behavioral chambers were presented with ACV, they did not all track upwind to the same extent, with some individuals not responding, continuing to walk crosswind,

Figure 3.14 | Dopaminergic Neurons Encode Orientation in Clean Air When Animals are Engaged in Upwind Tracking. (A) Linear filters predicting DAN activity (as in Figure 2.8A and Figure 3.5A) during bouts of continuous movement using |heading| centered on an eight second window as predictors ± 95% confidence interval for animals walking in closed loop experiencing high airflow and engaged in active tracking of the airstream (dark lines, N=22 flies, 41 five minute trials) and animals experiencing low airflow and not attending to the movement of the airstream (light lines, N=20 animals, 32 five minute trials, same as Figure 3.8B).

Figure 3.14

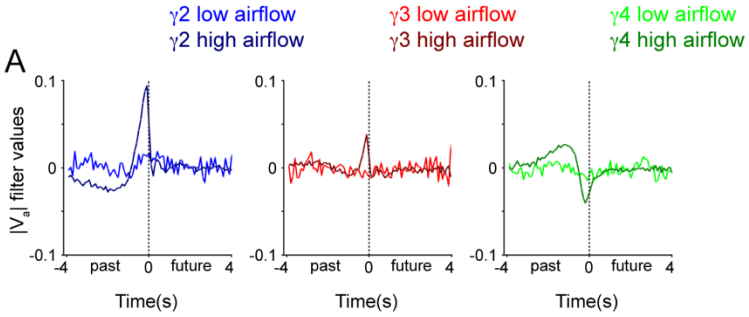
A
γ2 low airflow
γ2 high airflow
γ3 low airflow
γ3 high airflow
γ4 low airflow
γ4 high airflow
|V_a| filter values
0.1
0
-0.1
-4
past
0
future
4
Time(s)

or even occasionally moving away from the odor (Figure 3.1). Thus even an appetitive odor does not appear to trigger invariant approach behaviors. Similarly, when we presented freely moving flies in our behavioral chamber with CO_2, an aversive odor, we occasionally observed animals reorient and walk upwind towards the odor source (Figure 3.2C), suggesting that an aversive cue can sometimes produce approach behavior. Our findings suggest that the γ4 DANs reflect the strength of an animal's approach towards an olfactory cue, but not the cue itself, raising the possibility that these neurons should still respond even when animals tracked upwind towards an aversive odor.

To examine whether the relationships between DAN activity and behavioral responses to odor changed in the presence of an aversive stimulus, we repeated our previous protocol in the low airflow context but presented brief pulses of CO_2 rather than ACV. As expected, flies were much less likely to track upwind to CO_2 than to ACV, and the γ4 DAN odor responses were significantly diminished overall (Figures 3.15A-C). However, on the rare occasions that a fly did reorient and walk towards the fictive odor source, γ4 DAN activity increased and remained correlated with the animal's change in heading within the odor plume (Figure 3.15D). These data further support that γ4 DANs reflect an animal's engagement in olfactory approach behavior, independent of the identity of the odor.

Together, our data suggest that in the context of a sensory-triggered behavior, like odor tracking, the MB DANs neither strictly represent the animal's sensory experience, nor its physical movements, but rather reflect the strength or vigor of the behavioral response to the odor. We hypothesize that patterns of DAN activity are not encoding the specific physical actions of an

Figure 3.15 | Dopaminergic Neurons Correlate with Approach Behavior Regardless of Odor Identity. (A) Fictive 2D trajectories of representative tethered animal in closed loop being presented with ACV (left, orange) and CO_2 (right, grey). **(B)** Animals have diminished behavioral responses to CO_2 compared with ACV. Upwind displacement (left), average |heading| (middle), and average forward velocity (left) of tethered animals in closed loop during the presentation of ACV (black) and CO_2 (grey). Paired t-test with Bonferroni correction, $p<0.05$ (*), $p<0.001$ (**). N=7 flies, 98 odor presentations (48 ACV and 50 CO_2). **(C)** Dopaminergic neurons differentially respond to ACV and CO_2. Paired t-test with Bonferroni correction, $p<0.01$ (*), $p<0.001$ (**). N=7 flies, 98 odor presentations (48 ACV and 50 CO_2). **(D)** γ4 DAN responses to CO_2 are still correlated with an animal's reorientation behavior. Average γ DAN $\Delta F/F_o$ vs upwind displacement (left), Δ|heading| (middle), and Δforward velocity (right) during odor presentation. Upwind displacement normalized by average net motion during movement bouts. γ DAN $\Delta F/F_o$ is averaged over t=2 to t=10 sec after odor onset. F_o defined as in (Figure 3.7C and Figure 3.12C). Pearson correlation coefficient (r) indicated where relationship is statistically significant ($p<0.00001$ with Bonferroni correction). N=7 flies, 98 odor presentations (48 ACV and 50 CO_2).

Figure 3.15

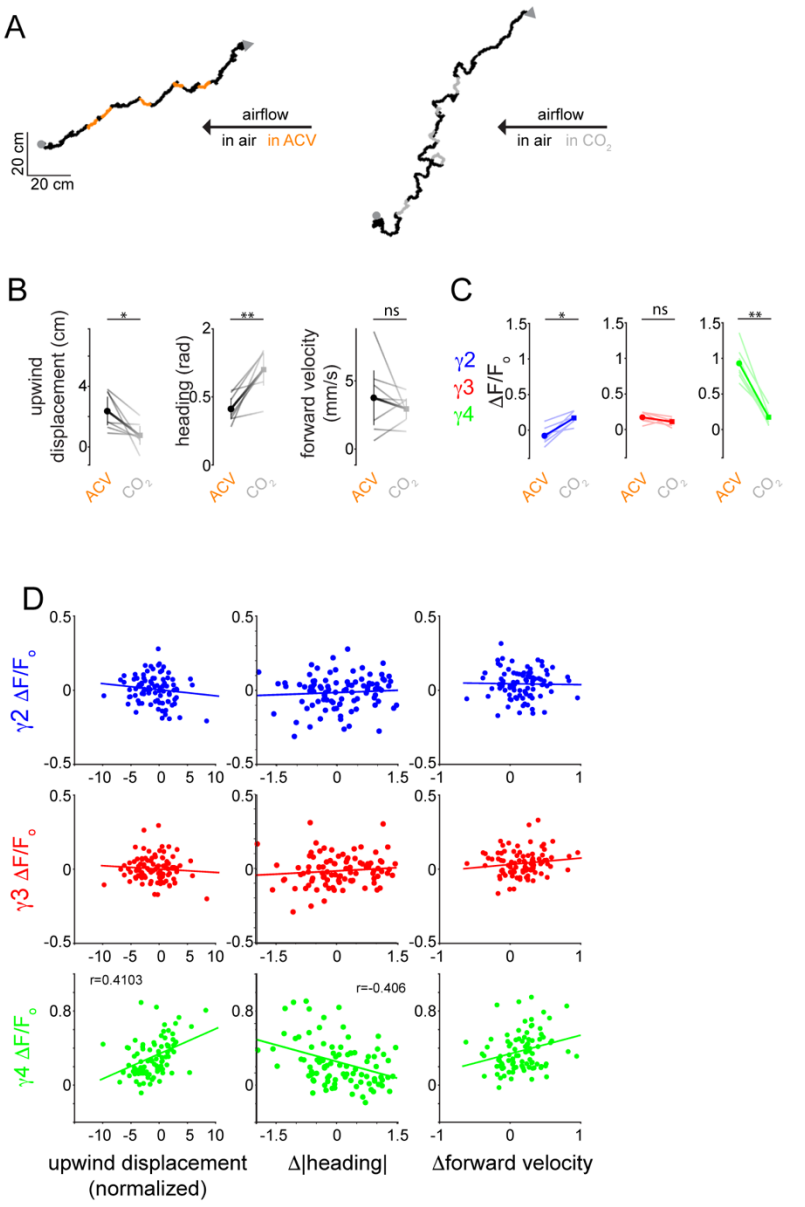
A
airflow
in air in ACV
20 cm
20 cm
airflow
in air in CO2
B
upwind displacement (cm)
heading (rad)
forward velocity (mm/s)
*
**
ns
ACV
CO2
C
γ2
γ3
γ4
ΔF/Fo
D
γ2 ΔF/Fo
γ3 ΔF/Fo
γ4 ΔF/Fo
r=0.4103
r=-0.406
upwind displacement (normalized)
Δ|heading|
Δforward velocity

animal, but rather are reflecting *why* an animal is performing a specific action or movement. DANs may therefore reflect the goal, purpose, or motivation underlying an animal's movements.

3.8 Discussion

Dopaminergic neurons innervating the mammalian striatum display heterogeneous patterns of activity and exhibit diverse sensory and motor correlates[147,179,198,208,218,220,222,225,227]. Understanding what features of an animal's experience are encoded in the ongoing activity of dopaminergic networks is key to unraveling the computations they perform and how they coordinate downstream circuits to shape behavior. Our work reveals that the DANs innervating the γ lobe of the MB bidirectionally signal reward and punishment to instruct learning, but they also contain detailed representations of the moment-by-moment movements of the animal. To gain insight into the nature of motor-related signals, we recorded from MB DANs as animals were actively engaged in sensory-triggered, purposive olfactory behaviors.

If the DANs strictly reflect the performance of a movement, then we expect those representations should be consistent regardless of the context in which they are executed. Alternatively, if the DANs were signaling the identity of a sensory stimulus, then their activity should be stereotypically linked to its presence or absence. Instead, we find that DAN activity reflects neither the precise kinematics nor the identity of an odor but the behavioral response to the odor. DAN activity, rather than passively denoting the presence of an appetitive food odor, appears to be contingent upon whether an animal engages in approach behavior and actively tracks

the stimulus. When behavioral tracking of the odor stimulus requires an animal to reorient, DAN activity correlates with its reorientations; when tracking requires an animal to instead increase its forward velocity, DAN activity correlates with its change in forward velocity. Furthermore, we observed a correlation with DAN activity and approach to an olfactory stimulus regardless of the identity of the odor itself. Our data suggest that the DANs are not simply correlated with the movements of the animal, but with the purpose or goal of a given movement. These observations invite speculation that the motor-related activity in DANs during spontaneous locomotion is likewise reflecting the purpose or motivation underlying specific movements. The non-stereotyped but tight temporal relationship between rapid changes in motor output and DAN activity supports a movement-tethered representation of motivation within certain MB dopaminergic pathways.

Although the activity of γ2 and γ3 DANs were able to anticipate future tracking behavior to some extent, anemotaxis appeared to be most robustly correlated with the γ4 DANs. Consistent with our previous findings that movement only negligibly contributed to γ5 DAN activity, neither the odor stimulus nor the behavioral response to it were apparent in this compartment (data not shown). These differences across the γ DAN subpopulations further support our hypothesis that each compartment may communicate unique information, with γ4, for instance, being especially relevant to avoidance or approach behaviors in the context of an airflow or odor and γ5 being tuned to gustatory signals and food ingestion.

These observations reinforce the striking parallels we have noted between the mammalian dopaminergic system and the MB. Striatal dopamine is argued to reflect the animal's underlying motivation to engage in a learned task and studies of mammalian dopaminergic pathways suggest

that these motivational signals promote and invigorate purposeful action[147,156,213,214,222,374]. A recent study reported that dopaminergic representations of movement reflect the animal's expectation of a rewarding outcome resulting from its actions[199]. Similarly, the γ DANs appear to encode the animal's drive to track upwind in our closed loop system. These mammalian representations of expected reward from a given movement may be directly analogous to the motor signals we observe in the DANs that indicate the goal or purpose of an action.

Studies of mammalian dopaminergic networks have struggled to understand how the heterogeneous sensorimotor correlates exhibited by dopaminergic neurons relate to their role in controlling locomotion and signaling reinforcement to instruct learning[147,160,215,216,218,220,227]. Models have attempted to unify correlates of reward and movement in dopaminergic populations by describing motor signals as movement-specific RPEs or framing all dopaminergic activity as encoding an effort-to-value ratio[144,147,208,222,436–438]. It has proven difficult, however, to elucidate the links between motor-related activity, reinforcement and reward signals, and representations of task-related variables in an experimental paradigm within dopaminergic pathways[160,199,227]. Furthermore, it has been challenging to disentangle motor-related signals from reflections of other features of the animal's experience while performing a task, such as choice[147,148,160,227].

The simple, concise, and stereotyped organization of the MB, however, allows us to appreciate that the same discrete DAN pathways that signals appetitive sugar reward to instruct the formation of positive olfactory associations also correlate with rapid changes in an animal's velocity and reflect the strength of real-time behavioral responses to odor. The MB therefore affords us the opportunity to specifically link reinforcement- and motor-related signals in the same

neural population, suggesting a fundamental connection between these variables within dopaminergic circuitry.

Multiplexed signals of movement and reward in mammalian striatal dopaminergic neurons may therefore be similar to the MB DANs and reflect the goal or motivation underlying a specific movement or action. This raises the possibility that representations of abstract, task-related variables reported in dopaminergic neurons innervating the basal ganglia and limbic structures, such as latency to initiate in a task, directional choice, and task engagement, may be intimately and fundamentally linked to the physical movements that make them manifest, thus bridging the gap between representations of movement and reward.

Our initial interest in examining DANs as animals walked in closed loop was to determine if the variability in the relationships between neural activity and behavior was due to a lack of sensory feedback generated by an animal's movements. The variability between specific parameters of movement and DAN activity persisted even when flies were transitioned into a sensory-responsive, closed loop environment. Distinct patterns of DAN activity, however, did map on to subtle differences in locomotor behavior not apparent in animals walking with no sensory feedback and the capacity of the DANs to predict certain behaviors improved. As these movements were still spontaneous, we lack insight into the external and internal variables that may have triggered them and we therefore cannot confidently explain this phenomenon. We can, however, speculate in light of what we observed during odor tracking. If DANs are encoding the goal or purpose of a movement, then perhaps in closed loop actions have a more consistent purpose. In a sensory-unresponsive context, initiation of a forward movement may be performed with the same

intention as a subsequent turning movement later on in the trial, producing variability in the DAN-behavior correlation. However, in closed loop, walking upwind or accelerating in the forward direction within a steady airflow is more likely to have the same ultimate goal within and across animals. For that reason, we may see increased coherence in how γ4 correlates with forward velocity and why extreme differences in γ2 and γ4 activity appear to relate to different aspects of how animals initiate movement.

The dominance of motor-related signals in the odor responses of the DANs presents the possibility that even signals in these neurons that have been ascribed as sensory responses may actually be more closely related to the movement triggered by a sensory cue. It is easy to think of sugar reward or electric shock as passive sensory processes, but in reality they are accompanied by a series of motor actions that DANs may reflect instead of the sensory stimulus directly.

Thus far, all of our experiments have been observational, examining how patterns of neural activity correlate with behavior. This prompts the question of what role these neural correlates play in shaping behavior. Our finding that DANs are capable of anticipating a fly's future actions suggests that DANs may be able to actively promote or invigorate a fly's movements. In subsequent chapters we exogenously alter the activity of these populations using optogenetic reagents to determine what role they play in concurrent sensory-motivated behaviors.

In this chapter, we have described how DAN activity correlates with the contextually relevant movements of an animal as it performs a goal-oriented action. MB DANs have been implicated in a number of different motivated behaviors[248–250,257–281] and it is unclear how DAN

representations of movement change when the internal motivational state of an animal is altered. In the next chapter, we explore how changing the satiety state of a fly affects behavioral and neural responses to olfactory stimuli.

Chapter 4

Odor Responses of Dopaminergic Neurons in States of Hunger and Satiety

4.1 Introduction

An animal's behavior will vary significantly depending on its level of satiety, with hungry individuals being more motile, exploratory, and likely to engage in food foraging, while at the same time being less risk-averse[29,30,57,276,439–443]. Without the immediate and pressing drive to locate nutrients, sated individuals have the opportunity to engage in other behaviors, including predator avoidance, play, courtship, mating, and other social interactions[444–453]. Access to nutrients, however, is a constant requirement for all animals and just as hungry individuals are in need of finding new food sources, fed ones are incentivized to remain in close proximity to their

current, food-rich location. Indeed, organisms from diverse species will engage in local search behaviors after encountering a food source and during states of satiety to remain in contact with previously identified resources[443,454–458]. Therefore, animals at different levels of hunger and satiety will not only behave differently, they may perform different actions for similar reasons or they may perform physically similar movements with different underlying goals or motivations.

In addition to altering locomotor behavior, satiety level also changes how animals evaluate sensory stimuli, altering which elements of the environment are deemed rewarding and gating an animal's capacity to learn and form associations[25–32,459–461]. It is not surprising, therefore, that dopaminergic pathways are modulated by satiety state and signaling from dopaminergic neurons affects foraging, local search, and other hunger-level-dependent behaviors[461–469]. It remains unclear, however, the extent to which differences in dopaminergic activity between hungry and fed individuals reflects altered locomotion or altered signaling of reward and reinforcement.

Multiple behaviors displayed by *Drosophila* are modulated by satiety state[276]. Starved flies will engage in robust foraging behavior while fed animals perform local search and are significantly less active[427–431]. The MB plays a critical role in controlling these food foraging behaviors and MB DAN activity is modulated by an animal's satiety, in part through the expression of circulating neuromodulators and neuropeptides that reflect metabolic state[273–276]. In addition, the perturbation of specific DAN subpopulations disrupts normal satiety-state-dependent responses to food and odor[248,275,427]. The degree to which differences in DAN responses to food odors in starved and fed animals reflects concurrent behavior is not known. Our data suggested that the MB DANs are encoding the goal or objective underlying sensory-triggered actions. We

were therefore interested in understanding how altering the fly's internal drive or motivation to track towards an odor affected both behavioral and neural responses to odor.

4.2 Satiety State Coordinately Influences Dopaminergic Neurons and Behavior

To directly examine how changing an animal's satiety state coordinately influenced DAN activity and behavior, we compared odor tracking in the low airflow context in flies fasted for 18-24 hours before and after feeding them sucrose (Figure 4.1A). As observed in freely moving animals (Figures 3.2A,B) once fed, flies maintained a lower overall velocity and frequently failed to reorient and track upwind when presented with ACV (Figures 4.1B,C and Figure 4.2A). DAN activity was correspondingly modulated, such that the attenuation in behavioral attraction after feeding was accompanied by a proportional reduction in γ4 and an increase in γ2 odor responses (Figures 4.2B,C). Interestingly, we observed that a significant correlation remained between an animal's heading and γ4 DAN activity within the odor plume in fed flies (Figure 4.2D), indicating that on occasions when a fed animal did reorient to walk upwind in the odor, γ4 DANs respond, albeit more weakly and variably than in starved animals. Together, these data demonstrate that alterations in satiety state are reflected in coordinated changes to both the behavioral response to an odor and activity across the DAN network.

Figure 4.1 | Changing the Internal Drive to Track Odors by Feeding Animals Alters Both Behavioral and Dopaminergic Olfactory Responses. (A) Schematic of closed loop experimental paradigm (as in Figure 3.3A) with additional ability to feed animals a sucrose solution between trials. **(B)** Fictive 2D trajectories of representative tethered animal in closed loop before (top) and after (bottom) feeding animal 1 M sucrose. Clean air presentation indicated in black and ACV presentation indicated in orange. **(C)** Fictive 2D position and DAN>sytGCAMP6s activity from indicated odor presentations in (B) before (top) and after (bottom) sugar feeding. Analyses performed as in Figure 3.7B.

Figure 4.1

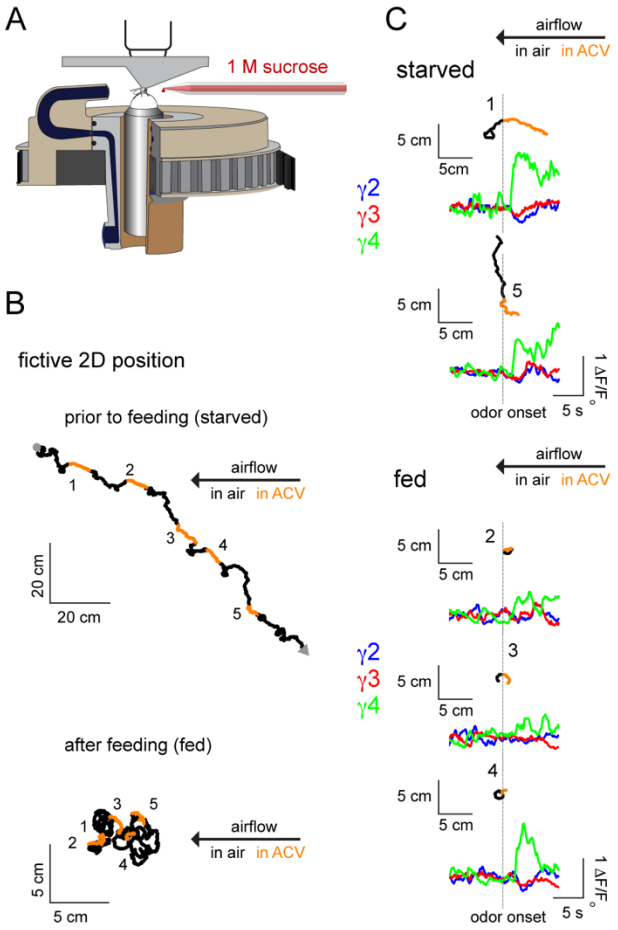
A
1 M sucrose
B
fictive 2D position
prior to feeding (starved)
airflow
in air in ACV
20 cm
20 cm
after feeding (fed)
airflow
in air in ACV
5 cm
5 cm
C
airflow
in air in ACV
starved
5 cm
5cm
γ2
γ3
γ4
5 cm
5 cm
1 ΔF/F
odor onset
5 s
fed
airflow
in air in ACV
5 cm
5 cm
5 cm
5 cm
5 cm
5 cm
odor onset
5 s

Figure 4.2 | Proportional Changes in Behavioral and Dopaminergic Olfactory Responses After Feeding. (A) Fed animals have diminished behavioral responses to ACV. Upwind displacement (left), average |heading| (middle), and average forward velocity (left) of tethered animals in closed loop during odor presentation before (black) and after (maroon) sugar feeding. Paired t-test with Bonferroni correction, $p<0.01$ (*). N=10 flies, 102 odor presentations (49 before and 53 after sugar feeding). **(B)** Fed animals have altered dopaminergic responses to ACV. Paired t-test with Bonferroni correction, $p<0.01$ (*). N=10 flies, 102 odor presentations (49 before and 53 after sugar feeding). **(C)** Feeding animals sugar proportionally diminishes both behavioral and γ4 dopaminergic olfactory responses. Change in average upwind displacement vs change in average γ DANs $\Delta F/F_o$ during odor presentation after sugar feeding. Upwind displacement normalized as in Figure 3.7C. γ DAN $\Delta F/F_o$ is calculated as in Figure 3.7C. Pearson correlation coefficient (r) indicated where relationship is statistically significant ($p<0.01$ with Bonferroni correction). N=10 flies, 102 odor presentations (49 before and 53 after sugar feeding). **(D)** In fed animals γ DAN odor responses are still correlated with an animal's reorientation behavior. γ DAN $\Delta F/F_o$, Δ|heading|, and Δforward velocity calculated as in Figure 3.7C and Figure 3.12C. Pearson correlation coefficient (r) indicated where relationship is statistically significant ($p<0.01$ with Bonferroni correction). N=10 flies, 53 odor presentations.

Figure 4.2

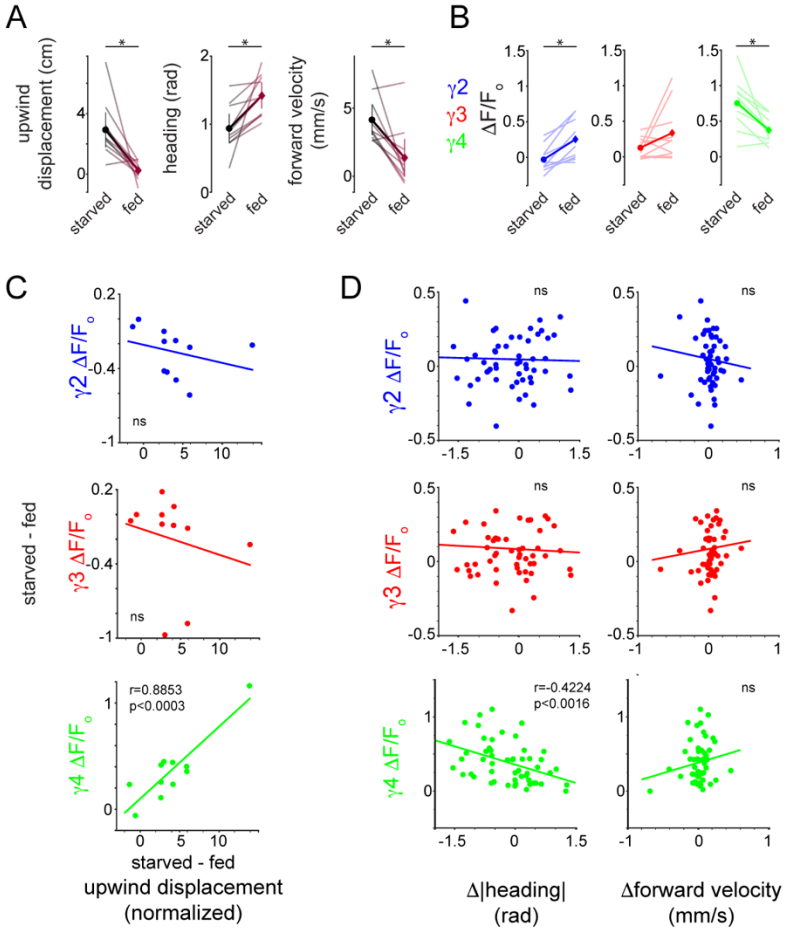
A
upwind displacement (cm)
heading (rad)
forward velocity (mm/s)
starved
fed
B
γ2
γ3
γ4
ΔF/F0
C
γ2 ΔF/F0
γ3 ΔF/F0
γ4 ΔF/F0
ns
r=0.8853
p<0.0003
starved - fed
upwind displacement (normalized)
D
r=-0.4224
p<0.0016
Δ|heading| (rad)
Δforward velocity (mm/s)

4.3 Discussion

The behavior of the fruit fly is profoundly affected by the satiety state of the animal, with hungry flies and sated flies displaying differential responses to stimuli of multiple modalities and exhibiting global differences in activity and arousal levels[275,276,427–431]. Dopaminergic pathways in the MB have been shown to be sensitive to the satiety state of an animal and thereby regulate both appetitive learning and food seeking behavior[274–276,427]. Genetic evidence indicates that DANs express an array of receptors for NPF, insulin, allostatin and other neuropeptides and neuromodulators, suggesting that their activity patterns may be directly influenced by an animal's metabolic needs[276]. This phenomenon has been attributed to dopaminergic tuning of KC-MBON synapses. Slowly varying neuropeptides and hormones act through dopamine to govern the configuration of MB circuitry, thereby gating MB odor responses in accordance with the requirements dictated by the animal's broader nutritional demands[275,276,427]. Likewise, we observe that fed flies were behaviorally indifferent to an appetitive food odor and infrequently tracked towards the fictive odor source. By directly comparing DAN activity in individual animals before and after feeding, we reveal that satiety state does not alter the magnitude of movement-related signals in γ lobe DANs (Figure 2.2D) and the reduced overall DAN activity was related to diminished overall level of locomotion. Indeed, the odor-evoked activity of γ4 DANs was comparable on the rare trials in which sated animals tracked the odor stimulus with similar vigor as a hungry fly. These observations suggest that the modulation of MB DANs by satiety reflects the differences in behavior between hungry and fed animals, underscoring how an animal's internal state is expressed through its actions. DAN activity therefore serves to bridge long-lasting states like hunger to the moment-by-moment actions of an animal.

Chapter 5

Mushroom Body Dopaminergic Neurons Actively Shape Odor-Tracking Behavior

5.1 Introduction

Dopamine's dual role in directing learning and motivating and invigorating movement has long been the subject of debate and speculation. The existence of distinct subsets of dopaminergic neurons tuned to specific reinforcing sensory stimuli or locomotor variables suggests that segregated and specialized pathways may underlie different neural processes[160,178,213,214]. Recent recordings, however, reveal that individual midbrain DANs contain multiplexed representations in which the kinematics of movements and task related variables are encoded by the same neurons that respond to rewards[220]. Yet the utility of motor-related activity in reward-signaling

dopaminergic neurons remains unknown. While correlates of movement have been proposed to reflect an expectation of future reward and thereby mediate learning rather than alter concurrent behavior[199], manipulation of dopaminergic neurons can affect task related behaviors in real-time[147]. Connecting the heterogeneous patterns of dopaminergic activity, with their diverse sensory and motor correlates, to the ongoing behavior of an animal has proven challenging.

Like mammalian dopaminergic pathways, MB DANs that signal reinforcement and instruct learning also contain representations of the moment-by-moment movements of the animal. Our work suggests that these motor-related signals appear to reflect the goal of the behavior, which could subserve learning and/or actively promote and invigorate concurrent behavior. Previous studies have demonstrated that ongoing DAN activity erodes the expression of previously learned olfactory behaviors, with no apparent effect on acute locomotion[362]. We, however, observe that MB DAN activity is related to the underlying end-goal of a movement, such that perturbations of their activity may only be appreciable in the context of performing a motivated task. The powerful and well-developed genetic tools available in *Drosophila* enable specific control over the different DAN subsets, allowing us to test the role of the exact same neurons across different contexts.

In this chapter, I demonstrate that inhibition and activation of MB DANs diminishes and enhances odor approach behavior, respectively, suggesting that these populations are playing an active role in shaping real-time locomotion.

5.2 Inhibition of Dopaminergic Pathways Diminishes Odor Approach

To assess whether DAN activity actively shapes odor tracking, we used intersectional genetic drivers to selectively express the light-gated Cl^- channel GtACR1[470] in different subsets of DANs, allowing us to transiently inhibit them during odor tracking in freely moving animals (Figure 5.1A). Previous studies demonstrated that optogenetic perturbation of DANs during the presentation of an odor leads to altered levels of approach upon subsequent presentations of the odor[356,471]. To dissociate the acute effects of DANs from learning, each cohort of animals received only a single optogenetic perturbation and our analysis focused on comparing behavioral responses to odor before and during, but not after, optogenetic intervention.

The protocerebral anterior medial (PAM) DANs innervate four different compartments, including γ4, and are sufficient to instruct appetitive olfactory memories[348,471]. Optogenetic inhibition of either this broader population of MB DANs or just the subset of DANs targeting the γ4 compartment both suppressed the number of starved flies tracking upwind towards the odor source and dampened the speed with which they tracked (Figures 5.1B,C). In contrast, silencing the protocerebral posterior lateral (PPL) cluster of DANs, a subset of DANs that convey negative reinforcement to the MB during learning and includes those targeting the γ2 compartment, had no effect on odor tracking behavior, highlighting the specificity of these behavioral deficits (Figure 5.1C). Thus the ongoing activity of the PAM DANs and specifically the γ4 DANs is required for the robust odor approach behaviors displayed in hungry animals.

Figure 5.1 | Optogenetic Inhibition of Mushroom Body Dopaminergic Neurons Diminishes Normal Upwind Approach to Appetitive Apple Cider Vinegar. Cohorts of freely moving animals in a behavioral chamber (as in Figures 3.1A-C) were presented with continuous clean airflow and a 1sec pulse of the appetitive food odor ACV. On designated trials, odor was paired with optogenetic inhibition (green light activating the light-gated Cl^- channel GtACR1) of select subsets of MB DANs. **(A)** Schematic of experimental paradigm where designated odor presentations are paired with optogenetic inhibition of genetically identified DANs. **(B)** Average upwind displacement (left panel), proportion of animals walking upwind (middle panel), and upwind speed (right panel) of PAM DANs (MB042B) > GtACR1 animals during consecutive odor presentations. On designated trials, odor is paired with optogenetic inhibition of PAM DANs. Thick dark line and circle marks indicate average behavior ± 95% confidence interval. Thin transparent lines represent behaviors during individual trials. Light-paired trial indicated by green bar. **(C)** Average upwind displacement (top), proportion of animals walking upwind (middle), and upwind speed (bottom) during the four odor presentations preceding optogenetic inhibition compared with light-paired trials for the indicated genotypes. From left to right: PAM DANs (MB042B)>GtACR1 (N=63), PAM DANs (MB196B)>GtACR1 (N=49), γ4 DANs (MB312B)>GtACR1 (N=54), PPL DANs (MB504B)>GtACR1 (N=30), PAM DANs (MB042B)-gal4 parental controls (N=33), >GtACR1 parental controls (N=157), PAM DANs (MB042B)>GtACR1 (no odor, only air) (N=38), R16A06 (γ KCs)>GtACR1 (N=69). $p<10^{-2}$ (*), $p<10^{-5}$ (**), $p<10^{-10}$ (***), $p<10^{-15}$ (****).

Figure 5.1

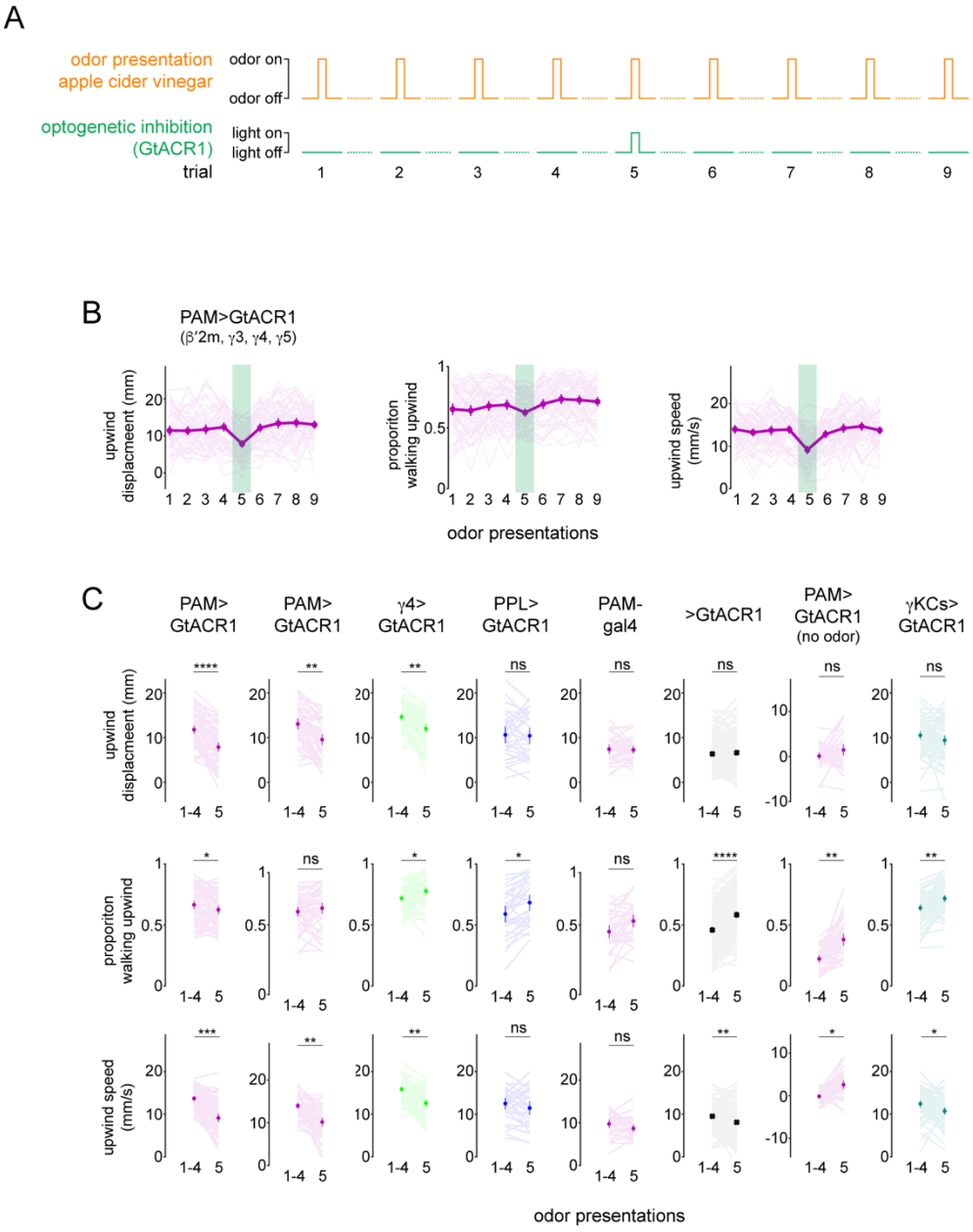
A
odor presentation
apple cider vinegar
odor on
odor off
optogenetic inhibition
(GtACR1)
light on
light off
trial
1 2 3 4 5 6 7 8 9
B
PAM>GtACR1
(β′2m, γ3, γ4, γ5)
upwind displacement (mm)
proporiton walking upwind
upwind speed (mm/s)
odor presentations
C
PAM> GtACR1
PAM> GtACR1
γ4> GtACR1
PPL> GtACR1
PAM-gal4
>GtACR1
PAM> GtACR1 (no odor)
γKCs> GtACR1
upwind displacement (mm)
proporiton walking upwind
upwind speed (mm/s)
1-4 5
odor presentations

5.3 Activation of Dopaminergic Pathways Enhances Appetitive Approach

Given that fed flies exhibited already strongly attenuated olfactory tracking behavior and correspondingly weak DAN activity, we asked whether DAN activation was sufficient to invigorate their behavioral response and enhance odor tracking. We therefore expressed the light-gated cation channel CsChrimson[472] in the PAM subset of DANs to transiently activate them in the presence of an olfactory stimulus. Optogenetic stimulation of the PAM DANs increased the proportion of fed flies that tracked upwind towards an odor (Figure 5.2A). Interestingly, activation of PAM DANs with CsChrimson in the absence of odor promoted upwind tracking (Figure 5.2B), indicating that odor is not strictly required for the DANs to bias animals towards approach behaviors. Thus inhibition or activation of the PAM DANs is sufficient to bidirectionally modulate olfactory approach behaviors, suppressing the strong attraction of hungry animals or enhancing the apathetic behavior of fed flies.

5.4 Kenyon Cells do not Modulate Approach Behaviors to the Same Extent as Dopaminergic Neurons

Given that KCs serve as a major conduit for olfactory information to the MB, we next asked whether this population played any role in shaping acute locomotor behavior. Dopamine may be functioning at the KC-MBON synapse, altering the tonic input of KCs onto efferent pathways to drive approach or avoidance. To address this question, we expressed GtACR1 in the γ KCs themselves and transiently inhibited their activity during odor presentation. Interestingly,

Figure 5.2 | Optogenetic Activation of Mushroom Body Dopaminergic Neurons Enhances Upwind Approach to Appetitive Apple Cider Vinegar and Clean Air. Cohorts of freely moving animals in a behavioral chamber (as in Figure 5.1) were presented with continuous clean airflow and a 1sec pulse of the appetitive food odor ACV. On designated trials, odor was paired with optogenetic excitation (red light activating the cation channel CsChrimson) of select subsets of MB DANs. **(A)** Average upwind displacement (top) and proportion of animals walking upwind (bottom) of PAM DANs (MB042B) > CsChrimson animals during consecutive odor presentations. Thick dark line and circle marks indicate average behavior ± 95% confidence interval. Thin transparent lines represent behaviors during individual trials. Activating light-paired trial indicated by red bar. Right panels: Average of above variables during the four odor presentations preceding optogenetic activation compared with light-paired trials in PAM DANs (MB042B) > CsChrimson animals (magenta) and >ChChrimson parental controls (black). Paired t-test with Bonferroni correction, $p=4.4321\times10^{-6}$ (*), $p=1.5\times10^{-7}$ (**). N=60. **(B)** Average upwind displacement (top) and proportion of animals walking upwind (bottom) of PAM DANs (MB042B) > CsChrimson animals during consecutive 10sec recordings of animals in an airflow with no odor presentation. Thick dark line and circle marks indicate average behavior ± 95% confidence interval. Thin transparent lines represent behaviors during individual trials. Activating light-paired trial indicated by red bar. Right panels: Average of above variables during the four trials preceding optogenetic activation compared with light-paired trials in PAM DANs (MB042B) > CsChrimson animals (magenta) and >ChChrimson parental controls (black). Paired t-test with Bonferroni correction, $p=3.7\times10^{-6}$ (**), $p=1.64\times10^{-10}$ (***), p=0.0027 (*). N=44.

Figure 5.2

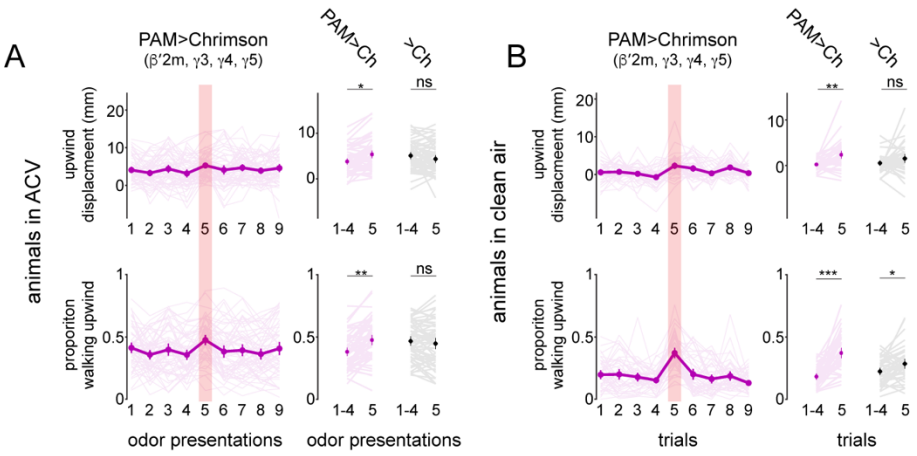
A
PAM>Chrimson
(β′2m, γ3, γ4, γ5)
PAM>Ch
>Ch
animals in ACV
upwind displacmeent (mm)
proporiton walking upwind
odor presentations
odor presentations
B
PAM>Chrimson
(β′2m, γ3, γ4, γ5)
PAM>Ch
>Ch
animals in clean air
upwind displacmeent (mm)
proporiton walking upwind
trials
trials

we found that silencing γ KCs in the presence of odor did not significantly alter the behavioral responses to odor (Figure 5.1C). This finding argues that real-time anemotaxis is independent of KC activity and that the influence of dopamine on approach behavior, even to an olfactory stimulus, is occurring beyond the KC-MBON synapse, potentially through direct connections between DANs and MBONs[398,405].

5.5 Mushroom Body Output Neuron Activity is Modulated by Movement

The MBONs are the only efferent pathways emanating from the MB. Representations of movement within DANs must be transmitted into changes in MBON activity in order for them to exert any influence on behavior. To assess if MBON activity, like DAN activity, is similarly affected by movement, we imaged the dendrites of the γ3 MBONs expressing soluble GCaMP6s. During spontaneous walking, where the fly was presented with no overt sensory stimuli, we observed a robust anticorrelation between γ3 MBON activity and locomotion onset (Figure 5.3), the reciprocal pattern of activity observed in γ3 DANs during similar movements. These findings present the possibility that DANs are exerting tight temporal control over the ongoing activity of MBONs to shape and influence concurrent behavior. These data posit that dopamine may function by inhibiting MBONs. Optogenetic activation of the γ4 MBON drives avoidance while activation of the γ2 MBON promotes approach[339]. If DANs are directly synapsing onto MBONs, then an inhibitory connection would be predicted because their corresponding DANs are activated by appetitive and aversive stimuli, respectively. In addition, we observed that activation of the γ4

DAN is correlated with and invigorates approach behavior (Figure 3.7 and Figure 5.2), corresponding to actions where the γ4 MBON activity is presumably depressed[339].

5.6 Discussion

Here we show that the ongoing activity of a population of DANs that instruct learning plays an active role in shaping the fly's concurrent behavior. While not precluding the role that baseline fluctuations in DANs may play in eroding memories[362], these results highlight the fact that they are simultaneously involved in the real-time processes of promoting and invigorating movement to achieve a designated task. The diverse functionality of dopamine therefore need not rely on discrete and separate subpopulations to affect both current and future behavior.

While dopamine's function in the formation of olfactory associations is localized to the KC-MBON synapse, we see that its ability to shape ongoing locomotion is independent of KC activity. This suggests that there may be alternative means for DANs to communicate with MBONs and modulate the net output of the MB. In accord with such a model, direct synaptic connections between DANs and MBONs have been observed in electron microscopy generated reconstruction of the MB lobes[398,405], and ongoing experiments by another student in the lab, Andrew Siliciano, suggest DAN activity is directly translated to fluctuations in the MBONs.

We see that even brief manipulations of DAN activity can alter the immediate behavior of flies. Odor presentations following inhibition or activation were comparable to those preceding

Figure 5.3 | Mushroom Body Output Neuron Activity Reflects Ongoing Behavior. (A) Overlay of five individual flies' net motion and γ3 MBON (MB083C) > GCaMP6s activity during spontaneous locomotion. **(B)** γ3 MBON activity during the initiation of movement. Top: average net motion ± 95% confidence interval as animals initiate sustained locomotion (≥3 sec) following a pause (≥2 sec). Middle: average activity of γ3 MBON activity aligned to changes movement onset ± 95%. MBON activity is z-score normalized over the five minute recording session. Bottom: heat map of z-score normalized γ3 MBON activity with each row representing MBON activity during a single instance of movement initiation. N=40 movements in 7 flies.

Figure 5.3

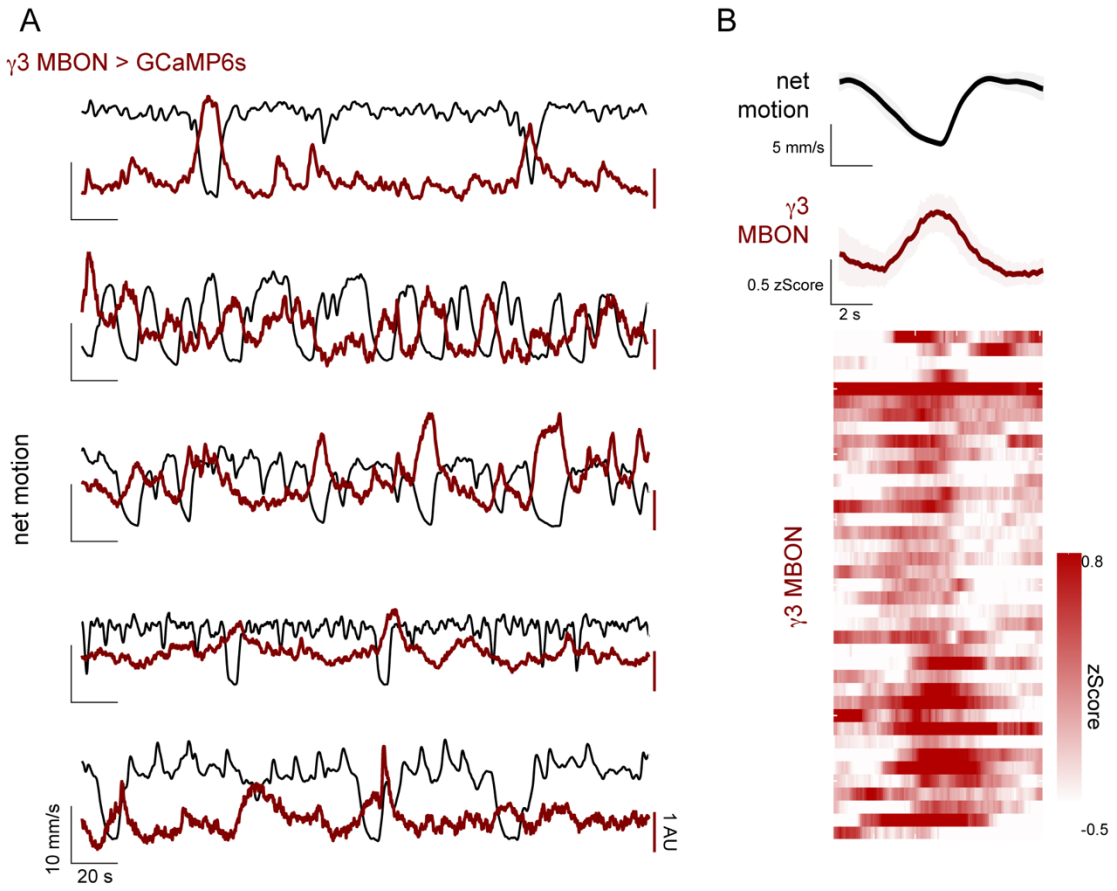
A
γ3 MBON > GCaMP6s
net motion
10 mm/s
20 s
1 AU
B
net motion
5 mm/s
γ3 MBON
0.5 zScore
2 s
γ3 MBON
0.8
zScore
-0.5

optogenetic perturbation, suggesting transient and acute effects of dopaminergic pathways. The DANs therefore appear poised to exert tight temporal control over the signals emanating from the MB to exert a dynamic influence on behavior.

Chapter 6

Discussion and Future Directions

6.1 Introduction

For my thesis I took advantage of the concise circuit architecture of the *Drosophila* MB to explore the nature of movement-related activity in a population of dopaminergic neurons that signal reinforcement and instruct the formation of olfactory associations. By recording from these populations during spontaneous and naturalistic locomotion I demonstrated that the ongoing activity of discrete subsets of DANs reflected specific aspects of movement, including rapid changes in velocity and transitions between different locomotor states.

To gain insight into what facets of an animal's experience were represented by these movement-related signals, I employed a closed loop virtual reality paradigm to observe animals as they performed goal-directed, sensory-triggered behaviors. Recording from the DANs as animals navigated within an odor plume revealed that their activity was contingent upon the strength or vigor with which an animal tracked upwind towards the fictive odor source. Moreover, in different experimental contexts where distinct motor actions were required to track the odor, DAN activity became emergently linked to the behavioral metric most relevant to the performance of olfactory navigation. Within the odor plume, DAN activity carried prospective information about an individual's future actions. The satiety state of an animal coordinately altered dopaminergic activity and behavior, but when fed animals did approach an odor, subsets of DANs continued to correlate with the robustness of upwind tracking. Together, these observations suggest that the complex activity patterns of MB DANs represent neither purely sensory nor motor variables but rather correlate with the goal or motivation underlying an animal's actions as it tracks an odor during a particular trial.

While motor signals have been previously observed in the MB DANs, they were believed to function as part the neuropil's well-established role in olfactory learning, acting to erode previously formed associations[362] or allowing an animal's behavioral state to serve as a reinforcement cue itself[351], altering future rather than concurrent behavior. Taking advantage of the powerful genetic tools available in the fly, I gained access to subsets of MB DANs to selectively express optogenetic reagents. I found that transient inhibition of DANs that are positively correlated with upwind tracking significantly diminished the normal approach responses to an appetitive olfactory cue. Conversely, activation of those same DANs enhanced upwind

tracking to odor and even drove anemotaxis in clean air. These findings suggest that ongoing activity of MB DANs that instruct learning also play an active role in shaping the concurrent behavior of the animal, biasing flies toward avoidance or approach behaviors in real-time.

6.2 Understanding the Mushroom Body Dopaminergic Neuron – Mushroom Body Output Neuron Network

While these studies offer a detailed description of how baseline fluctuations in DAN activity influence behavior, major questions persist and more work will be required to fully appreciate the MB's role in controlling and coordinating locomotion and affecting other adaptive behaviors.

I focused exclusively on the four DAN subpopulations innervating the medial portion of the γ lobe of the MB. Even within that restricted subset, we see heterogeneous representations of sensory stimuli and movement and only one of these subpopulations, the γ4 DANs, appears to be consistently tuned to anemotaxic actions. The MB is comprised of an additional 11 compartments[256] that, in the context of learning, are differentially responsive to different reinforcements, such as nutritive sugar, sweet taste, and water, and instruct either short- or long-term memories with distinct learning rules[334,336,350,352–355,363]. Each DAN-MBON pair may relay distinct features of the animal's experience, tuned to different behavioral contexts or sensory modalities. In future studies it will be interesting to examine all of the MB's dopaminergic

pathways to reveal what sensorimotor variables are encoded in the activity of the different dopaminergic subpopulations.

While it is tempting to segregate the MB's different compartments, assigning each one a set of associated variables and functions, ultimately it will be critical to conceive of the MB as a fundamentally unified structure whose various parts operate in concert. As my thesis and previous work from our lab and others[351,398,400,405] emphasizes, the MB DANs exist as a functional network formed through rich interconnections between compartments. Studies of MBONs demonstrate that only a small fraction of them can bias approach or avoidance behaviors autonomously while activation of distinct combinations of MBONs have more profound effects on behavior[339]. Thus the heterogeneous DAN activity in different compartments is likely to be integrated by downstream neurons rather than forming parallel pathways operating independently, a possibility supported by the overlapping axonal projections of the MBONs[256]. Variability in how individual DAN subsets represent sensorimotor variables over time may be due to their receiving flexible input from both discrete afferent channels and recurrent feedback from the MB itself, highlighting the importance of studying the MB as a functional unit. Future work to simultaneously record DAN activity across the entire MB and define the functional relationships between the different DAN compartments will therefore be critical. As my thesis work suggests, these recordings must be accomplished with minimal loss of temporal precision given that DANs are capable of signaling movements that occur over tens to hundreds of milliseconds, making it vital to capture the moment-by-moment changes in neural activity to fully appreciate how they relate to equally rapid changes in behavior. New technologies that permit fast volumetric functional imaging of neural activity present exciting avenues of research that will accomplish this goal[473]. A detailed exploration of

how information is flowing through the entire MB will constrain our understanding of this neuropil's broader role in shaping the fly's behavior.

The above questions are already being addressed in part by efforts to develop a complete connectome of the *Drosophila* brain[398,405]. A fully mapped connectome will offer knowledge of which pathways feed into the MB DANs and detailed insight into the destination of efferent signals emanating from the MB. These anatomic studies will undoubtedly constrain models and illuminate which compartments and DAN-MBON pairs are capable of influencing which behaviors. While a connectome will establish the boundaries of these investigations, it will most likely not be the coda to examinations of the MB. As the study of neuromodulators has aptly demonstrated, connectomics is not destiny[22–24], and an understanding of the functional connectivity of the MB will inevitably be required. Preliminary studies already illustrate that understanding the flow of information into and out of the MB will not be trivial. These networks appear to be highly recurrent, with MBONs directly and indirectly affecting the DANs and efferent pathways leading to other integrative centers like the fan-shaped body of the central complex whose output is also recurrent, functionally dynamic, and nebulously described[256,351,357–359,474–477]. Even a recent study that identified a functional connection between a MBON and a population of neurons in the lateral horn (LH), a brain region believed to mediate innate olfactory behaviors, found that these LH outputs fed back into MB associated neuropils innervated by the dendrites of DANs[358]. Although olfactory sensory input via KCs is the most well-characterized afferent signal into the MB, it is apparent that a wide array of both sensory and motor information flows into MB circuits, most likely through the DANs. Rather than a relay for learned olfactory responses, the MB appears to be an integrative nexus of

sensory and motor data, broadcasting signals throughout the brain to influence multiple aspects of the fly's behavior.

Although a daunting task, understanding how the MB is functionally integrated into the fly brain will provide vital insight into how this structure flexibly influences a fly's behavior over different time scales—in real-time while animals are engaged in decision making and navigation, over extended periods of time such as during sleep/wake cycles, or in the future through learning.

6.3 The Mushroom Body Dopaminergic Neurons and Fly Behavior

The MB DANs appear to be capable of influencing a diverse set of adaptive behaviors[248–250,257–281]. Examining their activity in only a single behavioral context may therefore obscure their broader functionality. Only by recording both spontaneous and sensory-motivated behaviors were we able to gain insight into which aspects of an animal's experience are encoded by the γ DANs. Future studies should take advantage of the fly's rich behavioral repertoire to examine how the MB DANs dynamically reflect sensorimotor variables while the animal is engaged in different tasks and under different internal and external conditions. During my thesis I performed preliminary experiments with the help of Cheng Lyu in Gaby Maimon's lab that suggest the DANs also reflect movements during flight and signal the onset or offset of flying bouts (data not shown), highlighting their context-dependent functionality and representations of movement.

My thesis work focused on how MB DANs reflect goal-directed behaviors in the context of tracking an olfactory plume, but it will be exciting to learn how their activity relates to other motivated behaviors, such as courtship and predator escape. Our lab is currently improving the closed loop paradigm to allow the concentration of odor to vary depending on the position of the fly in a fictive virtual reality. This will add an additional dynamic layer to the fly's environment and may allow us to more fully appreciate how the MB influences adaptive behavior.

While examining fly behavior within different contexts is critical, it will also be important to develop ways to precisely and accurately capture the fine features of movement. In this study, we relied on the relatively coarse metrics extracted from recording the rotation of the spherical treadmill. While we found neural correlates of parameters of movement such as forward and turning velocity, our experimental paradigm had no way to detect if other, more subtle motor actions, are represented in DAN activity. Recently, an unbiased, high-resolution monitoring and categorization of behavior in mice provided a detailed characterization and catalog of the motor repertoire displayed by a mouse that has facilitated insight into how striatal pathways differentially reflect specific movements[146,478]. Similarly, meticulous analyses of the gait of the fly has revealed the role of distinct pathways in specific motor actions[479]. Machine learning algorithms and emerging recording techniques will allow us to learn how the complexity and subtlety of a fly's movements are reflected and modulated by the MB DANs[480–482].

Representations of movement parameters in the MB DANs shift when animals are engaged in purposeful action. Similarly, there are profound differences in ongoing DAN activity in tethered flies suspended in midair compared to a tethered fly walking on a spherical treadmill. This

indicates that the broader experimental paradigm may have a large influence on DAN activity. In our experiments flies were able to walk with a regular gait and perform purposeful movements like anemotaxis, but they were still tethered, walked on an artificial foam surface, had their proboscis glued in place, and had their head cuticle removed. There is no way for us to appreciate the extent to which these experimental conditions influenced DAN activity or behavior. It will therefore be important for future investigations to develop ways to record from DANs in a minimally invasive manner to get as close to naturalistic locomotion as possible. Advances in three-photon microscopy and *in vivo* bioluminescence imaging of Ca^{2+} signaling offer exciting means to record from DANs in less intrusive and more ethologically realistic settings[483–487]. These new functional imaging techniques, coupled with the selective genetic access to neural populations of interest[235–237], provide a powerful platform to establish links between neural activity and behavior.

6.4 How Movement-Related Activity in Mushroom Body Dopaminergic Neurons Affects Downstream Circuits

While my thesis focused on the question of which sensorimotor variables are encoded in DAN activity and how they alter behavior, it is also critical to understand how representations of movement by the DANs affect downstream neurons[222]. Within a single compartment, all the DANs appear to act in concert and convey similar information about the ongoing behavior of an animal. In the γ4 compartment, we observe that the fluctuations in DAN activity during odor tracking resemble the phasic responses evoked by ingestion of a sugar reward. An important and exciting

remaining question for the future is how the downstream components of the MB circuitry differentiate between dopamine signals evoked by external reinforcements or arising from behavior. One possibility is that the ongoing dopamine release during odor tracking may engage the same synaptic plasticity mechanisms that drive memory formation, allowing both external reinforcements and the actions that predict them to similarly instruct learning. Indeed, dopamine release during ongoing behavior is proposed to regulate the strength of KC-MBON synapses such that the current circumstances of an animal can overwrite past associations[351,362]. Ongoing DAN activity may also serve to shape synaptic plasticity rules or gate an animal's capacity to learn, restricting it to epochs when animals are aroused and motivated. Appetitive memory formation in the fly appears to be gated by satiety and can only be expressed in hungry animals, underscoring the tight interplay between motivational drives and learning[274,400].

An alternative possibility is that DAN activity during ongoing behavior could contribute to acute modulation of the MB circuit through mechanisms that are distinct from associative plasticity. The MB's position at the nexus of sensory circuits conveying odor signals and the efferent MBON pathways that bias behavior make it an ideal site for dopaminergic reinforcement to shape olfactory preferences during learning. However, there is substantial evidence for a role for the MB beyond olfactory learning[257,263,272,275,281,361,427], suggesting dopamine may modulate MB circuits in distinct ways. A recent electron microscopy reconstruction of the MB lobes reveals the existence of direct DAN-MBON synapses, providing an alternative route for dopaminergic modulation that could act in parallel to presynaptic associative plasticity[398,405]. Such connections could allow different sensory modalities and movement variables to influence an animal's concurrent behavior. If, for instance, output neurons from the LH are in fact feeding into DANs[358]

that are in turn having a direct effect on MBON activity, then the same dopamine signal could function in parallel to motivate real-time odor responses while concurrently modulating the KC-MBON synapse to alter future olfactory-triggered behavior.

Moving forward, it will be critical to understand how ongoing DAN activity affects downstream MB pathways, specifically how movement-related activity in DANs is both propagated to MBONs and engages the MB's learning machinery. My experiments recording from the γ3 MBON suggest that like the DANs, the activity of MB efferent pathways are correlated with features of the animal's locomotor behavior (Figure 5.3). Mechanistic insight into the functional link between DANs and MBONs, however, is still required. One potential approach is to perform dual functional imaging of DANs and MBONs expressing genetically encoded calcium indicators with non-overlapping emissions spectra[371,488,489]. Such studies could provide an understanding of the temporal relationship between DANs and MBONs, demonstrating that fluctuations in DAN activity are consistently linked with comparable changes in the MBONs. More informative, however, would be studies in which the activity of MBONs is monitored while DAN activity is perturbed. Optogenetic inhibition of DANs with GtACR1 or activation with CsChrimson while recording from specific MBONs would provide insight into how altering dopaminergic signaling affects MBONs in real-time. By performing the same experiments but recording instead from KCs, we could determine if dopamine is influencing MBONs directly or indirectly via their KC input.

A current student in the lab, Andrew Siliciano, is already beginning to examine the functional relationships between DANs and MBONs. In *ex vivo* experiments, he has found that when a dopamine receptor antagonist is injected directly into the lobes of the MB, GCaMP

signaling from MBONs increases, while no such change in KC activity is observed (data not shown). Likewise, Andrew has observed that optogenetic inhibition of DANs produces increases in the activity of the γ4 MBON during tethered locomotion (data not shown). These preliminary studies support my findings suggesting that dopamine has an inhibitory effect on the γ3 MBON and indicate that the ongoing level of activity in MBONs is influenced by dopamine, possibly directly and independently of KCs.

An additional experimental approach to investigate the functional links between DANs and MBONs is to examine the expression of dopamine receptors in the MBONs. Dopamine receptors are highly expressed in KCs where they have a well-established role in synaptic plasticity[268,288,289,293,297,362,364,490,491]. These receptors, however, also appear to be expressed in MBONs where they are necessary for certain adaptive behaviors[427]. Cell-type specific knock-down of dopamine receptors in the MBONs could help to elucidate how dopamine directly affects MBON activity during locomotion. The complement of dopamine receptors or their expression level may differ across the different MBONs such that some can only be affected by dopamine via their KC inputs while others may be directly sensitive to dopaminergic neuromodulation. Different dopamine receptors are linked to different downstream signaling pathways in KCs[471,491] and they may likewise couple to distinct second messengers and signaling cascades in MBONs. Dopamine may therefore be able to exert differential effects on KCs and MBONs in a given compartment simultaneously or on different MBONs innervating different compartments.

Dopamine appears to have variable effects on its downstream partners within the MB lobes, presenting an especially challenging obstacle for future experiments aimed at understanding the

DANs' functional relationship with both KCs and MBONs. In learning paradigms, shifting the timing of a dopamine signal relative to an odor presentation by only a few hundred milliseconds can engage different dopamine receptor signaling cascades in KC axons and have opposite effects on KC-MBON plasticity[471]. If KCs are activated prior to DANs, the KC-MBON synapse is depressed, but if the temporal relationship is reversed such that DANs are activated before KCs, that same synapse becomes potentiated. The DAN-MBON synapses might exhibit similar temporal sensitivity, with dopamine dynamically modulating MBON activity depending on multiple different variables. For example, depending on the timing of KC inputs and locomotor fluctuations, different dopamine receptor pathways in the MBONs may be engaged. An alternative and exciting possibility is that the activity of other sub-circuits within the MB may regulate dopamine's diverse and dynamic effects. In the mammalian striatum, cholinergic interneurons have been proposed to act as a switch, indicating to dopaminergic targets when changes in dopamine are signaling reward and when they related to movement[222,492–494]. Similarly, the GABAergic neuron APL and the peptidergic neuron DPM innervates broadly within the lobes and may alter how dopamine is received by the MBONs[495–498]. This will be an intriguing area of exploration, as insight into how the effect of dopamine on its downstream targets is controlled and coordinated will further our understanding of dopaminergic circuitry flexibility.

In addition, it will be important to explore how ongoing, movement-related activity in the DANs engages the learning machinery of the MB to drive the formation of associations. Dopamine can have profound effects on pre-synaptic KC responses through different dopamine receptor G-protein-coupled signaling cascades. It will be interesting to investigate if motor-related activity in DANs can engage those same learning pathway. Preliminary experiments in our lab performed by

Andrew Siliciano suggest that during tethered locomotion, the concentration cyclic adenosine monophosphate (cAMP), a second messenger produced by the DopR1 dopamine receptor in KCs that underlies the plasticity at the KC-MBON synapse during associative learning[291,292,499], covaries with changes in DAN activity (data not shown). Therefore as animals move and cause the level of dopamine in a given compartment to fluctuate, we see the molecular pathways that drive synaptic plasticity are being activated as they would be when an animal encounters a reinforcing sensory cue. These findings agree with previous reports that movement-related DAN activity can erode past memories[362] and suggest that a fly's actions themselves could serve as a reinforcement in the formation of olfactory associations.

Ongoing experiments into the functional interactions between DANs and their KC and MBON targets within a compartment will address the critical question of *how* the ongoing, movement-related fluctuations in DANs that we have characterized here ultimately affect an animal's concurrent behavior. Such studies will uncover the circuit mechanism underlying our discovery that optogenetic perturbations of DAN activity reversibly tunes the vigor of behavioral tracking, suppressing the drive of hungry animals to track an appetitive food odor or inducing fed animals to track upwind, even in the absence of an olfactory stimulus.

6.5 The Mushroom Body as a Locus for Flexible Behaviors

Since the initial discovery that ablation of the *Drosophilaf* MB impaired the formation and expression of olfactory associations[285], the structure has been primarily associated with the study of learning. As a model system, the MB has proven incredibly useful in the quest to understand the molecular and circuit mechanisms underlying how memories are created, consolidated, and stored within neural structures. Progress was achieved in part by a focus on examining the MB within the narrow context of associative learning paradigms and this emphasis did indeed generate useful models that help us understand the basic molecular processes and system properties that allow for experience-dependent plasticity in neural circuits[234,256,286,298–301]. The attention to learning, however, has also led to an under-appreciation of the MB's functions in more general adaptive behaviors. Emerging evidence, including the work described in this thesis, indicates that the MB plays a far more expansive role in shaping the ongoing behavior of the fly, from decision making, to sleep and circadian rhythms, to control of movement[248–250,257–281]. While the non-learning functions of the MB are becoming better appreciated, it is vital that this new awareness be accompanied by an understanding of the intimate relationships between different adaptive behaviors. My thesis work demonstrates that the very same neurons that drive synaptic plasticity to bias future behavioral responses to odor are playing an active role in coordinating odor-tracking in real-time. The neural processes underlying these behaviors are fundamentally connected within the DANs of the MB and we should strive to conceptualize them as inherently related phenomena.

6.6 Conservation of Dopaminergic Circuitry

Dopaminergic pathways coordinate and modulate ongoing movement but also signal reinforcement to instruct learning[73,99–101]. While reports have proposed the existence of anatomically segregated subpopulations dedicated to either motor control or learning[213,214], individual dopaminergic neurons exhibit multiplexed representations of the animal's movements and reinforcing sensory stimuli[199,216,220]. As a further complication, dopaminergic pathways have been shown to correlate with more abstract variables such as engagement with a learned task or level of arousal[147,148,156,160,227,410], making it difficult to determine to what extent their activity is movement-related or connected to the structure of a given experimental paradigm. The literature investigating dopaminergic pathways is rife with conflicting reports and mutually exclusive interpretations[107,147,148,156,157,160,164,169,179,183,198–200,213–216,218,220,222,223,225–227,374,377,410,494], and there is little consensus as to how dopamine achieves its diverse functionality, the anatomic and functional logic of dopaminergic circuitry, the identify the variables encoded by dopaminergic neuron activity, and how ongoing dopaminergic activity affects downstream neural pathways to shape behavior.

In our study of only a subset of the ~120 MB DANs, we observe all of the complexity, heterogeneity, and variability of vertebrate dopaminergic systems recapitulated. Within the four subsets of DANs innervating the γ lobe alone, representing fewer than 50 individual neurons, we observe pathways oriented to signaling the presence of rewarding sensory stimuli and pathways that exhibit multiplexed encoding of both reinforcing external cues and movement. We likewise observe representations of locomotor state lasting up to minutes, correlates of rapid changes in

movement occurring over hundreds of milliseconds, and reflections of goal-oriented behaviors. These striking parallels between mammalian and insect dopaminergic circuits, despite their separation by several hundred million years of evolutionary divergence, suggest that these are fundamental features of dopaminergic signaling. Studies in zebrafish have revealed that their diencephalic dopaminergic nuclei may be similarly organized into discrete subcircuits with unique sensorimotor correlates, further supporting a conserved logic of dopaminergic systems across evolution[500]. Recent recordings from the mammalian midbrain has likewise provided evidence that neurons encoding similar motor- and task-related variables are anatomically clustered[220]. Our emerging understanding of the organization of mammalian dopaminergic circuits makes the MB appear a striatum-in-miniature.

The coupling of reinforcement signals and locomotor representations in the same neuromodulatory system across such distantly related phyla argues for an inherent connection between them that could contribute to the diverse roles of dopamine. If dopaminergic neurons are signaling the intention or motivation of specific actions or the value of a given sensory stimulus, they would represent a bridge linking the immediate behavior of the animal to its broader environmental and internal context. By imbuing sensorimotor variables with context-dependent meaning, a motivational dopaminergic signal would allow the activity of a single neural population to both promote and invigorate movements in real-time and simultaneously bias future behavior through learning. The goal or motivation of our actions is therefore integral to how our brains control and coordinate our movements and our ongoing behavior influences how we evaluate sensory stimuli and assess our experiences.

6.7 Implications for Mammalian Dopaminergic Pathways

This correspondence of dopaminergic circuitry across evolution not only elucidates fundamental features of dopaminergic signaling pathways, it also allows for insights gained from the study of the MB to potentially impact our understanding of the larger and more complicated mammalian dopaminergic system. Representations of movement in mammalian dopaminergic neurons have been suggested to reflect an expectation of reward resulting from an action[199]. Contravening studies, however, have posited that models cannot adequately describe movement-related activity in dopaminergic neurons as motor-associated RPEs alone[227]. It has been difficult to directly connect the multiplexed activity of dopaminergic neurons with their role in both learning and motor control. Like mammalian dopaminergic neurons, MB DANs reflect reward and contain detailed representations of movement, but the simple and organized architecture of the MB allows us to appreciate that the very same DANs that respond to reinforcing sensory stimuli also non-stereotypically encode forward velocity, are consistently correlated with purposeful, goal-oriented behaviors in the context of an olfactory stimulus, and their inhibition or activation attenuates or enhances anemotaxis, respectively. These findings suggest that these DANs are encoding the motivation and purpose underlying specific motor actions and that their activity promotes and invigorates those same actions in real-time. These and future insights gained from the study of the fly may translatable to the mammalian system as well. The MB will therefore be a powerful platform to understand how dopaminergic pathways encode different variables and how their ongoing activity affects downstream circuits and behavior.

One lesson immediately apparent from the study of the MB is the need to sample from midbrain dopaminergic neurons more extensively. Even within the MB's limited dopaminergic populations we observe distinct subpopulations dedicated to specific facets of the animal's experience and exhibiting non-equivalent representations of movement and sensory stimuli. Recent studies of the rodent striatum have made use of fiber photometry[199] or fast-scan cyclic voltammetry[147], which aggregates the activity of thousands of dopaminergic neurons together, or have used functional imaging[214,220] and electrophysiological[215,216] methods to record from individual dopaminergic neurons, where even capturing the activity from ~500 individual cells simultaneously accounts for less than 1% of the dopaminergic population. If, like the MB, the mammalian striatum is intricately innervated by many dopaminergic sub-pathways, each uniquely encoding different features of the animal's ongoing movements and sensory environment, more comprehensive methods of recording from dopaminergic neurons will be required to gain a coherent understanding of the system.

An additional potential insight gained from the study of MB DANs is that the activity of dopaminergic pathways may be the product of both dedicated sensorimotor afferents and recurrent feedback from output circuits. Although the cortico-basal ganglia-thalmo-cortical loop is fundamentally conceived of as a recurrent circuit, the flow of information into the dopaminergic neurons is conspicuously ill-defined. Indeed, the inputs into mammalian dopamine neurons are poorly described but revealing the functional and possibly flexible balance between sensory, motor, and recurrent data integrated by dopaminergic neurons may be critical to understanding their heterogeneous and variable patterns of activity.

6.8 Motor Correlates Across the Brain

As our ability to record from neural populations in more naturalistic and ethologically relevant settings improves[501], it is becoming increasingly clear that movement has a profound effect on the activity of neural circuits, even those not directly related to motor control[241,380,393,502–504]. Neurons in the visual cortex, for example, also contain representations of the facial movements of a mouse[505] and movement signals appear to be broadcast throughout the brain[504,505]. Given that the brain evolved from simple circuits dedicated to generating physical behavioral responses to sensory stimuli, it is not surprising to find locomotion at the foundation of diverse neural pathways. Multiplexed representations, like those seen in the striatal dopaminergic neurons, are therefore prevalent throughout the brain. It is important to appreciate, however, that reinforcement and movement need not be linked *a priori* in dopaminergic neurons. Recent studies of the mammalian amygdala posit that orthogonal populations in this neuropil represent stress and anxiety caused by learned sensory cues versus those caused by location within an environment[506]. Neural circuits have the capacity to separately encode distinct variables, making the coupling of multiple different sensorimotor variables in dopaminergic pathways notable and potentially functionally relevant. The motor deficits resulting from lesions to dopaminergic pathways highlight the critical role that dopamine play in both representing and influencing ongoing movement and make determining what features of the animal's experience are reflected in dopaminergic correlates of movement especially interesting and important. Moreover, the dopaminergic system may provide a template for understanding the nature and utility of motor-correlates in diverse neuropil across the brain.

6.9 The Study of Neuromodulatory Networks

The study of neuromodulators has profoundly impacted the way we think about how adaptive behaviors emerge from the flexible properties of neural circuits. The operation of neuromodulatory circuits themselves, however, are only beginning to be fully appreciated. It has proved challenging to decipher what features of the animal's experience are encoded in the complex, heterogeneous, and variable patterns of activity displayed by these broadly and intricately innervating pathways. Moreover, these neuromodulatory neurons themselves appear to function dynamically and flexibly, begging the recursive question: who neuromodulates the neuromodulators? Gaining a coherent description of the flow of information through these pathways is critical for our understanding of both the physiological and pathological functioning of our brains. Great progress in the study of neuromodulators has been achieved through the use of simplified model systems that share conserved features with our own nervous system[22–24]. My thesis work presented here suggests a fundamental conservation in the architecture and organization of neuromodulatory circuits themselves between mammals and invertebrates. Hopefully, the MB can serve as a platform to dissect the functional operations of neuromodulatory pathways and shed light on how they coordinately shape the activity of downstream circuits and behavior.

Materials and Methods

Fly Husbandry

Flies were maintained on conventional cornmeal-agar-molasses medium at 23-25°C and 60-70% relative humidity under a 12 hour light/dark cycle. Animals were removed from food and placed in vials containing only a water-soaked KimWipe 12-24 hours before all tethered locomotion experiments. Flies for optogenetic experiments were grown on retinoid-free sugar-and-yeast-based food medium[507] in 24 hour darkness. 1-2 day old females were transferred to conventional food containing .4mM all-trans-Retinal (Sigma #R2500) and placed in the dark for 24 hours. To food deprive the animals, they were subsequently removed from food and placed in empty vials containing only a KimWipe soaked in 2mL of .2mM all-trans-Retinal water placed in darkness for 12-18 hours prior to behavioral experiments.

Fly Strains

Strains and sources:

UAS-sytGCaMP6s[351]. TH-Gal4[508]. DDC-Gal4[509]. MB247-DsRed[347] (gift from Andre Fiala, University of Göttingen). UAS-GCaMP6f[371]. MB247-LexA[510] (gift from Scott Waddell,

University of Oxford). LexAop-GCaMP6s (#53747) (Bloomington Stock Center). UAS-CD8-GFP (#32185) (Bloomington Stock Center). 20X-UAS-IVS-CsChrimson.mVenus-attP18[471]. UAS-GtACR1[470]. 58E02-p65ADZp; 22E04-ZpGdbd [MB042B], 58E02-p65ADZp; 10G03-ZpGdbd [MB312B], 52H03-p65ADZp; TH-ZpGdbd [MB504B], 58E02-p65ADZp; 36B06-ZpGdbd [MB196B], 30G08-p65ADZp; 48B03-ZpGdbd [MB441B], 52G04-p65ADZp; 94B10-ZpGdbd [MB441B], 16A06-Gal4 (FlyLight, Janelia).

Genotypes used by figure (with neuronal expression description):

All experiments were performed using 3 day to 2 week old females. Unless noted below, all animals are of the genotype UAS-sytGCaMP6s, MB247(KCs)-DsRed; TH(DAN subset)-Gal4, DDC(DAN subset)-Gal4

Figure 2.3B: 58E02(DAN subset)-p65ADZp/UAS-GCaMP6s; 10G03(DAN subset)-ZpGdbd

Figure 2.9A: 30G08 (DAN subset)-p65ADZp/UAS-GCaMP6f; 48B03 (DAN subset)-ZpGdbd

Figure 2.9B: 58E02 (DAN subset)-p65ADZp/UAS-GCaMP6f; 10G03 (DAN subset)-ZpGdbd

Figure 2.9C: 30G08 (DAN subset)-p65ADZp/UAS-CD8-GFP; 48B03 (DAN subset)-ZpGdbd

Figure 3.8A: MB247(KCs)-LexA/LexAOP-GCaMP6s

Figure 5.1A: UAS-GtACR1; 58E02(DAN subset)-p65ADZp; 22E04(DAN subset)-ZpGdbd.

Figure 5.1B: UAS-GtACR1; 58E02(DAN subset)-p65ADZp; 22E04(DAN subset)-ZpGdbd.

UAS-GtACR1; 58E02(DAN subset)-p65ADZp; 36B06(DAN subset)-ZpGdbd.

UAS-GtACR1; 58E02(DAN subset)-p65ADZp; 10G03(DAN subset)-ZpGdbd.

UAS-GtACR1; 52H03(DAN subset)-p65ADZp; TH(DAN subset)-ZpGdbd.

58E02(DAN subset)-p65ADZp; 22E04(DAN subset)-ZpGdbd.

UAS-GtACR1.

UAS-GtACR1; 16A06(KC subset)-Gal4.

Figure 5.2B: UAS-ChChrimson; 58E02(DAN subset)-p65ADZp; 22E04(DAN subset)-ZpGdbd.

UAS-ChChrimson

Figure 5.3: UAS-GcAMP6s; 52G04 (MBON subset)-p65ADZp; 94B10 (DAN subset)-ZpGdbd.

Fly Tethering and Dissection

For *in vivo* imaging of neural activity flies were prepared as described previously[369] with minor modifications. Briefly, 3 day to 2 week old females were temporarily anesthetized using CO_2 (<30s) and tethered to a holder dish modified from that used in previous studies[369]. The fly was held in place with UV-curable glue (Loctite) applied to each eye and thorax and the proboscis was glued in an extended position to minimize movement during imaging. After a 30-minute to 2-hour recovery period, the dish was then filled with external saline (108mM NaCl, 5mM KCl, 2mM CaCl2, 8.2mM MgCl2, 4mM NaHCO3, 1mM NaH2PO4, 5mM trehalose, 10mM sucrose, 5mM HEPES sodium salt, pH 7.5 with osmolarity adjusted to 275 mOsm) and the cuticle covering the dorsal portion of the head was removed. Muscle 16 and obstructing trachea were removed with care taken to keep the antennae and antennal nerves intact.

Two-Photon Functional Imaging

All functional imaging experiments were performed on an Ultima two-photon laser scanning microscope (Bruker Nanosystems) equipped with galvanometers driving a Chameleon Ultra II Ti:Sapphire laser. Emitted fluorescence was detected with either photomultiplier-tube or GaAsP photodiode (Hamamatsu) detectors. Images were acquired with an Olympus 40x, 0.8 numerical aperture objective at 512 pixels × 512 pixels resolution. For fast-scanning volumetric imaging in vivo (Figure 2.3A), the laser was directed through an 8kHz resonant scanning galvonometer and the objective was controlled by a piezo-electric Zfocus. Z-planes were defined in order to visualize maximum number of γ4 DAN soma (~50m). Ten planes were recorded with the entire volume imaged at a rate of 2-5Hz.

Tethered Locomotion

A spherical treadmill was designed based on previous studies[368,369]. Briefly, a 6.35mm diameter ball was shaped from Last-A-Foam FR-4618 (General Plastics) by a steel concave file. The ball rested in an aluminum base with a concave hemisphere 6.75mm in diameter with a 1mm channel drilled through the bottom and connected to an airflow. The ball was recorded at 60-61 fps using a Point Grey Firefly Camera with Infinity Lens (94mm focal length) focused on the ball while being illuminated by infrared LED lights. Ball rotation was calculated in real time using FicTrac software[370] running on Ubuntu 12.04 on computers with processors with speeds of at least 3GHz.

Electrophysiology

γ3 DAN soma were targeted for patch recordings by fluorescence from expression of soluble CD8-GFP. Flies were tethered as above but after opening of the cuticle, brains were treated with 2mg/mL of collagenase (Sigma) in external saline for ~30sec to soften the perineural sheath and then washed with perfusion saline 3-5 times. The exposed neuropil was continuously perfused (~2-3 mL/min) with perfusion saline that was continuously bubbled with 95% O_2/5% CO_2 at a final pH of 7.3. To gain access to soma, the sheath was broken by positive pressure from ejection of saline through a large bore broken electrode. Intracellular recordings were performed with fire-polished patch electrodes (3-5MΩ) filled with internal saline (130mM potassium aspartate, 8mM KCl, .2mM $MgCl_2$, 5mM Sucrose, 10mM HEPES pH 7.3, 10mM EGTA). Current traces were acquired in voltage-clamp mode using Multiclamp 700B amplifier, digitized at 10Hz and filtered at 1kHz. Spikes were counted and plotted using custom Matlab scripts.

Closed loop arena

The heading of the fly, as calculated by FicTrac, was transmitted to an Arduino Mega via serial port. Custom Arduino code was used to translate heading into tube position controlled by motors described below.

The closed loop air-delivery system was custom designed using OnShape (www.onshape.com) and 3D printed using Visijet Crystal material at XHD resolution in a

3DSystems Projet 3510 HD Plus. O-ring OD and ID Gland surfaces were designed with excess material for printing then manually modified on a lathe for improved RMS [surface] finishing. 360° tube rotation was driven by a bipolar stepper motor (Pololu item #1206) controlled through a A4988 Stepper Motor Driver Carrier (Pololu #2980) coupled by a Dust-Free Timing Belt XL Series, 1/4" Width (McMaster-Carr, 1679K121, Trade No. 130×L025) to the rotating tube system, which rotated mounted on an Ultra-Corrosion-Resistant Stainless Steel Ball Bearing (3/4" Shaft Diameter, 1-5/8" OD, Mcmaster-Carr 5908K19). Air channel was kept airtight using oil resistant o-rings (1/16 Fractional Width, Dash Number 020, Mcmaster-Carr 2418T126). Motor rotation was measured by a rotary encoder (CUI Inc., AMT10 Series) to correct for skipped steps.

Odor stimulation and airflow

Odor stimulation was achieved by directing a continuous stream of either 100 mL/min or 400mL/min (high airflow conditions, Figure 3.12-3.14) of clean air through a 2mm diameter tube made of Visijet Crystal material directed at the fly's antenna. 10-20% of the total airstream was diverted through the headspace of a 500 mL glass bottle containing water. At a trigger, a custom-built solenoid valve controller system redirected the odor stream from the water bottle to a bottle containing the odorant, Apple Cider Vinegar (ACV, Heinz). To present CO_2 to tethered animals (Figure 3.15), an additional custom-built solenoid valve controller system was used to re-direct pressurized air containing 99% CO_2 into the clean airstream while simultaneously shunting away the same proportion of the total airflow at a designated trigger.

Sugar Feeding

Flies were tethered for imaging and locomotion as described above and presented with nanoliter volumes of 1M sucrose via a Nanoject II Auto-Nanoliter Injector (Drummon, Cat. No. 3-000-204) positioned with a motorized micromanipulator (Scientifica). Red food coloring was added to the sucrose and the fly abdomens were inspected after each experiment to confirm sucrose ingestion.

Freely Moving Behavior and Optogenetic Perturbations

Fly chamber component pieces were cut from acrylic sheets using a laser cutter. The lid and base of each chamber were cut from transparent acrylic (Clear Cast Acrylic Sheet, 12" x 24" x 1/16", McMaster Carr). Two holes on opposite sides of the lid were tapped for 10-32 threaded Luer lock connectors. A single hole was cut in the base to allow flies to be loaded and unloaded. A spacer was cut from a 3-mm black scratch-resistant acrylic sheet (McMaster-Carr) with a central empty chamber (20 mm x 50 mm) flanked by two manifolds. Narrow channels were etched between the manifolds and central chamber using a low-power setting of the laser cutter. This permitted airflow between the chamber and the manifolds while confining flies within the chamber. The dimensions of the inside chamber were 20 mm x 50 mm x 3 mm. The base, spacer, and lid were glued together using acrylic solvent and the edges of the chamber were further sealed with epoxy (Devcon 5 Minute® Epoxy) to make them airtight. 10-32 Luer connectors were screwed into the top of the chamber and sealed around the edges with epoxy.

Flies in chambers were assayed in a custom-built apparatus. Chambers were placed on a 3mm thick white acrylic sheet suspended on aluminum posts above a 3x4 array of 530nm LEDs (Luxeon Rebel). LEDs were attached to metal heat sinks (Mouser #532-374624B32G), which were secured at 5cm intervals to a 30x30 cm aluminum wire cloth sheet (McMaster-Carr #9227T53). LEDs were driven by Recom Power RCD-24-0.70/W/X2 drivers, which were powered by a variable DC power supply. Infrared LED strips (940 nm, LED Lights World) attached to the wire cloth between the heat sinks provided back-illumination of the platform. A Firefly camera (Point Grey) was mounted in a central hole within an acrylic lid suspended 30cm above the platform on aluminum posts. Flies were recorded at 30 frames/second. Odor presentation and airflow were controlled using 3-way micro solenoid valves. A vacuum line was used to draw air into each chamber at a rate of 0.75-1 L/min/chamber. Two valves were used to control the direction of airflow, and additional valves were used to switch between clean air and different odors. Odorants were placed in glass bottles with lids containing two Luer connectors. One connector was attached to an odor inlet valve and the other was left open to allow room air to enter the bottle. By default, air entered the apparatus through a bottle containing distilled water. To deliver odor pulses, the solenoid valve to the water bottle was closed while simultaneously opening the valve to an odor bottle. The valves were then switched back to their resting position after the specified odor presentation interval. Valves were powered by a 12V DC power supply and switched on and off using VO14642AT solid state relays. Valve relays and LED drivers were controlled by the output pins of an Arduino running custom software that allowed for independent control of each component. Custom software written in C was used for data acquisition and instrument control

during individual trials of odor/light presentation. Python scripts were used to execute sequences of trials.

To present CO_2 to freely moving animals, an additional valve system was built that instead of using a vacuum to pull air through a liquid containing bottle, pushed pressurized air through those same bottles. To prevent the build-up of pressure, air not being directed into the behavioral chambers was vented into the room. Valve relays and LED drivers were controlled by the output pins of an Arduino running custom software that allowed for independent control of each component.

Optogenetic inhibition and excitation were achieved using a 1-2 second illumination with either 520nm or 627nm LEDs. The intensity of light within each chamber during LED illumination was 20-40 μW/mm2.

Image Processing

All image processing was done using FIJI/ImageJ (NIH). Compartment (DAN subpopulation)-specific activity was computed by averaging all fluorescent signal within a MB γ lobe compartment. Compartments were identified and defined manually. All DAN>sytGCaMP6s signals are normalized by MB247(KC)>dsRed fluorescence within the same ROI.

Data Analysis

Unless otherwise noted, all analyses and visualizations were performed using custom scripts in ImageJ and Matlab.

All representations, normalizations, and averaging of behavior and DAN activity were generated by custom Matlab scripts.

Behavioral variables of net motion, forward velocity, angular velocity, and lateral velocity were convoluted by the biexponential rise and decay function of GCaMP6s (rise $t_{1/2}$=175ms and decay $t_{1/2}$=550ms) or GCaMP6f (Figure 2.9, rise $t_{1/2}$=50ms and decay $t_{1/2}$=100ms) except in Figures 2.6, 2.8, 3.5B, 3.9, 3.10,3.11, 3.13, 3.14, where non-convoluted behavior was used.

The following built in matlab functions were used to calculate the designated variables in the designated figures:

mnrval (probability of accurate walking state prediction; Figure 2.4B)

corrcoef (Pearson correlation coefficient and associated p-value calculation; Figures 2.4D, 2.5A, 2.6, 2.10C, 3.4A, 3.7C-E, 3.12B-C3.15D, 4.2C-D)

kmeans (K-means clustering; Figure 2.2A, 2.3A)

fitlm (fitting a linear model predicting forward velocity from γ DAN activity. Figure 3.5B)

K-means clustering analysis (Figure 2.3B) was performed as follows: FIJI/ImageJ was used to mask areas outside the γ lobe in recordings from DAN>sytGCaMP6s. The fluorescence

over time at each γ lobe pixel (independent of its original location within the MB) was fed into the Matlab function *kmeans*, which assigned it a cluster designation. Pixel cluster designation was then mapped onto original pixel location and plotted.

Probability of accurate walking state prediction (Figure 2.4B) was calculated as follows: Custom Matlab scripts used manually identified cutoff values to perform an *in silico* identification of periods of walking and periods of not walking during trials of spontaneous movement. Walking/still designations were then manually verified. Animals that were not designated as being still for at least 20% of time points were discarded. All data from a single animal were concatenated and 20% of time points were randomly set aside (using Matlab function *randperm*) while the remaining 80% were used to train a multinomial logistic regression model (*mnrval*) to predict locomotor state from compartmentalized DAN activity. The model was then tested on the previously allocated 20% of time points. During testing, the model produced both a prediction of locomotor state and probability of accuracy. Predictions were compared with actual locomotor state and the probability of accuracy of correct predictions were averaged (with incorrect predictions assigned a value of zero). This process was repeated 100 times for each animal and the mean probability of accuracy was averaged across all 100 repetitions.

Partial correlations for each pair-wise combination of γ DANs (Figure 2.10B) were generated using python scripts that subtracted out exiting correlations between each γ DAN and parameters of movement (net motion, forward velocity, turning velocity, and lateral velocity) and the activity of other γ DANs and then calculating the Pearson's correlation coefficient (r) for the residual DAN signals.

Instances of movement initiation (Figures 2.4C,D, 2.5, 2.6, 2.9A, 3.4) were identified *in silico* with custom Matlab scripts that used a manually set cutoff to find inflection points in net motion after a prolonged pauses (≥2sec) followed by sustained movement (≥3sec).

Principal component analysis (PCA) of behavioral variables during the onset of movement (Figure 2.6) was performed on net motion, forward velocity, turning velocity, and |lateral velocity| across a 4 second time window centered on instants of movement initiation (4 variables × 4sec time window × 10Hz sampling = 160 initial variables per start). All behaviors were z-score normalized over the 4sec window.

Linear filters (Figures 2.8, 3.5A, 3.8B, 3.14) were generated by custom python code that fit using standardized linear regression in which the least squared error between all true and predicted output was minimized to identify best-fit filters.

Cross correlation matrices (Figures 3.9, 3.13A,B) were generated using custom built python scripts calculating and plotting the Pearson's correlation coefficient of between DAN activity and behavior at each timepoint in a 20 second window.

The nested model analysis (Figures 3.11, 3.13C) used linear models, with significant levels for the increase in variance explained as stepwise predictors were added computed using an F-test. Models were generated using custom written python scripts.

Statistical analysis

All statistical analyses were performed using built in Matlab functions unless otherwise noted.

One-way ANOVA: *anova1* (Figures 2.2C,D, 2.4B, 2.10B, 3.8A)

2-tailed paired t-tests with Holm-Bonferroni post-hoc correction: *ttest* (Figures 2.8D, 3.2B,D, 3.6C, 3.15B,C, 4.2A,B, 5.1C, 5.2)

2-tailed t-tests for Pearson correlation coefficients with Holm-Bonferroni post-hoc correction: *corrcoef* (Figures 2.5A, 2.6C,D, 2.10C, 3.7C-E, 3.12B,C, 3.15D, 4.2C,D)

Figures and Illustrations

All schematics and illustrations were generated using Adobe® Illustrator® CS6, Version 16.0.0.

All figures were made using Adobe® Illustrator® CS6, Version 16.0.0.

References

1. Swanson, L. W. *et al. Beautiful Brain: The Drawings of Santiago Ramon y Cajal*. (Abrams, 2017).

2. Jones, E. G. Neuroanatomy: Cajal and after Cajal. *Brain Res. Rev.* **55**, 248–255 (2007).

3. Swanson, L. W. & Lichtman, J. W. From Cajal to Connectome and Beyond. *Annu. Rev. Neurosci.* **39**, 197–216 (2016).

4. Siegelbaum, S. A. & Hudspeth, A. J. *Principles of Neural Science, Fifth Edition*. (McGraw Hill Professional, 2013).

5. Blumenfeld, H. *Neuroanatomy through Clinical Cases*. (Sinauer, 2011).

6. Arber, S. Motor Circuits in Action: Specification, Connectivity, and Function. *Neuron* **74**, 975–989 (2012).

7. Svoboda, K. & Li, N. Neural mechanisms of movement planning: motor cortex and beyond. *Curr. Opin. Neurobiol.* **49**, 33–41 (2018).

8. Scoville, W. B. & Milner, B. Loss of recent memory after bilateral hippocampal lesions. *J. Neurol. Neurosurg. Psychiatry* **20**, 11–21 (1957).

9. Milner, B. & Klein, D. Loss of recent memory after bilateral hippocampal lesions: memory and memories—looking back and looking forward. *J Neurol Neurosurg Psychiatry* **87**, 230–230 (2016).

10. Milner, B., Petrides, M. & Smith, M. L. Frontal lobes and the temporal organization of memory. *Hum. Neurobiol.* **4**, 137–142 (1985).

11. Crane, J. & Milner, B. Do I know you? Face perception and memory in patients with selective amygdalo-hippocampectomy. *Neuropsychologia* **40**, 530–538 (2002).

12. Tremblay, P. & Dick, A. S. Broca and Wernicke are dead, or moving past the classic model of language neurobiology. *Brain Lang.* **162**, 60–71 (2016).

13. Ardila, A., Bernal, B. & Rosselli, M. How Localized are Language Brain Areas? A Review of Brodmann Areas Involvement in Oral Language. *Arch. Clin. Neuropsychol.* **31**, 112–122 (2016).

14. Filley, C. M. The Neuroanatomy of Attention. *Semin. Speech Lang.* **23**, 89–98 (2002).

15. Culpepper, L. Neuroanatomy and Physiology of Cognition. *J. Clin. Psychiatry* **76**, 900–900 (2015).

16. Xu, T. *et al.* Rapid formation and selective stabilization of synapses for enduring motor memories. *Nature* **462**, 915–919 (2009).

17. Fu, M., Yu, X., Lu, J. & Zuo, Y. Repetitive motor learning induces coordinated formation of clustered dendritic spines *in vivo*. *Nature* **483**, 92–95 (2012).

18. Clark, T. A., Fu, M., Dunn, A. K., Zuo, Y. & Jones, T. A. Preferential stabilization of newly formed dendritic spines in motor cortex during manual skill learning predicts performance gains, but not memory endurance. *Neurobiol. Learn. Mem.* **152**, 50–60 (2018).

19. Paolicelli, R. C. *et al.* Synaptic Pruning by Microglia Is Necessary for Normal Brain Development. *Science* **333**, 1456–1458 (2011).

20. Hong, S., Dissing-Olesen, L. & Stevens, B. New insights on the role of microglia in synaptic pruning in health and disease. *Curr. Opin. Neurobiol.* **36**, 128–134 (2016).

21. Sivachenko, A., Li, Y., Abruzzi, K. C. & Rosbash, M. The Transcription Factor Mef2 Links the Drosophila Core Clock to Fas2, Neuronal Morphology, and Circadian Behavior. *Neuron* **79**, 281–292 (2013).

22. Bargmann, C. I. Beyond the connectome: How neuromodulators shape neural circuits. *BioEssays* **34**, 458–465 (2012).

23. Bargmann, C. I. & Marder, E. From the connectome to brain function. *Nat. Methods* **10**, 483–490 (2013).

24. Marder, E. Neuromodulation of Neuronal Circuits: Back to the Future. *Neuron* **76**, 1–11 (2012).

25. Inagaki, H. K. *et al.* Visualizing Neuromodulation In Vivo: TANGO-Mapping of Dopamine Signaling Reveals Appetite Control of Sugar Sensing. *Cell* **148**, 583–595 (2012).

26. Hergarden, A. C., Tayler, T. D. & Anderson, D. J. Allatostatin-A neurons inhibit feeding behavior in adult Drosophila. *Proc. Natl. Acad. Sci.* **109**, 3967–3972 (2012).

27. Chao, M. Y., Komatsu, H., Fukuto, H. S., Dionne, H. M. & Hart, A. C. Feeding status and serotonin rapidly and reversibly modulate a Caenorhabditis elegans chemosensory circuit. *Proc. Natl. Acad. Sci.* **101**, 15512–15517 (2004).

28. Martelli, C. *et al.* SIFamide Translates Hunger Signals into Appetitive and Feeding Behavior in Drosophila. *Cell Rep.* **20**, 464–478 (2017).

29. Crossley, M., Staras, K. & Kemenes, G. A central control circuit for encoding perceived food value. *Sci. Adv.* **4**, (2018).

30. Sayin, S., Boehm, A. C., Kobler, J. M., De Backer, J.-F. & Grunwald Kadow, I. C. Internal State Dependent Odor Processing and Perception—The Role of Neuromodulation in the Fly Olfactory System. *Front. Cell. Neurosci.* **12**, (2018).

31. Lee, S., Kim, Y.-J. & Jones, W. D. Central peptidergic modulation of peripheral olfactory responses. *BMC Biol.* **15**, 35 (2017).

32. Root, C. M., Ko, K. I., Jafari, A. & Wang, J. W. Presynaptic Facilitation by Neuropeptide Signaling Mediates Odor-Driven Food Search. *Cell* **145**, 133–144 (2011).

33. Dielenberg, R. A. & McGregor, I. S. Defensive behavior in rats towards predatory odors: a review. *Neurosci. Biobehav. Rev.* **25**, 597–609 (2001).

34. Tank, A. W. & Lee Wong, D. Peripheral and central effects of circulating catecholamines. *Compr. Physiol.* **5**, 1–15 (2015).

35. Chamero, P. *et al.* Identification of protein pheromones that promote aggressive behaviour. *Nature* **450**, 899–902 (2007).

36. Yilmaz, M. & Meister, M. Rapid Innate Defensive Responses of Mice to Looming Visual Stimuli. *Curr. Biol.* **23**, 2011–2015 (2013).

37. Hermans, E. J. *et al.* Stress-Related Noradrenergic Activity Prompts Large-Scale Neural Network Reconfiguration. *Science* **334**, 1151–1153 (2011).

38. Pavlou, H. J. & Goodwin, S. F. Courtship behavior in Drosophila melanogaster: towards a 'courtship connectome'. *Curr. Opin. Neurobiol.* **23**, 76–83 (2013).

39. Andrews, J. C. *et al.* Octopamine Neuromodulation Regulates Gr32a-Linked Aggression and Courtship Pathways in Drosophila Males. *PLOS Genet.* **10**, e1004356 (2014).

40. Pereira, T. D. & Murthy, M. To Fight or Not to Fight. *Neuron* **95**, 986–988 (2017).

41. Watanabe, K. *et al.* A Circuit Node that Integrates Convergent Input from Neuromodulatory and Social Behavior-Promoting Neurons to Control Aggression in Drosophila. *Neuron* **95**, 1112-1128.e7 (2017).

42. Xia, X.-B. & Mills, S. L. Gap junctional regulatory mechanisms in the AII amacrine cell of the rabbit retina. *Vis. Neurosci.* **21**, 791–805 (2004).

43. Geffen, M. N., Vries, S. E. J. de & Meister, M. Retinal Ganglion Cells Can Rapidly Change Polarity from Off to On. *PLOS Biol.* **5**, e65 (2007).

44. Chang, A. J., Chronis, N., Karow, D. S., Marletta, M. A. & Bargmann, C. I. A Distributed Chemosensory Circuit for Oxygen Preference in C. elegans. *PLOS Biol.* **4**, e274 (2006).

45. Marder, E. Invertebrate Neurobiology: Polymorphic neural networks. *Curr. Biol.* **4**, 752–754 (1994).

46. Goldman, M. S., Golowasch, J., Marder, E. & Abbott, L. F. Global Structure, Robustness, and Modulation of Neuronal Models. *J. Neurosci.* **21**, 5229–5238 (2001).

47. Nadim, F. & Bucher, D. Neuromodulation of neurons and synapses. *Curr. Opin. Neurobiol.* **29**, 48–56 (2014).

48. Ursin, R. Serotonin and sleep. *Sleep Med. Rev.* **6**, 55–67 (2002).

49. Siegel, J. M. The Neurotransmitters of Sleep. *J. Clin. Psychiatry* **65**, 4–7 (2004).

50. Zeitzer, J. M. Control of sleep and wakefulness in health and disease. *Prog. Mol. Biol. Transl. Sci.* **119**, 137–154 (2013).

51. Becchetti, A. & Amadeo, A. Why we forget our dreams: Acetylcholine and norepinephrine in wakefulness and REM sleep. *Behav. Brain Sci.* **39**, (2016).

52. Berridge, C. W. & Waterhouse, B. D. The locus coeruleus–noradrenergic system: modulation of behavioral state and state-dependent cognitive processes. *Brain Res. Rev.* **42**, 33–84 (2003).

53. Berridge, C. W. Noradrenergic modulation of arousal. *Brain Res. Rev.* **58**, 1–17 (2008).

54. Gobrogge, K. & Wang, Z. The ties that bond: neurochemistry of attachment in voles. *Curr. Opin. Neurobiol.* **38**, 80–88 (2016).

55. Wang, Z. & Aragona, B. J. Neurochemical regulation of pair bonding in male prairie voles. *Physiol. Behav.* **83**, 319–328 (2004).

56. Anderson, D. J. Circuit modules linking internal states and social behaviour in flies and mice. *Nat. Rev. Neurosci.* **17**, 692–704 (2016).

57. Kim, S. M., Su, C.-Y. & Wang, J. W. Neuromodulation of Innate Behaviors in Drosophila. *Annu. Rev. Neurosci.* **40**, 327–348 (2017).

58. Corrales-Carvajal, V. M., Faisal, A. A. & Ribeiro, C. Internal states drive nutrient homeostasis by modulating exploration-exploitation trade-off. *eLife* **5**, e19920 (2016).

59. Yu, A. J. & Dayan, P. Uncertainty, Neuromodulation, and Attention. *Neuron* **46**, 681–692 (2005).

60. Noudoost, B. & Moore, T. The role of neuromodulators in selective attention. *Trends Cogn. Sci.* **15**, 585–591 (2011).

61. Lee, S.-H. & Dan, Y. Neuromodulation of Brain States. *Neuron* **76**, 209–222 (2012).

62. Anderson, D. J. & Adolphs, R. A Framework for Studying Emotions across Species. *Cell* **157**, 187–200 (2014).

63. Seyedabadi, M., Fakhfouri, G., Ramezani, V., Mehr, S. E. & Rahimian, R. The role of serotonin in memory: interactions with neurotransmitters and downstream signaling. *Exp. Brain Res.* **232**, 723–738 (2014).

64. Puig, M. V., Rose, J., Schmidt, R. & Freund, N. Dopamine modulation of learning and memory in the prefrontal cortex: insights from studies in primates, rodents, and birds. *Front. Neural Circuits* **8**, (2014).

65. Uematsu, A. *et al.* Modular organization of the brainstem noradrenaline system coordinates opposing learning states. *Nat. Neurosci.* **20**, 1602–1611 (2017).

66. Aggarwal, M., Hyland, B. I. & Wickens, J. R. Neural control of dopamine neurotransmission: implications for reinforcement learning. *Eur. J. Neurosci.* **35**, 1115–1123 (2012).

67. Huertas, M. A., Schwettmann, S. E. & Shouval, H. Z. The Role of Multiple Neuromodulators in Reinforcement Learning That Is Based on Competition between Eligibility Traces. *Front. Synaptic Neurosci.* **8**, (2016).

68. Goodman, W. K., Grice, D. E., Lapidus, K. A. B. & Coffey, B. J. Obsessive-Compulsive Disorder. *Psychiatr. Clin. North Am.* **37**, 257–267 (2014).

69. Hendrickson, R. C. & Raskind, M. A. Noradrenergic dysregulation in the pathophysiology of PTSD. *Exp. Neurol.* **284**, 181–195 (2016).

70. Harrison, P. J., Geddes, J. R. & Tunbridge, E. M. The Emerging Neurobiology of Bipolar Disorder. *Trends Neurosci.* **41**, 18–30 (2018).

71. Sharma, A. & Couture, J. A Review of the Pathophysiology, Etiology, and Treatment of Attention-Deficit Hyperactivity Disorder (ADHD). *Ann. Pharmacother.* **48**, 209–225 (2014).

72. Grace, A. A. Dysregulation of the dopamine system in the pathophysiology of schizophrenia and depression. *Nat. Rev. Neurosci.* **17**, 524–532 (2016).

73. Lang, A. E. & Lozano, A. M. Parkinson's Disease. *N. Engl. J. Med.* **339**, 1044–1053 (1998).

74. Marder, E., O'Leary, T. & Shruti, S. Neuromodulation of Circuits with Variable Parameters: Single Neurons and Small Circuits Reveal Principles of State-Dependent and Robust Neuromodulation. *Annu. Rev. Neurosci.* **37**, 329–346 (2014).

75. Beaulieu, J.-M. & Gainetdinov, R. R. The Physiology, Signaling, and Pharmacology of Dopamine Receptors. *Pharmacol. Rev.* **63**, 182–217 (2011).

76. Tritsch, N. X. & Sabatini, B. L. Dopaminergic Modulation of Synaptic Transmission in Cortex and Striatum. *Neuron* **76**, 33–50 (2012).

77. Schultz, W., Dayan, P. & Montague, P. R. A Neural Substrate of Prediction and Reward. *Science* **275**, 1593–1599 (1997).

78. Brunelli, M., Castellucci, V. & Kandel, E. R. Synaptic facilitation and behavioral sensitization in Aplysia: possible role of serotonin and cyclic AMP. *Science* **194**, 1178–1181 (1976).

79. Kandel, E. R. The Molecular Biology of Memory Storage: A Dialogue Between Genes and Synapses. *Science* **294**, 1030–1038 (2001).

80. Barbas, D., DesGroseillers, L., Castellucci, V. F., Carew, T. J. & Marinesco, S. Multiple Serotonergic Mechanisms Contributing to Sensitization in Aplysia: Evidence of Diverse Serotonin Receptor Subtypes. *Learn. Mem.* **10**, 373–386 (2003).

81. Lee, Y.-S. *et al.* Identification of a serotonin receptor coupled to adenylyl cyclase involved in learning-related heterosynaptic facilitation in Aplysia. *Proc. Natl. Acad. Sci.* **106**, 14634–14639 (2009).

82. Kim, Y., Chen, L., McCarley, R. W. & Strecker, R. E. Sleep allostasis in chronic sleep restriction: The role of the norepinephrine system. *Brain Res.* **1531**, 9–16 (2013).

83. Aston-Jones, G. & Cohen, J. D. An integrative theory of locus coeruleus-norepinephrine function: adaptive gain and optimal performance. *Annu. Rev. Neurosci.* **28**, 403–450 (2005).

84. Schwarz, L. A. & Luo, L. Organization of the Locus Coeruleus-Norepinephrine System. *Curr. Biol.* **25**, R1051–R1056 (2015).

85. Aston-Jones, G. & Waterhouse, B. Locus coeruleus: From global projection system to adaptive regulation of behavior. *Brain Res.* **1645**, 75–78 (2016).

86. Benarroch, E. E. Locus coeruleus. *Cell Tissue Res.* **373**, 221–232 (2018).

87. Ogawa, S. K., Cohen, J. Y., Hwang, D., Uchida, N. & Watabe-Uchida, M. Organization of Monosynaptic Inputs to the Serotonin and Dopamine Neuromodulatory Systems. *Cell Rep.* **8**, 1105–1118 (2014).

88. Li, Y. *et al.* Serotonin neurons in the dorsal raphe nucleus encode reward signals. *Nat. Commun.* **7**, 10503 (2016).

89. Pollak Dorocic, I. *et al.* A Whole-Brain Atlas of Inputs to Serotonergic Neurons of the Dorsal and Median Raphe Nuclei. *Neuron* **83**, 663–678 (2014).

90. Weissbourd, B. *et al.* Presynaptic Partners of Dorsal Raphe Serotonergic and GABAergic Neurons. *Neuron* **83**, 645–662 (2014).

91. Parkinson, J. *An essay on the shaking palsy*. (Printed by Whittingham & Rowland ..., for Sherwood, Neely & Jones ..., 1817).

92. Ehringer, H. & Hornykiewicz, O. [Distribution of noradrenaline and dopamine (3-hydroxytyramine) in the human brain and their behavior in diseases of the extrapyramidal system]. *Klin. Wochenschr.* **38**, 1236–1239 (1960).

93. Birkmayer, W. & Hornykiewicz, O. [The L-3,4-dioxyphenylalanine (DOPA)-effect in Parkinson-akinesia]. *Wien. Klin. Wochenschr.* **73**, 787–788 (1961).

94. Anden, N. E. *et al.* Demonstration and mapping out of nigro-neostriatal dopamine neurons. *Life Sci. 1962* **3**, 523–530 (1964).

95. Cotzias, G. C., Van Woert, M. H. & Schiffer, L. M. Aromatic Amino Acids and Modification of Parkinsonism. *N. Engl. J. Med.* **276**, 374–379 (1967).

96. Cotzias, G. C., Papavasiliou, P. S. & Gellene, R. Modification of Parkinsonism — Chronic Treatment with L-Dopa. *N. Engl. J. Med.* **280**, 337–345 (1969).

97. Fahn, S. The history of dopamine and levodopa in the treatment of Parkinson's disease. *Mov. Disord.* **23**, S497–S508 (2008).

98. Riederer, P. & Wuketich, S. Time course of nigrostriatal degeneration in parkinson's disease. A detailed study of influential factors in human brain amine analysis. *J. Neural Transm.* **38**, 277–301 (1976).

99. Bergman, H. & Deuschl, G. Pathophysiology of Parkinson's disease: from clinical neurology to basic neuroscience and back. *Mov. Disord. Off. J. Mov. Disord. Soc.* **17 Suppl 3**, S28-40 (2002).

100. Steinberg, E. E. *et al.* A causal link between prediction errors, dopamine neurons and learning. *Nat. Neurosci.* **16**, 966–973 (2013).

101. Higa, K. K. *et al.* Striatal dopamine D1 receptor suppression impairs reward-associative learning. *Behav. Brain Res.* **323**, 100–110 (2017).

102. Seip-Cammack, K. M., Young, J. J., Young, M. E. & Shapiro, M. L. Partial lesion of the nigrostriatal dopamine pathway in rats impairs egocentric learning but not spatial learning or behavioral flexibility. *Behav. Neurosci.* **131**, 135–142 (2017).

103. Wise, R. A. & Schwartz, H. V. Pimozide attenuates acquisition of lever-pressing for food in rats. *Pharmacol. Biochem. Behav.* **15**, 655–656 (1981).

104. Parker, J. G. *et al.* Attenuating GABAA Receptor Signaling in Dopamine Neurons Selectively Enhances Reward Learning and Alters Risk Preference in Mice. *J. Neurosci.* **31**, 17103–17112 (2011).

105. Oishi, Y. & Lazarus, M. The control of sleep and wakefulness by mesolimbic dopamine systems. *Neurosci. Res.* **118**, 66–73 (2017).

106. Cooper, S., Robison, A. J. & Mazei-Robison, M. S. Reward Circuitry in Addiction. *Neurotherapeutics* **14**, 687–697 (2017).

107. Phillips, P. E. M., Stuber, G. D., Heien, M. L. A. V., Wightman, R. M. & Carelli, R. M. Subsecond dopamine release promotes cocaine seeking. *Nature* **422**, 614–618 (2003).

108. Gerdeman, G. L., Partridge, J. G., Lupica, C. R. & Lovinger, D. M. It could be habit forming: drugs of abuse and striatal synaptic plasticity. *Trends Neurosci.* **26**, 184–192 (2003).

109. Laruelle, M. Imaging dopamine transmission in schizophrenia. A review and meta-analysis. *Q. J. Nucl. Med. Off. Publ. Ital. Assoc. Nucl. Med. AIMN Int. Assoc. Radiopharmacol. IAR* **42**, 211–221 (1998).

110. Guillin, O., Abi-Dargham, A. & Laruelle, M. Neurobiology of Dopamine in Schizophrenia. in *International Review of Neurobiology* **78**, 1–39 (Academic Press, 2007).

111. van Os, J. & Kapur, S. Schizophrenia. *The Lancet* **374**, 635–645 (2009).

112. Tarver, J., Daley, D. & Sayal, K. Attention-deficit hyperactivity disorder (ADHD): an updated review of the essential facts. *Child Care Health Dev.* **40**, 762–774 (2014).

113. Tye, K. M. *et al.* Dopamine neurons modulate neural encoding and expression of depression-related behaviour. *Nature* **493**, 537–541 (2013).

114. Chinta, S. J. & Andersen, J. K. Dopaminergic neurons. *Int. J. Biochem. Cell Biol.* **37**, 942–946 (2005).

115. Regehr, W. G., Carey, M. R. & Best, A. R. Activity-Dependent Regulation of Synapses by Retrograde Messengers. *Neuron* **63**, 154–170 (2009).

116. Higley, M. J. & Sabatini, B. L. Competitive regulation of synaptic Ca^{2+} influx by D2 dopamine and A2A adenosine receptors. *Nat. Neurosci.* **13**, 958–966 (2010).

117. Sun, X., Zhao, Y. & Wolf, M. E. Dopamine Receptor Stimulation Modulates AMPA Receptor Synaptic Insertion in Prefrontal Cortex Neurons. *J. Neurosci.* **25**, 7342–7351 (2005).

118. McKay, B. E., Placzek, A. N. & Dani, J. A. Regulation of synaptic transmission and plasticity by neuronal nicotinic acetylcholine receptors. *Biochem. Pharmacol.* **74**, 1120–1133 (2007).

119. Flores-Hernández, J. *et al.* Dopamine Enhancement of NMDA Currents in Dissociated Medium-Sized Striatal Neurons: Role of D1 Receptors and DARPP-32. *J. Neurophysiol.* **88**, 3010–3020 (2002).

120. Flores-Hernandez, J. *et al.* D1 Dopamine Receptor Activation Reduces GABAA Receptor Currents in Neostriatal Neurons Through a PKA/DARPP-32/PP1 Signaling Cascade. *J. Neurophysiol.* **83**, 2996–3004 (2000).

121. Rice, M. E., Patel, J. C. & Cragg, S. J. Dopamine release in the basal ganglia. *Neuroscience* **198**, 112–137 (2011).

122. Lanciego, J. L., Luquin, N. & Obeso, J. A. Functional Neuroanatomy of the Basal Ganglia. *Cold Spring Harb. Perspect. Med.* **2**, a009621 (2012).

123. Carta, M. & Bezard, E. Contribution of pre-synaptic mechanisms to l-DOPA-induced dyskinesia. *Neuroscience* **198**, 245–251 (2011).

124. Cloud, L. J., Zutshi, D. & Factor, S. A. Tardive Dyskinesia: Therapeutic Options for an Increasingly Common Disorder. *Neurotherapeutics* **11**, 166–176 (2014).

125. Beninger, R. J. The role of dopamine in locomotor activity and learning. *Brain Res. Rev.* **6**, 173–196 (1983).

126. Berridge, K. C., Venier, I. L. & Robinson, T. E. Taste reactivity analysis of 6-hydroxydopamine-induced aphagia: Implications for arousal and anhedonia hypotheses of dopamine function. *Behav. Neurosci.* **103**, 36–45 (1989).

127. Castan˜eda, E., Whishaw, I. Q., Lermer, L. & Robinson, T. E. Dopamine depletion in neonatal rats: effects on behavior and striatal dopamine release assessed by intracerebral microdialysis during adulthood. *Brain Res.* **508**, 30–39 (1990).

128. Schultz, W. Depletion of dopamine in the striatum as an experimental model of parkinsonism: direct effects and adaptive mechanisms. *Prog. Neurobiol.* **18**, 121–166 (1982).

129. DeLong, M. R. Primate models of movement disorders of basal ganglia origin. *Trends Neurosci.* **13**, 281–285 (1990).

130. Mink, J. W. The Basal Ganglia and Involuntary Movements: Impaired Inhibition of Competing Motor Patterns. *Arch. Neurol.* **60**, 1365–1368 (2003).

131. Kravitz, A. V. *et al.* Regulation of parkinsonian motor behaviours by optogenetic control of basal ganglia circuitry. *Nature* **466**, 622–626 (2010).

132. Roseberry, T. K. *et al.* Cell-Type-Specific Control of Brainstem Locomotor Circuits by Basal Ganglia. *Cell* **164**, 526–537 (2016).

133. Freeze, B. S., Kravitz, A. V., Hammack, N., Berke, J. D. & Kreitzer, A. C. Control of Basal Ganglia Output by Direct and Indirect Pathway Projection Neurons. *J. Neurosci.* **33**, 18531–18539 (2013).

134. Redgrave, P., Prescott, T. J. & Gurney, K. The Basal Ganglia: A Vertebrate Solution to the Selection Problem? *Neuroscience* **89**, 1009–1023 (1999).

135. Mink, J. W. The Basal Ganglia: Focused Selection and Inhibition of Competing Motor Programs. *Prog. Neurobiol.* **50**, 381–425 (1996).

136. Suryanarayana, S. M., Hellgren Kotaleski, J., Grillner, S. & Gurney, K. N. Roles for globus pallidus externa revealed in a computational model of action selection in the basal ganglia. *Neural Netw.* **109**, 113–136 (2019).

137. Aldridge, J. W. & Berridge, K. C. Coding of Serial Order by Neostriatal Neurons: A "Natural Action" Approach to Movement Sequence. *J. Neurosci.* **18**, 2777–2787 (1998).

138. Jaeger, D., Gilman, S. & Wayne Aldridge, J. Neuronal activity in the striatum and pallidum of primates related to the execution of externally cued reaching movements. *Brain Res.* **694**, 111–127 (1995).

139. Barbera, G. *et al.* Spatially Compact Neural Clusters in the Dorsal Striatum Encode Locomotion Relevant Information. *Neuron* **92**, 202–213 (2016).

140. Kim, N., Barter, J. W., Sukharnikova, T. & Yin, H. H. Striatal firing rate reflects head movement velocity. *Eur. J. Neurosci.* **40**, 3481–3490 (2014).

141. Meyer-Luehmann, M., Thompson, J. F., Berridge, K. C. & Aldridge, J. W. Substantia nigra pars reticulata neurons code initiation of a serial pattern: implications for natural action sequences and sequential disorders. *Eur. J. Neurosci.* **16**, 1599–1608 (2002).

142. Klaus, A. *et al.* The Spatiotemporal Organization of the Striatum Encodes Action Space. *Neuron* **95**, 1171-1180.e7 (2017).

143. Tecuapetla, F., Matias, S., Dugue, G. P., Mainen, Z. F. & Costa, R. M. Balanced activity in basal ganglia projection pathways is critical for contraversive movements. *Nat. Commun.* **5**, 4315 (2014).

144. Yttri, E. A. & Dudman, J. T. Opponent and bidirectional control of movement velocity in the basal ganglia. *Nature* **533**, 402–406 (2016).

145. Cui, G. *et al.* Concurrent activation of striatal direct and indirect pathways during action initiation. *Nature* **494**, 238–242 (2013).

146. Markowitz, J. E. *et al.* The Striatum Organizes 3D Behavior via Moment-to-Moment Action Selection. *Cell* **174**, 44-58.e17 (2018).

147. Hamid, A. A. *et al.* Mesolimbic dopamine signals the value of work. *Nat. Neurosci.* **19**, 117–126 (2016).

148. Howe, M. W., Tierney, P. L., Sandberg, S. G., Phillips, P. E. M. & Graybiel, A. M. Prolonged dopamine signalling in striatum signals proximity and value of distant rewards. *Nature* **500**, 575–579 (2013).

149. Romo, R. & Schultz, W. Dopamine neurons of the monkey midbrain: contingencies of responses to active touch during self-initiated arm movements. *J. Neurophysiol.* **63**, 592–606 (1990).

150. Cohen, J. Y., Haesler, S., Vong, L., Lowell, B. B. & Uchida, N. Neuron-type-specific signals for reward and punishment in the ventral tegmental area. *Nature* **482**, 85–88 (2012).

151. Day, J. J., Roitman, M. F., Wightman, R. M. & Carelli, R. M. Associative learning mediates dynamic shifts in dopamine signaling in the nucleus accumbens. *Nat. Neurosci.* **10**, 1020–1028 (2007).

152. Mirenowicz, J. & Schultz, W. Importance of unpredictability for reward responses in primate dopamine neurons. *J. Neurophysiol.* **72**, 1024–1027 (1994).

153. Pan, W.-X., Schmidt, R., Wickens, J. R. & Hyland, B. I. Dopamine Cells Respond to Predicted Events during Classical Conditioning: Evidence for Eligibility Traces in the Reward-Learning Network. *J. Neurosci.* **25**, 6235–6242 (2005).

154. Hollerman, J. R. & Schultz, W. Dopamine neurons report an error in the temporal prediction of reward during learning. *Nat. Neurosci.* **1**, 304–309 (1998).

155. Bunney, B. S., Chiodo, L. A. & Grace, A. A. Midbrain dopamine system electrophysiological functioning: a review and new hypothesis. *Synap. N. Y. N* **9**, 79–94 (1991).

156. Palmiter, R. D. Dopamine Signaling in the Dorsal Striatum Is Essential for Motivated Behaviors. *Ann. N. Y. Acad. Sci.* **1129**, 35–46 (2008).

157. Bayer, H. M. & Glimcher, P. W. Midbrain Dopamine Neurons Encode a Quantitative Reward Prediction Error Signal. *Neuron* **47**, 129–141 (2005).

158. Reynolds, J. N. J., Hyland, B. I. & Wickens, J. R. A cellular mechanism of reward-related learning. *Nature* **413**, 67–70 (2001).

159. Tobler, P. N., Fiorillo, C. D. & Schultz, W. Adaptive Coding of Reward Value by Dopamine Neurons. *Science* **307**, 1642–1645 (2005).

160. Parker, N. F. *et al.* Reward and choice encoding in terminals of midbrain dopamine neurons depends on striatal target. *Nat. Neurosci.* **19**, 845–854 (2016).

161. Wang, D. V. & Tsien, J. Z. Convergent Processing of Both Positive and Negative Motivational Signals by the VTA Dopamine Neuronal Populations. *PLOS ONE* **6**, e17047 (2011).

162. Gan, J. O., Walton, M. E. & Phillips, P. E. M. Dissociable cost and benefit encoding of future rewards by mesolimbic dopamine. *Nat. Neurosci.* **13**, 25–27 (2010).

163. Roesch, M. R., Calu, D. J. & Schoenbaum, G. Dopamine neurons encode the better option in rats deciding between differently delayed or sized rewards. *Nat. Neurosci.* **10**, 1615–1624 (2007).

164. Lammel, S. *et al.* Input-specific control of reward and aversion in the ventral tegmental area. *Nature* **491**, 212–217 (2012).

165. Lammel, S., Lim, B. K. & Malenka, R. C. Reward and aversion in a heterogeneous midbrain dopamine system. *Neuropharmacology* **76**, 351–359 (2014).

166. Watabe-Uchida, M., Eshel, N. & Uchida, N. Neural Circuitry of Reward Prediction Error. *Annu. Rev. Neurosci.* **40**, 373–394 (2017).

167. Waelti, P., Dickinson, A. & Schultz, W. Dopamine responses comply with basic assumptions of formal learning theory. *Nature* **412**, 43–48 (2001).

168. Jay, T. M. Dopamine: a potential substrate for synaptic plasticity and memory mechanisms. *Prog. Neurobiol.* **69**, 375–390 (2003).

169. Pignatelli, M. & Bonci, A. Role of Dopamine Neurons in Reward and Aversion: A Synaptic Plasticity Perspective. *Neuron* **86**, 1145–1157 (2015).

170. Sutton, R. S. Learning to predict by the methods of temporal differences. *Mach. Learn.* **3**, 9–44 (1988).

171. Barto, A. G. Reinforcement learning control. *Curr. Opin. Neurobiol.* **4**, 888–893 (1994).

172. Sutton, R. S. & Barto, A. G. Toward a modern theory of adaptive networks: expectation and prediction. *Psychol. Rev.* **88**, 135–170 (1981).

173. Sharp, M. E., Foerde, K., Daw, N. D. & Shohamy, D. Dopamine selectively remediates 'model-based' reward learning: a computational approach. *Brain* **139**, 355–364 (2016).

174. Langdon, A. J., Sharpe, M. J., Schoenbaum, G. & Niv, Y. Model-based predictions for dopamine. *Curr. Opin. Neurobiol.* **49**, 1–7 (2018).

175. Dayan, P. Dopamine, Reinforcement Learning, and Addiction. *Pharmacopsychiatry* **42**, S56–S65 (2009).

176. Fiorillo, C. D., Song, M. R. & Yun, S. R. Multiphasic Temporal Dynamics in Responses of Midbrain Dopamine Neurons to Appetitive and Aversive Stimuli. *J. Neurosci.* **33**, 4710–4725 (2013).

177. Zweifel, L. S. *et al.* Activation of dopamine neurons is critical for aversive conditioning and prevention of generalized anxiety. *Nat. Neurosci.* **14**, 620–626 (2011).

178. Lerner, T. N. *et al.* Intact-Brain Analyses Reveal Distinct Information Carried by SNc Dopamine Subcircuits. *Cell* **162**, 635–647 (2015).

179. Bromberg-Martin, E. S., Matsumoto, M. & Hikosaka, O. Dopamine in Motivational Control: Rewarding, Aversive, and Alerting. *Neuron* **68**, 815–834 (2010).

180. Costa, V. D., Tran, V. L., Turchi, J. & Averbeck, B. B. Dopamine modulates novelty seeking behavior during decision making. *Behav. Neurosci.* **128**, 556–566 (2014).

181. Menegas, W., Babayan, B. M., Uchida, N. & Watabe-Uchida, M. Opposite initialization to novel cues in dopamine signaling in ventral and posterior striatum in mice. *eLife* **6**, e21886 (2017).

182. Rangel-Gomez, M. & Meeter, M. Neurotransmitters and Novelty: A Systematic Review. *J. Psychopharmacol. (Oxf.)* **30**, 3–12 (2016).

183. Matsumoto, H., Tian, J., Uchida, N. & Watabe-Uchida, M. Midbrain dopamine neurons signal aversion in a reward-context-dependent manner. *eLife* **5**, e17328 (2016).

184. Fee, M. S. & Goldberg, J. H. A hypothesis for basal ganglia-dependent reinforcement learning in the songbird. *Neuroscience* **198**, 152–170 (2011).

185. Gadagkar, V. *et al.* Dopamine neurons encode performance error in singing birds. *Science* **354**, 1278–1282 (2016).

186. Hoffmann, L. A., Saravanan, V., Wood, A. N., He, L. & Sober, S. J. Dopaminergic Contributions to Vocal Learning. *J. Neurosci.* **36**, 2176–2189 (2016).

187. Joel, D., Niv, Y. & Ruppin, E. Actor–critic models of the basal ganglia: new anatomical and computational perspectives. *Neural Netw.* **15**, 535–547 (2002).

188. Kreitzer, A. C. & Malenka, R. C. Striatal Plasticity and Basal Ganglia Circuit Function. *Neuron* **60**, 543–554 (2008).

189. Graybiel, A. M. The Basal Ganglia and Chunking of Action Repertoires. *Neurobiol. Learn. Mem.* **70**, 119–136 (1998).

190. Kravitz, A. V. & Kreitzer, A. C. Striatal Mechanisms Underlying Movement, Reinforcement, and Punishment. *Physiology* **27**, 167–177 (2012).

191. Chang, C. Y., Gardner, M., Di Tillio, M. G. & Schoenbaum, G. Optogenetic Blockade of Dopamine Transients Prevents Learning Induced by Changes in Reward Features. *Curr. Biol.* **27**, 3480-3486.e3 (2017).

192. Zis, A. P., Fibiger, H. C. & Phillips, A. G. Reversal by L-Dopa of Impaired Learning Due to Destruction of the Dopaminergic Nigro-Neostriatal Projection. *Science* **185**, 960–962 (1974).

193. Shohamy, D., Myers, C. E., Grossman, S., Sage, J. & Gluck, M. A. The role of dopamine in cognitive sequence learning: evidence from Parkinson's disease. *Behav. Brain Res.* **156**, 191–199 (2005).

194. Collins, A. L. *et al.* Dynamic mesolimbic dopamine signaling during action sequence learning and expectation violation. *Sci. Rep.* **6**, 20231 (2016).

195. Beigi, M., Wilkinson, L., Gobet, F., Parton, A. & Jahanshahi, M. Levodopa medication improves incidental sequence learning in Parkinson's disease. *Neuropsychologia* **93**, 53–60 (2016).

196. Tremblay, P.-L. *et al.* Movement chunking during sequence learning is a dopamine-dependant process: a study conducted in Parkinson's disease. *Exp. Brain Res.* **205**, 375–385 (2010).

197. Badgaiyan, R. D., Fischman, A. J. & Alpert, N. M. Striatal dopamine release in sequential learning. *NeuroImage* **38**, 549–556 (2007).

198. Saunders, B. T., Richard, J. M., Margolis, E. B. & Janak, P. H. Dopamine neurons create Pavlovian conditioned stimuli with circuit-defined motivational properties. *Nat. Neurosci.* **21**, 1072 (2018).

199. Coddington, L. T. & Dudman, J. T. The timing of action determines reward prediction signals in identified midbrain dopamine neurons. *Nat. Neurosci.* **21**, 1563 (2018).

200. Berridge, K. C. The debate over dopamine's role in reward: the case for incentive salience. *Psychopharmacology (Berl.)* **191**, 391–431 (2007).

201. Adamantidis, A. R. *et al.* Optogenetic Interrogation of Dopaminergic Modulation of the Multiple Phases of Reward-Seeking Behavior. *J. Neurosci.* **31**, 10829–10835 (2011).

202. Chang, C. Y. *et al.* Brief optogenetic inhibition of dopamine neurons mimics endogenous negative reward prediction errors. *Nat. Neurosci.* **19**, 111–116 (2016).

203. D'Ardenne, K., McClure, S. M., Nystrom, L. E. & Cohen, J. D. BOLD Responses Reflecting Dopaminergic Signals in the Human Ventral Tegmental Area. *Science* **319**, 1264–1267 (2008).

204. Barron, A. B., Søvik, E. & Cornish, J. L. The Roles of Dopamine and Related Compounds in Reward-Seeking Behavior Across Animal Phyla. *Front. Behav. Neurosci.* **4**, (2010).

205. Waddell, S. Reinforcement signalling in Drosophila; dopamine does it all after all. *Curr. Opin. Neurobiol.* **23**, 324–329 (2013).

206. Schultz, W. The phasic reward signal of primate dopamine neurons. *Adv. Pharmacol. San Diego Calif* **42**, 686–690 (1998).

207. Sharpe, M. J. & Schoenbaum, G. Evaluation of the hypothesis that phasic dopamine constitutes a cached-value signal. *Neurobiol. Learn. Mem.* **153**, 131–136 (2018).

208. Schultz, W. Multiple Dopamine Functions at Different Time Courses. *Annu. Rev. Neurosci.* **30**, 259–288 (2007).

209. Grace, A. A. The tonic/phasic model of dopamine system regulation and its implications for understanding alcohol and psychostimulant craving. *Addict. Abingdon Engl.* **95 Suppl 2**, S119-128 (2000).

210. Grace, A. A. Phasic versus tonic dopamine release and the modulation of dopamine system responsivity: A hypothesis for the etiology of schizophrenia. *Neuroscience* **41**, 1–24 (1991).

211. Wightman, R. M. & Robinson, D. L. Transient changes in mesolimbic dopamine and their association with 'reward'. *J. Neurochem.* **82**, 721–735 (2002).

212. Freed, C. R. & Yamamoto, B. K. Regional brain dopamine metabolism: a marker for the speed, direction, and posture of moving animals. *Science* **229**, 62–65 (1985).

213. da Silva, J. A., Tecuapetla, F., Paixão, V. & Costa, R. M. Dopamine neuron activity before action initiation gates and invigorates future movements. *Nature* **554**, 244–248 (2018).

214. Howe, M. W. & Dombeck, D. A. Rapid signalling in distinct dopaminergic axons during locomotion and reward. *Nature* **535**, 505–510 (2016).

215. Dodson, P. D. *et al.* Representation of spontaneous movement by dopaminergic neurons is cell-type selective and disrupted in parkinsonism. *Proc. Natl. Acad. Sci.* **113**, E2180–E2188 (2016).

216. Barter, J. W. *et al.* Beyond reward prediction errors: the role of dopamine in movement kinematics. *Front. Integr. Neurosci.* **9**, (2015).

217. Barter, J. W., Castro, S., Sukharnikova, T., Rossi, M. A. & Yin, H. H. The role of the substantia nigra in posture control. *Eur. J. Neurosci.* **39**, 1465–1473 (2014).

218. Syed, E. C. J. *et al.* Action initiation shapes mesolimbic dopamine encoding of future rewards. *Nat. Neurosci.* **19**, 34–36 (2016).

219. Wang, D. V. & Tsien, J. Z. Conjunctive Processing of Locomotor Signals by the Ventral Tegmental Area Neuronal Population. *PLOS ONE* **6**, e16528 (2011).

220. Engelhard, B. *et al.* Specialized and spatially organized coding of sensory, motor, and cognitive variables in midbrain dopamine neurons. (2018). doi:10.1101/456194

221. Nicola, S. M. The Flexible Approach Hypothesis: Unification of Effort and Cue-Responding Hypotheses for the Role of Nucleus Accumbens Dopamine in the Activation of Reward-Seeking Behavior. *J. Neurosci.* **30**, 16585–16600 (2010).

222. Berke, J. D. What does dopamine mean? *Nat. Neurosci.* **21**, 787 (2018).

223. Panigrahi, B. *et al.* Dopamine Is Required for the Neural Representation and Control of Movement Vigor. *Cell* **162**, 1418–1430 (2015).

224. Fan, D., Rossi, M. A. & Yin, H. H. Mechanisms of Action Selection and Timing in Substantia Nigra Neurons. *J. Neurosci.* **32**, 5534–5548 (2012).

225. Salamone, J. D. & Correa, M. The Mysterious Motivational Functions of Mesolimbic Dopamine. *Neuron* **76**, 470–485 (2012).

226. Berridge, K. C. & Robinson, T. E. What is the role of dopamine in reward: hedonic impact, reward learning, or incentive salience? *Brain Res. Rev.* **28**, 309–369 (1998).

227. Lee, R. S., Mattar, M. G., Parker, N. F., Witten, I. B. & Daw, N. D. Reward prediction error does not explain movement selectivity in DMS-projecting dopamine neurons. *eLife* **8**, e42992 (2019).

228. Matsuda, W. *et al.* Single Nigrostriatal Dopaminergic Neurons Form Widely Spread and Highly Dense Axonal Arborizations in the Neostriatum. *J. Neurosci.* **29**, 444–453 (2009).

229. Fiorillo, C. D., Yun, S. R. & Song, M. R. Diversity and Homogeneity in Responses of Midbrain Dopamine Neurons. *J. Neurosci.* **33**, 4693–4709 (2013).

230. Lammel, S. *et al.* Diversity of Transgenic Mouse Models for Selective Targeting of Midbrain Dopamine Neurons. *Neuron* **85**, 429–438 (2015).

231. Stephenson, R. & Metcalfe, N. H. Drosophila melanogaster: a fly through its history and current use. *J. R. Coll. Physicians Edinb.* **43**, 70–75 (2013).

232. Arias, A. M. Drosophila melanogaster and the development of biology in the 20th century. *Methods Mol. Biol. Clifton NJ* **420**, 1–25 (2008).

233. Green, M. M. 2010: A Century of Drosophila Genetics Through the Prism of the white Gene. *Genetics* **184**, 3–7 (2010).

234. Bellen, H. J., Tong, C. & Tsuda, H. 100 years of Drosophila research and its impact on vertebrate neuroscience: a history lesson for the future. *Nat. Rev. Neurosci.* **11**, 514–522 (2010).

235. Jenett, A. *et al.* A GAL4-Driver Line Resource for Drosophila Neurobiology. *Cell Rep.* **2**, 991–1001 (2012).

236. Dolan, M.-J. *et al.* Facilitating Neuron-Specific Genetic Manipulations in Drosophila melanogaster Using a Split GAL4 Repressor. *Genetics* **206**, 775–784 (2017).

237. Dionne, H., Hibbard, K. L., Cavallaro, A., Kao, J.-C. & Rubin, G. M. Genetic Reagents for Making Split-GAL4 Lines in Drosophila. *Genetics* **209**, 31–35 (2018).

238. Yoshihara, M. & Ito, K. Acute Genetic Manipulation of Neuronal Activity for the Functional Dissection of Neural Circuits—A Dream Come True for the Pioneers of Behavioral Genetics. *J. Neurogenet.* **26**, 43–52 (2012).

239. Olsen, S. R. & Wilson, R. I. Cracking neural circuits in a tiny brain: new approaches for understanding the neural circuitry of Drosophila. *Trends Neurosci.* **31**, 512–520 (2008).

240. Simpson, J. H. & Looger, L. L. Functional Imaging and Optogenetics in Drosophila. *Genetics* **208**, 1291–1309 (2018).

241. Strother, J. A. *et al.* Behavioral state modulates the ON visual motion pathway of Drosophila. *Proc. Natl. Acad. Sci.* **115**, E102–E111 (2018).

242. van Breugel, F. & Dickinson, M. H. Plume-Tracking Behavior of Flying Drosophila Emerges from a Set of Distinct Sensory-Motor Reflexes. *Curr. Biol.* **24**, 274–286 (2014).

243. Pang, R., Breugel, F. van, Dickinson, M., Riffell, J. A. & Fairhall, A. History dependence in insect flight decisions during odor tracking. *PLOS Comput. Biol.* **14**, e1005969 (2018).

244. Álvarez-Salvado, E. *et al.* Elementary sensory-motor transformations underlying olfactory navigation in walking fruit-flies. *eLife* **7**, e37815 (2018).

245. Markow, T. A. & Hanson, S. J. Multivariate analysis of Drosophila courtship. *Proc. Natl. Acad. Sci. U. S. A.* **78**, 430–434 (1981).

246. Ewing, A. W. Functional Aspects of Drosophila Courtship. *Biol. Rev.* **58**, 275–292 (1983).

247. Demir, E. & Dickson, B. J. fruitless Splicing Specifies Male Courtship Behavior in Drosophila. *Cell* **121**, 785–794 (2005).

248. Bräcker, L. B. *et al.* Essential Role of the Mushroom Body in Context-Dependent CO2 Avoidance in Drosophila. *Curr. Biol.* **23**, 1228–1234 (2013).

249. Siju, K. P., Bräcker, L. B. & Kadow, I. G. Neural mechanisms of context-dependent processing of CO2 avoidance behavior in fruit flies. *Fly (Austin)* **8**, 68–74 (2014).

250. Lewis, L. P. C. *et al.* A Higher Brain Circuit for Immediate Integration of Conflicting Sensory Information in Drosophila. *Curr. Biol.* **25**, 2203–2214 (2015).

251. Pascual, A. & Préat, T. Localization of Long-Term Memory Within the Drosophila Mushroom Body. *Science* **294**, 1115–1117 (2001).

252. Quinn, W. G., Harris, W. A. & Benzer, S. Conditioned Behavior in Drosophila melanogaster. *Proc. Natl. Acad. Sci. U. S. A.* **71**, 708–712 (1974).

253. Davis, R. L. Mushroom bodies and drosophila learning. *Neuron* **11**, 1–14 (1993).

254. Heisenberg, M. What Do the Mushroom Bodies Do for the Insect Brain? An Introduction. *Learn. Mem.* **5**, 1–10 (1998).

255. Busto, G. U., Cervantes-Sandoval, I. & Davis, R. L. Olfactory Learning in Drosophila. *Physiology* **25**, 338–346 (2010).

256. Aso, Y. *et al.* The neuronal architecture of the mushroom body provides a logic for associative learning. *eLife* **3**, e04577 (2014).

257. Ueno, T. *et al.* Identification of a dopamine pathway that regulates sleep and arousal in *Drosophila*. *Nat. Neurosci.* **15**, 1516–1523 (2012).

258. Pitman, J. L., McGill, J. J., Keegan, K. P. & Allada, R. A dynamic role for the mushroom bodies in promoting sleep in *Drosophila*. *Nature* **441**, 753–756 (2006).

259. Tomita, J., Ban, G. & Kume, K. Genes and neural circuits for sleep of the fruit fly. *Neurosci. Res.* **118**, 82–91 (2017).

260. Sitaraman, D. *et al.* Propagation of Homeostatic Sleep Signals by Segregated Synaptic Microcircuits of the Drosophila Mushroom Body. *Curr. Biol.* **25**, 2915–2927 (2015).

261. Joiner, W. J., Crocker, A., White, B. H. & Sehgal, A. Sleep in *Drosophila* is regulated by adult mushroom bodies. *Nature* **441**, 757–760 (2006).

262. Artiushin, G. & Sehgal, A. The Drosophila circuitry of sleep–wake regulation. *Curr. Opin. Neurobiol.* **44**, 243–250 (2017).

263. Sitaraman, D., Aso, Y., Rubin, G. M. & Nitabach, M. N. Control of Sleep by Dopaminergic Inputs to the Drosophila Mushroom Body. *Front. Neural Circuits* **9**, (2015).

264. Hong, S.-T. *et al.* cAMP signalling in mushroom bodies modulates temperature preference behaviour in *Drosophila*. *Nature* **454**, 771–775 (2008).

265. Bang, S. *et al.* Dopamine Signalling in Mushroom Bodies Regulates Temperature-Preference Behaviour in Drosophila. *PLOS Genet.* **7**, e1001346 (2011).

266. Azanchi, R., Kaun, K. R. & Heberlein, U. Competing dopamine neurons drive oviposition choice for ethanol in Drosophila. *Proc. Natl. Acad. Sci.* **110**, 21153–21158 (2013).

267. Neckameyer, W. S. Dopamine and Mushroom Bodies in Drosophila: Experience-Dependent and -Independent Aspects of Sexual Behavior. *Learn. Mem.* **5**, 157–165 (1998).

268. Lim, J. *et al.* The mushroom body D1 dopamine receptor controls innate courtship drive. *Genes Brain Behav.* **17**, 158–167 (2018).

269. Liu, L., Wolf, R., Ernst, R. & Heisenberg, M. Context generalization in *Drosophila* visual learning requires the mushroom bodies. *Nature* **400**, 753–756 (1999).

270. Zhang, K., Guo, J. Z., Peng, Y., Xi, W. & Guo, A. Dopamine-Mushroom Body Circuit Regulates Saliency-Based Decision-Making in Drosophila. *Science* **316**, 1901–1904 (2007).

271. Swinderen, B. van *et al.* Shared Visual Attention and Memory Systems in the Drosophila Brain. *PLOS ONE* **4**, e5989 (2009).

272. Manjila, S. B., Kuruvilla, M., Ferveur, J.-F., Sane, S. P. & Hasan, G. Extended Flight Bouts Require Disinhibition from GABAergic Mushroom Body Neurons. *Curr. Biol.* **29**, 283-293.e5 (2019).

273. Colomb, J., Kaiser, L., Chabaud, M.-A. & Preat, T. Parametric and genetic analysis of Drosophila appetitive long-term memory and sugar motivation. *Genes Brain Behav.* **8**, 407–415 (2009).

274. Krashes, M. J. *et al.* A Neural Circuit Mechanism Integrating Motivational State with Memory Expression in Drosophila. *Cell* **139**, 416–427 (2009).

275. Landayan, D., Feldman, D. S. & Wolf, F. W. Satiation state-dependent dopaminergic control of foraging in Drosophila. *Sci. Rep.* **8**, 5777 (2018).

276. Grunwald Kadow, I. C. State-dependent plasticity of innate behavior in fruit flies. *Curr. Opin. Neurobiol.* **54**, 60–65 (2019).

277. Martin, J.-R., Ernst, R. & Heisenberg, M. Mushroom Bodies Suppress Locomotor Activity in Drosophila melanogaster. *Learn. Mem.* **5**, 179–191 (1998).

278. Serway, C. N. *et al.* Mushroom Bodies Enhance Initial Motor Activity in drosophila. *J. Neurogenet.* **23**, 173–184 (2009).

279. Mabuchi, I. *et al.* Mushroom body signaling is required for locomotor activity rhythms in Drosophila. *Neurosci. Res.* **111**, 25–33 (2016).

280. Sun, J. *et al.* Neural Control of Startle-Induced Locomotion by the Mushroom Bodies and Associated Neurons in Drosophila. *Front. Syst. Neurosci.* **12**, (2018).

281. Fuenzalida-Uribe, N. & Campusano, J. M. Unveiling the Dual Role of the Dopaminergic System on Locomotion and the Innate Value for an Aversive Olfactory Stimulus in Drosophila. *Neuroscience* **371**, 433–444 (2018).

282. Dujardin, F. Mémoire sur le système nerveux des insectes. *Ann Sci Nat Zool* **14**, 195–206 (1850).

283. Strausfeld, N. J., Hansen, L., Li, Y., Gomez, R. S. & Ito, K. Evolution, Discovery, and Interpretations of Arthropod Mushroom Bodies. *Learn. Mem.* **5**, 11–37 (1998).

284. Heisenberg, M., Borst, A., Wagner, S. & Byers, D. Drosophila mushroom body mutants are deficient in olfactory learning. *J. Neurogenet.* **2**, 1–30 (1985).

285. Belle, J. de & Heisenberg, M. Associative odor learning in Drosophila abolished by chemical ablation of mushroom bodies. *Science* **263**, 692–695 (1994).

286. Gerber, B., Tanimoto, H. & Heisenberg, M. An engram found? Evaluating the evidence from fruit flies. *Curr. Opin. Neurobiol.* **14**, 737–744 (2004).

287. Dubnau, J., Grady, L., Kitamoto, T. & Tully, T. Disruption of neurotransmission in *Drosophila* mushroom body blocks retrieval but not acquisition of memory. *Nature* **411**, 476–480 (2001).

288. Tully, T. & Quinn, W. G. Classical conditioning and retention in normal and mutant Drosophila melanogaster. *J. Comp. Physiol. [A]* **157**, 263–277 (1985).

289. Tempel, B. L., Bonini, N., Dawson, D. R. & Quinn, W. G. Reward learning in normal and mutant Drosophila. *Proc. Natl. Acad. Sci.* **80**, 1482–1486 (1983).

290. Waddell, S., Armstrong, J. D., Kitamoto, T., Kaiser, K. & Quinn, W. G. The amnesiac Gene Product Is Expressed in Two Neurons in the Drosophila Brain that Are Critical for Memory. *Cell* **103**, 805–813 (2000).

291. Levin, L. R. *et al.* The Drosophila learning and memory gene rutabaga encodes a Ca2+/calmodulin-responsive adenylyl cyclase. *Cell* **68**, 479–489 (1992).

292. Nighorn, A., Healy, M. J. & Davis, R. L. The cyclic AMP phosphodiesterase encoded by the drosophila dunce gene is concentrated in the mushroom body neuropil. *Neuron* **6**, 455–467 (1991).

293. Akalal, D.-B. G. *et al.* Roles for Drosophila mushroom body neurons in olfactory learning and memory. *Learn. Mem.* **13**, 659–668 (2006).

294. Han, P.-L., Levin, L. R., Reed, R. R. & Davis, R. L. Preferential expression of the drosophila rutabaga gene in mushroom bodies, neural centers for learning in insects. *Neuron* **9**, 619–627 (1992).

295. Skoulakis, E. M. C., Kalderon, D. & Davis, R. L. Preferential expression in mushroom bodies of the catalytic subunit of protein kinase A and its role in learning and memory. *Neuron* **11**, 197–208 (1993).

296. Hitier, R., Heisenberg, M. & Préat, T. Abnormal mushroom body plasticity in the Drosophila memory mutant amnesiac. *Neuroreport* **9**, 2717–2719 (1998).

297. Roman, G. & Davis, R. L. Molecular biology and anatomy of Drosophila olfactory associative learning. *BioEssays* **23**, 571–581 (2001).

298. Keene, A. C. & Waddell, S. *Drosophila* olfactory memory: single genes to complex neural circuits. *Nat. Rev. Neurosci.* **8**, 341–354 (2007).

299. McGuire, S. E., Deshazer, M. & Davis, R. L. Thirty years of olfactory learning and memory research in Drosophila melanogaster. *Prog. Neurobiol.* **76**, 328–347 (2005).

300. Davis, R. L. Olfactory memory formation in Drosophila: from Molecular to Systems Neuroscience. *Annu. Rev. Neurosci.* **28**, 275–302 (2005).

301. Heisenberg, M. Mushroom body memoir: from maps to models. *Nat. Rev. Neurosci.* **4**, 266–275 (2003).

302. Tanaka, N. K., Tanimoto, H. & Ito, K. Neuronal assemblies of the Drosophila mushroom body. *J. Comp. Neurol.* **508**, 711–755 (2008).

303. Lin, H.-H., Lai, J. S.-Y., Chin, A.-L., Chen, Y.-C. & Chiang, A.-S. A Map of Olfactory Representation in the Drosophila Mushroom Body. *Cell* **128**, 1205–1217 (2007).

304. Wong, A. M., Wang, J. W. & Axel, R. Spatial Representation of the Glomerular Map in the Drosophila Protocerebrum. *Cell* **109**, 229–241 (2002).

305. Vosshall, L. B. & Stocker, R. F. Molecular Architecture of Smell and Taste in Drosophila. *Annu. Rev. Neurosci.* **30**, 505–533 (2007).

306. Marin, E. C., Jefferis, G. S. X. E., Komiyama, T., Zhu, H. & Luo, L. Representation of the Glomerular Olfactory Map in the Drosophila Brain. *Cell* **109**, 243–255 (2002).

307. Jefferis, G. S. X. E. *et al.* Comprehensive Maps of Drosophila Higher Olfactory Centers: Spatially Segregated Fruit and Pheromone Representation. *Cell* **128**, 1187–1203 (2007).

308. Masse, N. Y., Turner, G. C. & Jefferis, G. S. X. E. Olfactory Information Processing in Drosophila. *Curr. Biol.* **19**, R700–R713 (2009).

309. Wilson, R. I. Early Olfactory Processing in Drosophila: Mechanisms and Principles. *Annu. Rev. Neurosci.* **36**, 217–241 (2013).

310. Kremer, M. C. *et al.* Structural Long-Term Changes at Mushroom Body Input Synapses. *Curr. Biol.* **20**, 1938–1944 (2010).

311. Gruntman, E. & Turner, G. C. Integration of the olfactory code across dendritic claws of single mushroom body neurons. *Nat. Neurosci.* **16**, 1821–1829 (2013).

312. Campbell, R. A. A. *et al.* Imaging a Population Code for Odor Identity in the Drosophila Mushroom Body. *J. Neurosci.* **33**, 10568–10581 (2013).

313. Leiss, F., Groh, C., Butcher, N. J., Meinertzhagen, I. A. & Tavosanis, G. Synaptic organization in the adult Drosophila mushroom body calyx. *J. Comp. Neurol.* **517**, 808–824 (2009).

314. Perez-Orive, J. *et al.* Oscillations and Sparsening of Odor Representations in the Mushroom Body. *Science* **297**, 359–365 (2002).

315. Turner, G. C., Bazhenov, M. & Laurent, G. Olfactory Representations by Drosophila Mushroom Body Neurons. *J. Neurophysiol.* **99**, 734–746 (2008).

316. Honegger, K. S., Campbell, R. A. A. & Turner, G. C. Cellular-Resolution Population Imaging Reveals Robust Sparse Coding in the Drosophila Mushroom Body. *J. Neurosci.* **31**, 11772–11785 (2011).

317. Caron, S. J. C., Ruta, V., Abbott, L. F. & Axel, R. Random convergence of olfactory inputs in the *Drosophila* mushroom body. *Nature* **497**, 113–117 (2013).

318. Litwin-Kumar, A., Harris, K. D., Axel, R., Sompolinsky, H. & Abbott, L. F. Optimal Degrees of Synaptic Connectivity. *Neuron* **93**, 1153-1164.e7 (2017).

319. Itskov, V. & Abbott, L. F. Pattern Capacity of a Perceptron for Sparse Discrimination. *Phys. Rev. Lett.* **101**, 018101 (2008).

320. Arena, P. *et al.* Modeling the insect mushroom bodies: Application to a delayed match-to-sample task. *Neural Netw.* **41**, 202–211 (2013).

321. Groschner, L. N., Chan Wah Hak, L., Bogacz, R., DasGupta, S. & Miesenböck, G. Dendritic Integration of Sensory Evidence in Perceptual Decision-Making. *Cell* **173**, 894-905.e13 (2018).

322. Ito, K., Awano, W., Suzuki, K., Hiromi, Y. & Yamamoto, D. The Drosophila mushroom body is a quadruple structure of clonal units each of which contains a virtually identical set of neurones and glial cells. *Development* **124**, 761–771 (1997).

323. Lee, T., Lee, A. & Luo, L. Development of the Drosophila mushroom bodies: sequential generation of three distinct types of neurons from a neuroblast. *Development* **126**, 4065–4076 (1999).

324. Zhu, S., Chiang, A.-S. & Lee, T. Development of the Drosophila mushroom bodies: elaboration, remodeling and spatial organization of dendrites in the calyx. *Development* **130**, 2603–2610 (2003).

325. Krashes, M. J., Keene, A. C., Leung, B., Armstrong, J. D. & Waddell, S. Sequential Use of Mushroom Body Neuron Subsets during Drosophila Odor Memory Processing. *Neuron* **53**, 103–115 (2007).

326. Cervantes-Sandoval, I., Martin-Peña, A., Berry, J. A. & Davis, R. L. System-Like Consolidation of Olfactory Memories in Drosophila. *J. Neurosci.* **33**, 9846–9854 (2013).

327. Isabel, G., Pascual, A. & Preat, T. Exclusive Consolidated Memory Phases in Drosophila. *Science* **304**, 1024–1027 (2004).

328. Yu, D., Akalal, D.-B. G. & Davis, R. L. Drosophila α/β Mushroom Body Neurons Form a Branch-Specific, Long-Term Cellular Memory Trace after Spaced Olfactory Conditioning. *Neuron* **52**, 845–855 (2006).

329. Scheunemann, L. *et al.* Consolidated and Labile Odor Memory Are Separately Encoded within the Drosophila Brain. *J. Neurosci.* **32**, 17163–17171 (2012).

330. Akalal, D.-B. G., Yu, D. & Davis, R. L. A Late-Phase, Long-Term Memory Trace Forms in the γ Neurons of Drosophila Mushroom Bodies after Olfactory Classical Conditioning. *J. Neurosci.* **30**, 16699–16708 (2010).

331. Zhao, J. *et al.* Dissociation of rugose-dependent short-term memory component from memory consolidation in Drosophila. *Genes Brain Behav.* **12**, 626–632 (2013).

332. Trannoy, S., Redt-Clouet, C., Dura, J.-M. & Preat, T. Parallel Processing of Appetitive Short- and Long-Term Memories In Drosophila. *Curr. Biol.* **21**, 1647–1653 (2011).

333. Krashes, M. J. & Waddell, S. Rapid Consolidation to a radish and Protein Synthesis-Dependent Long-Term Memory after Single-Session Appetitive Olfactory Conditioning in Drosophila. *J. Neurosci.* **28**, 3103–3113 (2008).

334. Blum, A. L., Li, W., Cressy, M. & Dubnau, J. Short- and Long-Term Memory in Drosophila Require cAMP Signaling in Distinct Neuron Types. *Curr. Biol.* **19**, 1341–1350 (2009).

335. Scholz-Kornehl, S. & Schwärzel, M. Circuit Analysis of a Drosophila Dopamine Type 2 Receptor That Supports Anesthesia-Resistant Memory. *J. Neurosci.* **36**, 7936–7945 (2016).

336. Murakami, S., Minami-Ohtsubo, M., Nakato, R., Shirahige, K. & Tabata, T. Two Components of Aversive Memory in Drosophila, Anesthesia-Sensitive and Anesthesia-Resistant Memory, Require Distinct Domains Within the Rgk1 Small GTPase. *J. Neurosci.* **37**, 5496–5510 (2017).

337. Pavlopoulos, E., Anezaki, M. & Skoulakis, E. M. C. Neuralized is expressed in the α/β lobes of adult Drosophila mushroom bodies and facilitates olfactory long-term memory formation. *Proc. Natl. Acad. Sci.* **105**, 14674–14679 (2008).

338. Folkers, E., Waddell, S. & Quinn, W. G. The Drosophila radish gene encodes a protein required for anesthesia-resistant memory. *Proc. Natl. Acad. Sci.* **103**, 17496–17500 (2006).

339. Aso, Y. *et al.* Mushroom body output neurons encode valence and guide memory-based action selection in Drosophila. *eLife* **3**, e04580 (2014).

340. Owald, D. *et al.* Activity of Defined Mushroom Body Output Neurons Underlies Learned Olfactory Behavior in Drosophila. *Neuron* **86**, 417–427 (2015).

341. Wu, J.-K. *et al.* Long-term memory requires sequential protein synthesis in three subsets of mushroom body output neurons in Drosophila. *Sci. Rep.* **7**, 7112 (2017).

342. Séjourné, J. *et al.* Mushroom body efferent neurons responsible for aversive olfactory memory retrieval in *Drosophila*. *Nat. Neurosci.* **14**, 903–910 (2011).

343. Owald, D. & Waddell, S. Olfactory learning skews mushroom body output pathways to steer behavioral choice in Drosophila. *Curr. Opin. Neurobiol.* **35**, 178–184 (2015).

344. Plaçais, P.-Y., Trannoy, S., Friedrich, A. B., Tanimoto, H. & Preat, T. Two Pairs of Mushroom Body Efferent Neurons Are Required for Appetitive Long-Term Memory Retrieval in Drosophila. *Cell Rep.* **5**, 769–780 (2013).

345. Hige, T., Aso, Y., Rubin, G. M. & Turner, G. C. Plasticity-driven individualization of olfactory coding in mushroom body output neurons. *Nature* **526**, 258–262 (2015).

346. Mao, Z. & Davis, R. L. Eight different types of dopaminergic neurons innervate the Drosophila mushroom body neuropil: anatomical and physiological heterogeneity. *Front. Neural Circuits* **3**, (2009).

347. Riemensperger, T., Völler, T., Stock, P., Buchner, E. & Fiala, A. Punishment Prediction by Dopaminergic Neurons in Drosophila. *Curr. Biol.* **15**, 1953–1960 (2005).

348. Liu, C. *et al.* A subset of dopamine neurons signals reward for odour memory in Drosophila. *Nature* **488**, 512–516 (2012).

349. Burke, C. J. *et al.* Layered reward signalling through octopamine and dopamine in Drosophila. *Nature* **492**, 433–437 (2012).

350. Lin, S. *et al.* Neural correlates of water reward in thirsty Drosophila. *Nat. Neurosci.* **17**, 1536–1542 (2014).

351. Cohn, R., Morantte, I. & Ruta, V. Coordinated and Compartmentalized Neuromodulation Shapes Sensory Processing in Drosophila. *Cell* **163**, 1742–1755 (2015).

352. Aso, Y. *et al.* Three Dopamine Pathways Induce Aversive Odor Memories with Different Stability. *PLOS Genet.* **8**, e1002768 (2012).

353. Das, G. *et al.* Drosophila Learn Opposing Components of a Compound Food Stimulus. *Curr. Biol.* **24**, 1723–1730 (2014).

354. Yamagata, N. *et al.* Distinct dopamine neurons mediate reward signals for short- and long-term memories. *Proc. Natl. Acad. Sci.* **112**, 578–583 (2015).

355. Aso, Y. *et al.* Specific Dopaminergic Neurons for the Formation of Labile Aversive Memory. *Curr. Biol.* **20**, 1445–1451 (2010).

356. Claridge-Chang, A. *et al.* Writing Memories with Light-Addressable Reinforcement Circuitry. *Cell* **139**, 405–415 (2009).

357. Ichinose, T. *et al.* Reward signal in a recurrent circuit drives appetitive long-term memory formation. *eLife* **4**, e10719 (2015).

358. Dolan, M.-J. *et al.* Neurogenetic dissection of the Drosophila innate olfactory processing center. *bioRxiv* 404277 (2018). doi:10.1101/404277

359. Dolan, M.-J. *et al.* Communication from Learned to Innate Olfactory Processing Centers Is Required for Memory Retrieval in Drosophila. *Neuron* **100**, 651-668.e8 (2018).

360. Vogt, K. *et al.* Shared mushroom body circuits underlie visual and olfactory memories in Drosophila. *eLife* **3**, e02395 (2014).

361. Hattori, D. *et al.* Representations of Novelty and Familiarity in a Mushroom Body Compartment. *Cell* **169**, 956-969.e17 (2017).

362. Berry, J. A., Cervantes-Sandoval, I., Chakraborty, M. & Davis, R. L. Sleep Facilitates Memory by Blocking Dopamine Neuron-Mediated Forgetting. *Cell* **161**, 1656–1667 (2015).

363. Huetteroth, W. *et al.* Sweet Taste and Nutrient Value Subdivide Rewarding Dopaminergic Neurons in Drosophila. *Curr. Biol.* **25**, 751–758 (2015).

364. Qin, H. *et al.* Gamma Neurons Mediate Dopaminergic Input during Aversive Olfactory Memory Formation in Drosophila. *Curr. Biol.* **22**, 608–614 (2012).

365. Seelig, J. D. *et al.* Two-photon calcium imaging from head-fixed during optomotor walking behavior. *Nat. Methods* **7**, 535–540 (2010).

366. Seelig, J. D. & Jayaraman, V. Studying Sensorimotor Processing With Physiology in Behaving Drosophila. in *International Review of Neurobiology* (ed. Atkinson, N.) **99**, 169–189 (Academic Press, 2011).

367. Seelig, J. D. & Jayaraman, V. Feature detection and orientation tuning in the Drosophila central complex. *Nature* **503**, 262–266 (2013).

368. Seelig, J. D. & Jayaraman, V. Neural dynamics for landmark orientation and angular path integration. *Nature* **521**, 186–191 (2015).

369. Green, J. *et al.* A neural circuit architecture for angular integration in Drosophila. *Nature* **546**, 101–106 (2017).

370. Moore, R. J. D. *et al.* FicTrac: A visual method for tracking spherical motion and generating fictive animal paths. *J. Neurosci. Methods* **225**, 106–119 (2014).

371. Chen, T.-W. *et al.* Ultrasensitive fluorescent proteins for imaging neuronal activity. *Nature* **499**, 295–300 (2013).

372. Yapici, N., Cohn, R., Schusterreiter, C., Ruta, V. & Vosshall, L. B. A Taste Circuit that Regulates Ingestion by Integrating Food and Hunger Signals. *Cell* **165**, 715–729 (2016).

373. Aimon, S. *et al.* Fast near-whole–brain imaging in adult Drosophila during responses to stimuli and behavior. *PLOS Biol.* **17**, e2006732 (2019).

374. Howard, C. D., Li, H., Geddes, C. E. & Jin, X. Dynamic Nigrostriatal Dopamine Biases Action Selection. *Neuron* **93**, 1436-1450.e8 (2017).

375. Wichmann, T. & DeLong, M. R. Pathophysiology of Parkinson's Disease: The MPTP Primate Model of the Human Disorder. *Ann. N. Y. Acad. Sci.* **991**, 199–213 (2003).

376. Jankovic, J. Parkinson's disease: clinical features and diagnosis. *J. Neurol. Neurosurg. Psychiatry* **79**, 368–376 (2008).

377. Jin, X. & Costa, R. M. Start/stop signals emerge in nigrostriatal circuits during sequence learning. *Nature* **466**, 457–462 (2010).

378. Lee, I. H. & Assad, J. A. Putaminal Activity for Simple Reactions or Self-Timed Movements. *J. Neurophysiol.* **89**, 2528–2537 (2003).

379. Maimon, G. & Assad, J. A. Parietal Area 5 and the Initiation of Self-Timed Movements versus Simple Reactions. *J. Neurosci.* **26**, 2487–2498 (2006).

380. Kim, A. J., Fitzgerald, J. K. & Maimon, G. Cellular evidence for efference copy in Drosophila visuomotor processing. *Nat. Neurosci.* **18**, 1247–1255 (2015).

381. Stetson, C. & Andersen, R. A. Early planning activity in frontal and parietal cortex in a simplified task. *J. Neurophysiol.* **113**, 3915–3922 (2015).

382. Fried, I., Mukamel, R. & Kreiman, G. Internally Generated Preactivation of Single Neurons in Human Medial Frontal Cortex Predicts Volition. *Neuron* **69**, 548–562 (2011).

383. Rajan, R. Pre-Bout Neural Activity Changes in Premotor Nucleus HVC Correlate with Successful Initiation of Learned Song Sequence. *J. Neurosci.* **38**, 5925–5938 (2018).

384. Tuthill, J. C. & Azim, E. Proprioception. *Curr. Biol.* **28**, R194–R203 (2018).

385. Mamiya, A., Gurung, P. & Tuthill, J. C. Neural Coding of Leg Proprioception in Drosophila. *Neuron* **100**, 636-650.e6 (2018).

386. Bosco, G. & Poppele, R. E. Proprioception From a Spinocerebellar Perspective. *Physiol. Rev.* **81**, 539–568 (2001).

387. Hasan, Z. & Stuart, D. G. Animal Solutions to Problems of Movement Control: The Role of Proprioceptors. *Annu. Rev. Neurosci.* **11**, 199–223 (1988).

388. Heinze, S., Narendra, A. & Cheung, A. Principles of Insect Path Integration. *Curr. Biol.* **28**, R1043–R1058 (2018).

389. Moser, E. I., Kropff, E. & Moser, M.-B. Place Cells, Grid Cells, and the Brain's Spatial Representation System. *Annu. Rev. Neurosci.* **31**, 69–89 (2008).

390. Taube, J. S., Muller, R. U. & Ranck, J. B. Head-direction cells recorded from the postsubiculum in freely moving rats. I. Description and quantitative analysis. *J. Neurosci.* **10**, 420–435 (1990).

391. Rubin, A., Yartsev, M. M. & Ulanovsky, N. Encoding of Head Direction by Hippocampal Place Cells in Bats. *J. Neurosci.* **34**, 1067–1080 (2014).

392. Sargolini, F. *et al.* Conjunctive Representation of Position, Direction, and Velocity in Entorhinal Cortex. *Science* **312**, 758–762 (2006).

393. Maimon, G., Straw, A. D. & Dickinson, M. H. Active flight increases the gain of visual motion processing in *Drosophila*. *Nat. Neurosci.* **13**, 393–399 (2010).

394. Blair, H. T. & Sharp, P. E. Anticipatory head direction signals in anterior thalamus: evidence for a thalamocortical circuit that integrates angular head motion to compute head direction. *J. Neurosci.* **15**, 6260–6270 (1995).

395. Kathman, N. D. & Fox, J. L. Representation of haltere oscillations and integration with visual inputs in the fly central complex. *J. Neurosci.* 1707–18 (2019). doi:10.1523/JNEUROSCI.1707-18.2019

396. Diedrichsen, J., Hashambhoy, Y., Rane, T. & Shadmehr, R. Neural Correlates of Reach Errors. *J. Neurosci.* **25**, 9919–9931 (2005).

397. Holroyd, C. B. & Coles, M. G. H. The neural basis of human error processing: Reinforcement learning, dopamine, and the error-related negativity. *Psychol. Rev.* **109**, 679–709 (2002).

398. Eichler, K. *et al.* The complete connectome of a learning and memory centre in an insect brain. *Nature* **548**, 175–182 (2017).

399. Cognigni, P., Felsenberg, J. & Waddell, S. Do the right thing: neural network mechanisms of memory formation, expression and update in Drosophila. *Curr. Opin. Neurobiol.* **49**, 51–58 (2018).

400. Felsenberg, J. *et al.* Integration of Parallel Opposing Memories Underlies Memory Extinction. *Cell* **175**, 709-722.e15 (2018).

401. Grace, A. A., Floresco, S. B., Goto, Y. & Lodge, D. J. Regulation of firing of dopaminergic neurons and control of goal-directed behaviors. *Trends Neurosci.* **30**, 220–227 (2007).

402. Miyamoto, T. & Amrein, H. Diverse roles for the Drosophila fructose sensor Gr43a. *Fly (Austin)* **8**, 19–25 (2014).

403. Heinze, S. & Pfeiffer, K. Editorial: The Insect Central Complex—From Sensory Coding to Directing Movement. *Front. Behav. Neurosci.* **12**, (2018).

404. Boyan, G. S. & Liu, Y. Development of the Neurochemical Architecture of the Central Complex. *Front. Behav. Neurosci.* **10**, (2016).

405. Takemura, S. *et al.* A connectome of a learning and memory center in the adult Drosophila brain. *eLife* **6**, e26975 (2017).

406. Talay, M. *et al.* Transsynaptic Mapping of Second-Order Taste Neurons in Flies by trans-Tango. *Neuron* **96**, 783-795.e4 (2017).

407. Vogt, N. Neuroscience: It takes two to *trans*-Tango. *Nat. Methods* **15**, 11 (2018).

408. Paulk, A. C., Kirszenblat, L., Zhou, Y. & Swinderen, B. van. Closed-Loop Behavioral Control Increases Coherence in the Fly Brain. *J. Neurosci.* **35**, 10304–10315 (2015).

409. Souman, J. L., Frissen, I., Sreenivasa, M. N. & Ernst, M. O. Walking Straight into Circles. *Curr. Biol.* **19**, 1538–1542 (2009).

410. Ikemoto, S. & Panksepp, J. The role of nucleus accumbens dopamine in motivated behavior: a unifying interpretation with special reference to reward-seeking. *Brain Res. Rev.* **31**, 6–41 (1999).

411. McGuire, S. E., Le, P. T. & Davis, R. L. The Role of Drosophila Mushroom Body Signaling in Olfactory Memory. *Science* **293**, 1330–1333 (2001).

412. Togunov, R. R., Derocher, A. E. & Lunn, N. J. Windscapes and olfactory foraging in a large carnivore. *Sci. Rep.* **7**, 46332 (2017).

413. Yu, Y. S. W., Graff, M. M., Bresee, C. S., Man, Y. B. & Hartmann, M. J. Z. Whiskers aid anemotaxis in rats. *Sci. Adv.* **2**, (2016).

414. Hansson, B. S., Knaden, M., Sachse, S., Stensmyr, M. C. & Wicher, D. Towards plant-odor-related olfactory neuroethology in Drosophila. *Chemoecology* **20**, 51–61 (2010).

415. Kennedy, J. S. & Marsh, D. Pheromone-Regulated Anemotaxis in Flying Moths. *Science* **184**, 999–1001 (1974).

416. Bell, J. S. & Wilson, R. I. Behavior Reveals Selective Summation and Max Pooling among Olfactory Processing Channels. *Neuron* **91**, 425–438 (2016).

417. Gaudry, Q., Hong, E. J., Kain, J., de Bivort, B. L. & Wilson, R. I. Asymmetric neurotransmitter release enables rapid odour lateralization in *Drosophila*. *Nature* **493**, 424–428 (2013).

418. Wolf, H. & Wehner, R. Pinpointing food sources: olfactory and anemotactic orientation in desert ants, Cataglyphis fortis. *J. Exp. Biol.* **203**, 857–868 (2000).

419. Cardé, R. T. Odour plumes and odour-mediated flight in insects. *Ciba Found. Symp.* **200**, 54–66; discussion 66-70 (1996).

420. Jovanic, T. *et al.* Neural Substrates of Drosophila Larval Anemotaxis. *Curr. Biol.* **29**, 554-566.e4 (2019).

421. Baker, K. L. *et al.* Algorithms for Olfactory Search across Species. *J. Neurosci.* **38**, 9383–9389 (2018).

422. Baggett, V. *et al.* Place learning overrides innate behaviors in Drosophila. *Learn. Mem.* **25**, 122–128 (2018).

423. Cardé, R. T. & Willis, M. A. Navigational Strategies Used by Insects to Find Distant, Wind-Borne Sources of Odor. *J. Chem. Ecol.* **34**, 854–866 (2008).

424. Liberzon, A. *et al.* Moth-inspired navigation algorithm in a turbulent odor plume from a pulsating source. *PLOS ONE* **13**, e0198422 (2018).

425. Giang, T., He, J., Belaidi, S. & Scholz, H. Key Odorants Regulate Food Attraction in Drosophila melanogaster. *Front. Behav. Neurosci.* **11**, (2017).

426. Calabrese, R. L. Cider vinegar rules. *eLife* **7**,

427. Tsao, C.-H., Chen, C.-C., Lin, C.-H., Yang, H.-Y. & Lin, S. Drosophila mushroom bodies integrate hunger and satiety signals to control innate food-seeking behavior. *eLife* **7**, e35264 (2018).

428. Kim, I. S. & Dickinson, M. H. Idiothetic Path Integration in the Fruit Fly Drosophila melanogaster. *Curr. Biol.* **27**, 2227-2238.e3 (2017).

429. Sachse, S. & Beshel, J. The good, the bad, and the hungry: how the central brain codes odor valence to facilitate food approach in Drosophila. *Curr. Opin. Neurobiol.* **40**, 53–58 (2016).

430. Chow, D. M. & Frye, M. A. The neuro-ecology of resource localization in Drosophila: behavioral components of perception and search. *Fly (Austin)* **3**, 50–61 (2009).

431. Herrero, P. Fruit fly behavior in response to chemosensory signals. *Peptides* **38**, 228–237 (2012).

432. Suh, G. S. B. *et al.* A single population of olfactory sensory neurons mediates an innate avoidance behaviour in Drosophila. *Nature* **431**, 854 (2004).

433. Faucher, C., Forstreuter, M., Hilker, M. & Bruyne, M. de. Behavioral responses of Drosophila to biogenic levels of carbon dioxide depend on life-stage, sex and olfactory context. *J. Exp. Biol.* **209**, 2739–2748 (2006).

434. Guerenstein, P. G. & Hildebrand, J. G. Roles and Effects of Environmental Carbon Dioxide in Insect Life. *Annu. Rev. Entomol.* **53**, 161–178 (2008).

435. Budick, S. A., Reiser, M. B. & Dickinson, M. H. The role of visual and mechanosensory cues in structuring forward flight in Drosophila melanogaster. *J. Exp. Biol.* **210**, 4092–4103 (2007).

436. Niv, Y., Daw, N. D., Joel, D. & Dayan, P. Tonic dopamine: opportunity costs and the control of response vigor. *Psychopharmacology (Berl.)* **191**, 507–520 (2007).

437. Schultz, W. Behavioral dopamine signals. *Trends Neurosci.* **30**, 203–210 (2007).

438. Schultz, W. Reward functions of the basal ganglia. *J. Neural Transm.* **123**, 679–693 (2016).

439. Yates, D. Neural circuits: The influence of hunger. *Nat. Rev. Neurosci.* **18**, 451 (2017).

440. Allen, W. E. *et al.* Thirst regulates motivated behavior through modulation of brainwide neural population dynamics. *Science* **364**, eaav3932 (2019).

441. Nie, L.-J., Cao, Z.-D. & Fu, S.-J. Digesting or swimming? Integration of the postprandial metabolism, behavior and locomotion in a frequently foraging fish. *Comp. Biochem. Physiol. A. Mol. Integr. Physiol.* **204**, 205–210 (2017).

442. Branch, A. & Shen, P. Central and Peripheral Regulation of Appetite and Food Intake in Drosophila. in *Appetite and Food Intake: Central Control* (ed. Harris, R. B. S.) (CRC Press/Taylor & Francis, 2017).

443. Schadegg, A. C. & Herberholz, J. Satiation level affects anti-predatory decisions in foraging juvenile crayfish. *J. Comp. Physiol. A* **203**, 223–232 (2017).

444. Egecioglu, E., Prieto-Garcia, L., Studer, E., Westberg, L. & Jerlhag, E. The role of ghrelin signalling for sexual behaviour in male mice. *Addict. Biol.* **21**, 348–359 (2016).

445. Catano, L. B., Barton, M. B., Boswell, K. M. & Burkepile, D. E. Predator identity and time of day interact to shape the risk–reward trade-off for herbivorous coral reef fishes. *Oecologia* **183**, 763–773 (2017).

446. Sternson, S. M., Nicholas Betley, J. & Cao, Z. F. H. Neural circuits and motivational processes for hunger. *Curr. Opin. Neurobiol.* **23**, 353–360 (2013).

447. Wang, S.-P. *et al.* Mating experience and food deprivation modulate odor preference and dispersal in Drosophila melanogaster males. *J. Insect Sci.* **14**, (2014).

448. Garcia, N. W., Pfennig, K. S. & Burmeister, S. S. Leptin Manipulation Reduces Appetite and Causes a Switch in Mating Preference in the Plains Spadefoot Toad (Spea bombifrons). *PLOS ONE* **10**, e0125981 (2015).

449. Micevych, P. E. & Meisel, R. L. Integrating Neural Circuits Controlling Female Sexual Behavior. *Front. Syst. Neurosci.* **11**, (2017).

450. Wormington, J. & Juliano, S. Hunger-dependent and Sex-specific Antipredator Behaviour of Larvae of a Size-dimorphic Mosquito. *Ecol. Entomol.* **39**, 548–555 (2014).

451. Blecha, K. A., Boone, R. B. & Alldredge, M. W. Hunger mediates apex predator's risk avoidance response in wildland–urban interface. *J. Anim. Ecol.* **87**, 609–622 (2018).

452. Phillips-Farfán, B. V. & Fernández-Guasti, A. Endocrine, neural and pharmacological aspects of sexual satiety in male rats. *Neurosci. Biobehav. Rev.* **33**, 442–455 (2009).

453. Clinchy Michael, Zanette Liana, Boonstra Rudy, Wingfield John C. & Smith James N. M. Balancing food and predator pressure induces chronic stress in songbirds. *Proc. R. Soc. Lond. B Biol. Sci.* **271**, 2473–2479 (2004).

454. Weimerskirch, H., Pinaud, D., Pawlowski, F. & Bost, C. Does Prey Capture Induce Area-Restricted Search? A Fine-Scale Study Using GPS in a Marine Predator, the Wandering Albatross. *Am. Nat.* **170**, 734–743 (2007).

455. Nathan, R. *et al.* A movement ecology paradigm for unifying organismal movement research. *Proc. Natl. Acad. Sci.* **105**, 19052–19059 (2008).

456. López-Cruz, A. *et al.* Parallel Multimodal Circuits Control an Innate Foraging Behavior. *Neuron* **102**, 407-419.e8 (2019).

457. Salvador Liliana C. M., Bartumeus Frederic, Levin Simon A. & Ryu William S. Mechanistic analysis of the search behaviour of Caenorhabditis elegans. *J. R. Soc. Interface* **11**, 20131092 (2014).

458. Humphries, N. E. *et al.* Environmental context explains Lévy and Brownian movement patterns of marine predators. *Nature* **465**, 1066–1069 (2010).

459. Medic, N. *et al.* Dopamine Modulates the Neural Representation of Subjective Value of Food in Hungry Subjects. *J. Neurosci.* **34**, 16856–16864 (2014).

460. Hebart, M. N. & Gläscher, J. Serotonin and dopamine differentially affect appetitive and aversive general Pavlovian-to-instrumental transfer. *Psychopharmacology (Berl.)* **232**, 437–451 (2015).

461. Hsu, T. M., McCutcheon, J. E. & Roitman, M. F. Parallels and Overlap: The Integration of Homeostatic Signals by Mesolimbic Dopamine Neurons. *Front. Psychiatry* **9**, (2018).

462. Stouffer, M. A. *et al.* Insulin enhances striatal dopamine release by activating cholinergic interneurons and thereby signals reward. *Nat. Commun.* **6**, 8543 (2015).

463. Cassidy, R. M. & Tong, Q. Hunger and Satiety Gauge Reward Sensitivity. *Front. Endocrinol.* **8**, (2017).

464. Cone, J. J., McCutcheon, J. E. & Roitman, M. F. Ghrelin Acts as an Interface between Physiological State and Phasic Dopamine Signaling. *J. Neurosci.* **34**, 4905–4913 (2014).

465. Liu, Q. *et al.* Branch-specific plasticity of a bifunctional dopamine circuit encodes protein hunger. *Science* **356**, 534–539 (2017).

466. Friedman, D. A. *et al.* The Role of Dopamine in the Collective Regulation of Foraging in Harvester Ants. *iScience* **8**, 283–294 (2018).

467. Li, F. *et al.* Roles of NMDA and dopamine in food-foraging decision-making strategies of rats in the social setting. *BMC Neurosci.* **17**, 3 (2016).

468. Stern, S., Kirst, C. & Bargmann, C. I. Neuromodulatory Control of Long-Term Behavioral Patterns and Individuality across Development. *Cell* **171**, 1649-1662.e10 (2017).

469. Papageorgiou, G. K., Baudonnat, M., Cucca, F. & Walton, M. E. Mesolimbic Dopamine Encodes Prediction Errors in a State-Dependent Manner. *Cell Rep.* **15**, 221–228 (2016).

470. Govorunova, E. G., Sineshchekov, O. A., Janz, R., Liu, X. & Spudich, J. L. Natural light-gated anion channels: A family of microbial rhodopsins for advanced optogenetics. *Science* **349**, 647–650 (2015).

471. Handler, A. *et al.* Distinct dopamine receptor pathways underlie the temporal sensitivity of associative learning. *Cell Press*

472. Klapoetke, N. C. *et al.* Independent optical excitation of distinct neural populations. *Nat. Methods* **11**, 338–346 (2014).

473. Prevedel, R. *et al.* Fast volumetric calcium imaging across multiple cortical layers using sculpted light. *Nat. Methods* **13**, 1021–1028 (2016).

474. Cervantes-Sandoval, I., Phan, A., Chakraborty, M. & Davis, R. L. Reciprocal synapses between mushroom body and dopamine neurons form a positive feedback loop required for learning. *eLife* **6**, e23789 (2017).

475. Collett, M. & Collett, T. S. How does the insect central complex use mushroom body output for steering? *Curr. Biol.* **28**, R733–R734 (2018).

476. Solanki, N., Wolf, R. & Heisenberg, M. Central complex and mushroom bodies mediate novelty choice behavior in Drosophila. *J. Neurogenet.* **29**, 30–37 (2015).

477. Franconville, R., Beron, C. & Jayaraman, V. Building a functional connectome of the Drosophila central complex. *eLife* **7**, e37017 (2018).

478. Wiltschko, A. B. *et al.* Mapping Sub-Second Structure in Mouse Behavior. *Neuron* **88**, 1121–1135 (2015).

479. Mendes, C. S., Bartos, I., Akay, T., Márka, S. & Mann, R. S. Quantification of gait parameters in freely walking wild type and sensory deprived Drosophila melanogaster. *eLife* **2**, e00231 (2013).

480. Tastekin, I. *et al.* Sensorimotor pathway controlling stopping behavior during chemotaxis in the Drosophila melanogaster larva. *eLife* **7**, e38740 (2018).

481. Tao, L., Ozarkar, S., Beck, J. M. & Bhandawat, V. Statistical structure of locomotion and its modulation by odors. *eLife* **8**, e41235 (2019).

482. Costa, A. C., Ahamed, T. & Stephens, G. J. Adaptive, locally linear models of complex dynamics. *Proc. Natl. Acad. Sci.* **116**, 1501–1510 (2019).

483. Lark, A. R., Kitamoto, T. & Martin, J.-R. In Vivo Functional Brain Imaging Approach Based on Bioluminescent Calcium Indicator GFP-aequorin. *JoVE J. Vis. Exp.* e53705 (2016). doi:10.3791/53705

484. Martin, J.-R., Rogers, K. L., Chagneau, C. & Brûlet, P. In vivo Bioluminescence Imaging of Ca2+ Signalling in the Brain of Drosophila. *PLOS ONE* **2**, e275 (2007).

485. Ware, L. A. Three photons are better than tWO. *BioTechniques* **57**, 237–239 (2014).

486. Karagyozov, D., Mihovilovic Skanata, M., Lesar, A. & Gershow, M. Recording Neural Activity in Unrestrained Animals with Three-Dimensional Tracking Two-Photon Microscopy. *Cell Rep.* **25**, 1371-1383.e10 (2018).

487. Hsu, K.-J., Lin, Y.-Y., Chiang, A.-S. & Chu, S.-W. Whole-brain imaging and characterization of Drosophila brains based on one-, two-, and three-photon excitations. *bioRxiv* 339531 (2018). doi:10.1101/339531

488. Dana, H. *et al.* Sensitive red protein calcium indicators for imaging neural activity. *eLife* **5**, e12727 (2016).

489. Akerboom, J. *et al.* Genetically encoded calcium indicators for multi-color neural activity imaging and combination with optogenetics. *Front. Mol. Neurosci.* **6**, (2013).

490. Han, K.-A., Millar, N. S., Grotewiel, M. S. & Davis, R. L. DAMB, a Novel Dopamine Receptor Expressed Specifically in Drosophila Mushroom Bodies. *Neuron* **16**, 1127–1135 (1996).

491. Himmelreich, S. *et al.* Dopamine Receptor DAMB Signals via Gq to Mediate Forgetting in Drosophila. *Cell Rep.* **21**, 2074–2081 (2017).

492. Threlfell, S. *et al.* Striatal Dopamine Release Is Triggered by Synchronized Activity in Cholinergic Interneurons. *Neuron* **75**, 58–64 (2012).

493. Cachope, R. *et al.* Selective Activation of Cholinergic Interneurons Enhances Accumbal Phasic Dopamine Release: Setting the Tone for Reward Processing. *Cell Rep.* **2**, 33–41 (2012).

494. Howe, M. *et al.* Coordination of rapid cholinergic and dopaminergic signaling in striatum during spontaneous movement. *eLife* **8**, e44903 (2019).

495. Liu, X. & Davis, R. L. The GABAergic anterior paired lateral neuron suppresses and is suppressed by olfactory learning. *Nat. Neurosci.* **12**, 53–59 (2009).

496. Zhou, M. *et al.* Suppression of GABAergic neurons through D2-like receptor secures efficient conditioning in Drosophila aversive olfactory learning. *Proc. Natl. Acad. Sci.* **116**, 5118–5125 (2019).

497. Sugie, A., Marchetti, G. & Tavosanis, G. Structural aspects of plasticity in the nervous system of Drosophila. *Neural Develop.* **13**, 14 (2018).

498. Yu, D., Keene, A. C., Srivatsan, A., Waddell, S. & Davis, R. L. Drosophila DPM Neurons Form a Delayed and Branch-Specific Memory Trace after Olfactory Classical Conditioning. *Cell* **123**, 945–957 (2005).

499. Walkinshaw, E. *et al.* Identification of Genes That Promote or Inhibit Olfactory Memory Formation in Drosophila. *Genetics* **199**, 1173–1182 (2015).

500. Reinig, S., Driever, W. & Arrenberg, A. B. The Descending Diencephalic Dopamine System Is Tuned to Sensory Stimuli. *Curr. Biol.* **27**, 318–333 (2017).

501. Meyer, A. F., Poort, J., O'Keefe, J., Sahani, M. & Linden, J. F. A Head-Mounted Camera System Integrates Detailed Behavioral Monitoring with Multichannel Electrophysiology in Freely Moving Mice. *Neuron* **100**, 46-60.e7 (2018).

502. Ayaz, A., Stäuble, A., Saleem, A. B. & Helmchen, F. Layer-specific integration of locomotion and concurrent wall touching in mouse barrel cortex. *bioRxiv* 265165 (2018). doi:10.1101/265165

503. Pakan, J. M. *et al.* Behavioral-state modulation of inhibition is context-dependent and cell type specific in mouse visual cortex. *eLife* **5**, e14985 (2016).

504. Clancy, K. B., Orsolic, I. & Mrsic-Flogel, T. D. Locomotion-dependent remapping of distributed cortical networks. *Nat. Neurosci.* 1 (2019). doi:10.1038/s41593-019-0357-8

505. Stringer, C. *et al.* Spontaneous behaviors drive multidimensional, brainwide activity. *Science* **364**, eaav7893 (2019).

506. Gründemann, J. *et al.* Amygdala ensembles encode behavioral states. *Science* **364**, eaav8736 (2019).

507. Toivonen, J. M. *et al.* No Influence of Indy on Lifespan in Drosophila after Correction for Genetic and Cytoplasmic Background Effects. *PLOS Genet.* **3**, e95 (2007).

508. Friggi-Grelin, F., Iché, M. & Birman, S. Tissue-specific developmental requirements of Drosophila tyrosine hydroxylase isoforms. *genesis* **35**, 260–269 (2003).

509. Li, H., Chaney, S., Forte, M. & Hirsh, J. Ectopic G-protein expression in dopamine and serotonin neurons blocks cocaine sensitization in Drosophila melanogaster. *Curr. Biol.* **10**, 211–214 (2000).

510. Pitman, J. L. *et al.* A Pair of Inhibitory Neurons Are Required to Sustain Labile Memory in the Drosophila Mushroom Body. *Curr. Biol.* **21**, 855–861 (2011).